Thermorheology of Long Chain Branched Metallocene Polyethylene

Kang Zhu

A Thesis

in

The Department

of

Mechanical and Industrial Engineering

Presented in Partial Fulfillment of the Requirements

for the Degree of Master of Applied Science (Mechanical Engineering)

Concordia University

Montreal, Quebec, Canada

May 2003

Your file Votre référence
ISBN: 0-612-83893-5
Our file Notre référence
ISBN: 0-612-83893-5

Abstract

Thermorheology of Long Chain Branched Metallocene Polyethylene

Kang Zhu

Thermorheology is the study of the interrelationships between time and temperature in the rheological behavior of polymers. Metallocene polyethylene has a controlled and relatively simple molecular structure making it useful for the study of the relationships between rheological properties and molecular structure. Long chain branched metallocene polyethylene is thermorheologically complex, this means that the temperature sensitivity is time dependent, in other words the activation energy is time dependent.

In previous work this time dependent activation energy has been represented as an activation energy spectrum, an idea that was validated in the current work.The activation energy spectrum should be calculated from the relaxation spectrum, but small inaccuracies in the relaxation spectrum result in large errors in the activation energy spectrum. Therefore an alternate technique for determining this material function was needed. In this study, it was found that the activation energy spectrum could be calculated from the relaxation modulus and we demonstrated that the activation energy spectrum is a characteristic material function. Therefore by combining it with the relaxation spectrum at the reference temperature, viscoelastic properties at different temperatures can be predicted.

The thermorheological complexity of long chain branched polymers is caused by a particular relaxation mechanism called arm retraction. An equivalent relaxation

mechanism is exhibited by linear polymers at short time scales. According to this theory, linear polymers should be thermorheologically complex in the time range that this mechanism is active, however this has never been observed experimentally. The primary reason for the lack of experimental proof of that theory is the difficulty in accessing experimentally the necessary time scales. In order to make it possible to observe this behavior within the experimental window, a very high molecular weight, monodisperse linear polyethylene was studied. Thermorheological complexity of this material was observed in the expected time range, thus validating the theory of arm retraction and its linear polymer equivalent as the source of thermorheological complexity

From experimental results and arm retraction theory models, the apparent activation energy increases linearly with a product of the fraction of long chain branches and the arm molecular weight. The activation energy spectrum converges to the activation energy of the linear material before the Rouse time, then it increases until the arm is relaxed. The arm molecular weight not only affects the magnitude of the spectrum, but also affects its breadth. The volume fraction of long chain branches only affects the magnitude of the activation energy spectrum.

Acknowledgements

First of all, I would like to give my most heartfelt thanks to my supervisor Prof. Wood-Adams for her guidance and encouragement both in this project and in my life.

I would like to give my most heartfelt thanks to Prof. John Dealy of McGill University for his generous support and supervision. I would like to thanks the rheology research group of Chemical Engineering Department of McGill University, special thanks to Dr. Stephane Costeux, Dr. Chengxia He, Hee Park, Miguel Mbaque, Nannan Lui, Jack Xue, Siripon Anantawaraskul and Matthew Campbell for their help and useful discussion.

I would like to thanks my colleges Weiping Lui, Yijiu Jiang and Heng Wang for their help. The department staff deserves the acknowledgement for their technical and administrative assistance. Special thanks to Mr. John Elliott and Dr. Ming Xie for their help.

I would like to thank my parents, my sister and my brothers-in-law, my mother-in-law, my father-in-law, my wife and my daughter for their support. Without their love and support, my study in Concordia University would never be possible.

At last, I would like to express my appreciation of Dow Chemical Company and the Natural Science and Engineering Research Council of Canada for the funding of this project.

Table of Contents

List of Figures

List of Tables

1 Introduction

1.1 Rheology

Rheology is the science that deals with the way materials deform when forces are applied. There are two principal aspects of rheology. One involves the development of quantitative relationships between deformation and force for a material of interest. The second is the development of relationships that show how rheological behavior is influenced by the structure and composition of the material and temperature and pressure. Thermorheology is the study of the interrelationships between time and temperature in the rheological behavior of polymers.

The rheological properties of polymers are extremely important, they govern flow behavior in the processing and fabrication of plastic parts. Rheology is also important for the characterization of polymers. The rheological behavior of polymers can give us information about molecular structure, such as molecular weight, molecular weight distribution, and level of long chain branching. This information is an important part of material characterization and is also important for designing polymers for particular applications.

1.2 Long Chain Branched Metallocene Polyethylenes

The traditional lineup of polyethylenes includes low-density polyethylene (LDPE), linear low-density polyethylene (LLDPE) and high-density polyethylene (HDPE). Metallocene polyethylene (mPE) is a new commercial class that has been developed

since 1980's. Figure 1.1 schematically shows the molecular structures of different polyethylenes.[1]

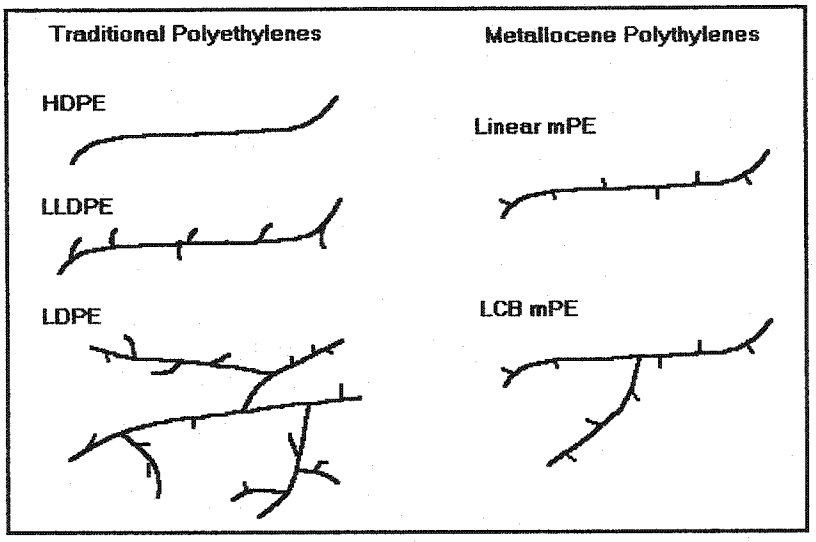

Figure 1.1 Schematic of Molecular Structures of Different Polyethylenes

Compared to traditional polyethylenes, mPEs exhibit good physical properties and better control of molecular structure, such as molecular weight distribution (MWD), chemical composition (CCD), and long chain branching (LCB)[2-4]. Long chain branches (LCB) can improve the processability of mPEs.

Because mPEs have unique and precisely controlled molecular structure, it is possible to study independently the effects of various molecular characteristics on rheological behaviors.[1, 5]

1.3 Linear Viscoelastic Behavior of Polymers [6-8]

1.3.1 Shear Relaxation Modulus and Creep Compliance

Polymers typically exhibit nonlinear viscoelastisity. This means that the response of materials to an imposed deformation depends on: (1) the size of the deformation, (2) the rate of the deformation, and (3) the kinematics of the deformation.

When the deformation is sufficiently mild, that the molecules of the polymer are disturbed from their equilibrium configuration to a negligible extent, linear viscoelasticity can be observed. In this case, the shear stress and the shear rate have a linear relationship, $\sigma = \eta_0 \dot{\gamma}$, The viscosity, η_0, is called the zero shear viscosity.

A linear viscoelastic response is independent of the kinematics of the deformation and the magnitude of past strains. Therefore, the effects of successive deformations can simply be added. The Boltzmann superposition principle (Eq.1.1) describes the stress response of a linear viscoelastic material to an arbitrary strain history.

$$\tau_{ij}(t) = \int_{-\infty} G(t-t')\dot{\gamma}_{ij}dt' \qquad [1.1]$$

The linear relaxation modulus, G(t), is defined as $G(t) = \sigma(t)/\gamma_0$ in a step strain experiment.

For high molecular weight polymers, there is a plateau zone between the glassy zone and the terminal zone on the G(t)-t curve, shown as Fig.1.2 [6]. The modulus in this region is called the plateau modulus, G_N^0.

The existence of the plateau implies that there are strong interactions between molecules. These strong interactions between molecules are called entanglements. The

plateau modulus is used to define the average molecular weight between entanglements, M_e.

$$G_N^0 = \frac{\rho RT}{M_e} \qquad [1.2]$$

In a creep experiment, a sample is suddenly subjected a constant shear stress, σ_0, and the strain, $\gamma(t)$, is recorded as a function of time. The creep compliance, J(t), is defined as $J(t) = \gamma(t)/\sigma_0$.

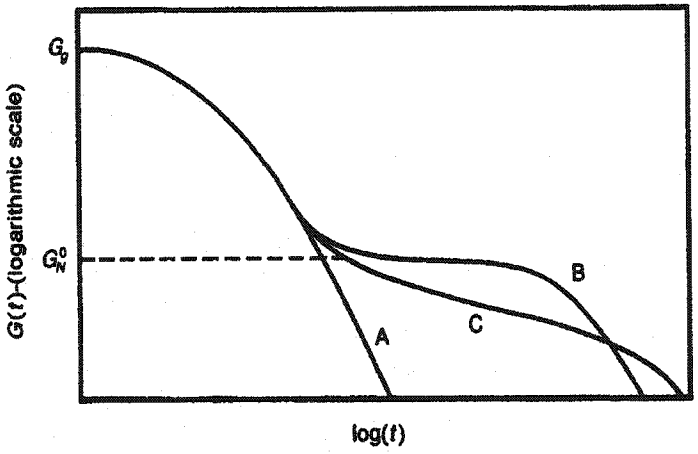

Figure 1.2 Relaxation modulus for three samples of a typical linear polymer. A is monodisperse with $M<M_C$; B is monodisperse with $M \gg M_C$, and C is polydisperse with $M_W \gg M_C$.

By using the Generalized Maxwell (Eq.1.3) and Voigt Models (Eq.1.4), the shear relaxation modulus, G(t), and the creep compliance, J(t), can be described as follows:

$$G(t) = \sum_{i=1}^{N} G_i[\exp(-t/\lambda_i)] \qquad [1.3]$$

$$J(t) = \sum_{i=1}^{N} J_i[1-\exp(-t/\lambda_i)] \qquad [1.4]$$

1.3.2 The Relaxation Spectrum and Retardation Spectrum

In the generalized Maxwell model, Eq.1.3, when the number of elements N increases without limit, the shear relaxation modulus, G(t), can be presented in terms of a continuous function H(λ), Eq.1.5, where H(λ)*d*ln(λ) is the contribution to the relaxation modulus between lnλ and lnλ+dlnλ.

$$G(t) = \int_0^\infty H(\lambda)[\exp(-t/\lambda)]d\ln\lambda \qquad [1.5]$$

The zero shear viscosity, η_0, can be expressed in form of H(λ):

$$\eta_0 = \int_0^\infty H(\lambda)\lambda d\ln\lambda \qquad [1.6]$$

Also, the shear creep compliance, J(t) can be presented in terms of a continuous spectrum which is called the retardation spectrum L(λ):

$$J(t) = J_g + \int_{-\infty}^{\infty} L(\lambda)(1-e^{-t/\lambda})d(\ln\lambda) + t/\eta_0 \qquad [1.7]$$

The relaxation spectrum is a fundamental quality in the linear viscoelastic theory. If this spectrum is known, other viscoelastic properties can be calculated easily. Unfortunately, it is not directly accessible by an experiment, it must be calculated from experiment data for viscoelastic properties, and the calculation is an ill-posed problem. Honerkamp and Weese[9] developed a nonlinear regularization technique (NLRG) for the calculation of a smooth relaxation spectra, the resulting relaxation spectra is reliable in the region approximately corresponding to the experimental time window.

1.3.3 The Complex Modulus and the Complex Viscosity

In a small amplitude oscillatory shear experiment, a shear strain as a sinusoidal function of time is imposed on a sample, $\gamma(t) = \gamma_0 \sin(\omega t)$. If γ_0 is sufficiently small the response is linear, and the resulting stress is a sinusoidal function of the same frequency as the strain, $\sigma(t) = \sigma_0 \sin(\omega t + \delta)$, with a phase angle δ which is called the mechanical loss angle. The stress can be written in the form:

$$\sigma(t)=\gamma_0\left[G'(\omega)\sin(\omega t)+G''(\omega)\cos(\omega t)\right] \qquad [1.8]$$

where G'(ω) is the storage modulus, and G"(ω) is the loss modulus, they are calculated from experimental data with Eq.1.9 and 1.10.

$$G'=\frac{\sigma_0}{\gamma_0}\cos(\delta) \qquad [1.9]$$

$$G''=\frac{\sigma_0}{\gamma_0}\sin(\delta) \qquad [1.10]$$

Using the relaxation spectrum, the storage modulus and loss modulus can be represented as:

$$G'(\omega)=\int_{-\infty}^{\infty}\left[H(\lambda)\omega^2\lambda^2/\left(1+\omega^2\lambda^2\right)\right]d(\ln\lambda) \qquad [1.11]$$

$$G''(\omega)=\int_{-\infty}^{\infty}\left[H(\lambda)\omega\lambda/\left(1+\omega^2\lambda^2\right)\right]d(\ln\lambda) \qquad [1.12]$$

An alternate description of the stress can be carried out using the complex viscosity instead of the complex modulus:

$$\sigma(t)=\dot{\gamma}_0\left[\eta'(\omega)\sin(\omega t)+\eta''(\omega)\cos(\omega t)\right] \qquad [1.13]$$

The complex viscosity is:

$$\eta^*(\omega)=\eta'(\omega)-i\eta''(\omega) \qquad [1.14]$$

and:

$$|\eta^*| = \frac{\sigma_0}{\dot{\gamma}_0} = \sqrt{(\eta')^2 + (\eta'')^2} \qquad [1.15]$$

1.4 Time-Temperature Superposition

Rheological properties are usually highly temperature dependent. It is often found that the viscoelastic properties, for example G' and G", taken at different temperatures can be brought together on a single master curve at temperature T_0 by means of time-temperature superposition. The materials which behave this way are said to be thermorheologically simple.

In this case the temperature dependence of viscosity can be described using a time shift factor, a_T, and a modulus shift factor, b_T, as shown as Eq.1.16 and 1.17.

$$\eta_0(T) = a_T(T) b_T(T) \eta_0(T_0) \qquad [1.16]$$

$$b_T(T) = G_N^0(T) / G_N^0(T_0) \qquad [1.17]$$

The modulus shift factor b_T is often neglected. Therefore, the time shift factor, a_T, can be determined by measuring the temperature dependence of the zero shear viscosity, and the activation energy for flow, E_a, can be calculated by the Arrhenius equation:

$$a_T = \frac{\eta_0(T)}{\eta_0(T_0)} = \exp\left[\frac{E_a}{R}\left(\frac{1}{T} - \frac{1}{T_0}\right)\right] \qquad [1.18]$$

The time-temperature superposition can be accomplished by plotting:

G(t), J(t) versus t/a_T

G'(ω), G"(ω) and $\eta^*(\omega)/a_T$ versus ωa_T

In some cases, the effect of temperature cannot be described by a single time-shift factor. The time-temperature superposition is no longer valid. This kind of materials is called thermorheologically complex, as shown in Fig.1.3[10].

For thermorheologically complex materials, there is no single time shift factor. The apparent activation flow energy, $\hat{E}_a$, is used to describe the temperature sensitivity of the zero shear viscosity:

$$\frac{\eta_0(T)}{\eta_0(T_0)} = \exp\left[\frac{\hat{E}_a}{R}\left(\frac{1}{T} - \frac{1}{T_0}\right)\right] \qquad [1.19]$$

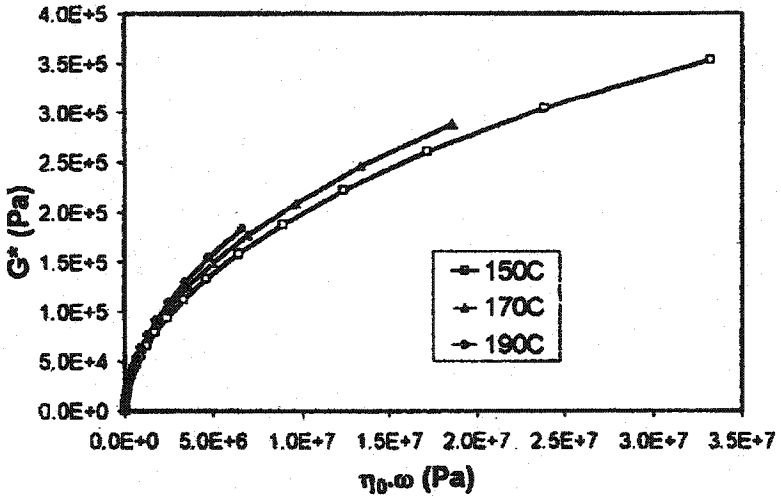

Figure 1.3 An example of thermorheologically complex behavior (HDB4).

2 Overview of Previous Work

2.1 Thermorheology of Polyethylene

2.1.1 Polyolefins

Because of a wide range of structures, commercial polyethylene materials (HDPE, LDPE and LLDPE) are not well suited for studying the relationships between molecular structures and rheological properties. Hydrogenated 1,4-polybutadiene (HPBD) has a similar molecular structure and properties to polyethylene, and can be synthesized by anionic polymerization with a very narrow-molecular-weight distribution and with specific branching structure. It is often used to study the rheological behaviors of polyethylene[11-14].

Fractions of linear polyethylene are also used to study the relationships between the melt viscoelasticity and molecular weight or temperature[15].

Metallocene polyethylenes have controllable, well-defined molecular structures, recently, they have been used to study the thermorheology of polyethylene[1, 10].

2.1.2 Linear Polyethylene

Linear polyethylene is well known as a thermorheological simple material, i.e. time-temperature superposition is valid. This has been confirmed with linear hydrogenated polybutadiene[11-14], fractions of linear polyethylene[15], and commercial linear polyethylenes[6-8].

The activation energy of flow of linear polyethylene is independent of molecular weight and molecular weight distribution[10, 11, 15].

For high-density polyethylene (HDPE) [6-8], the activation energy for flow E_a is about 28 kJ/mole. For linear low-density polyethylene (LLDPE) [10, 16, 17], the E_a is about 34 kJ/mole. For linear hydrogenated polybutadiene[11-14], the E_a is about 31 kJ/mole.

2.1.3 Long Chain Branched Polyethylene

Long chain branches dramatically affect rheological behaviors of polyethylene. Thermorheological complexity is observed in long chain branched polyethylene[6, 10-15]. The apparent activation flow energy $\hat{E}_a$ can increase as high as 57 kJ/mol.[6-8, 10, 18]

Raju, Graessley and Carella et al.[11-14] studied three-arm and four-arm hydrogenated polybutadiene stars. They discovered that the apparent flow activation energy, $\hat{E}_a$, increased linearly with arm length of HPBD stars[11]. For blends of linear and star HPBD, $\hat{E}_a$ increases linearly with the product ϕM_a[12, 13], where ϕ is the volume fraction of branched polymer and M_a is arm molecular weight. The results for three-arm and four-arm HPB stars can be expressed as:

$$\left(\hat{E}_a\right)_B = \left(E_a\right)_L + \wedge\phi\frac{M_a}{M_e} \qquad [2.1]$$

where subscript B represents branched, L represents linear, M_e is the entanglement molecular weight, and $\wedge$ is the activation coefficient which depends on chain microstructure.

Carella et al[14] studied the effect of the chain microstructure on the activation coefficient by using HPBD and hydrogenated polyisoprene (HPI). The HPBD samples correspond in microstructure to copolymers of ethylene and 1-butene with 4%-99% 1-butene content. The results are shown in Figure 2.1.

Wood-Adams and Costeux.[10] studied the thermorheological behavior of metallocene polyethylene. They found that Eq. 2.1 is valid for long chain branched mPE including high-density and low-density polyethylene, as shown in Fig.2.2.

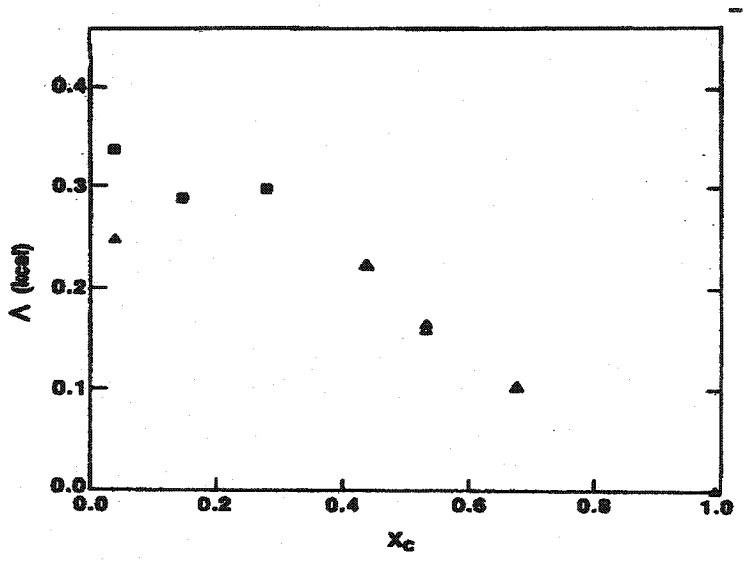

Figure 2.1 Activation coefficients for HPI and HPBD as a function of microstructure. ▲: three-arm HPBD, Δ: three-arm HPI, ■: four-arm HPBD; X_c: the equivalent mole fraction of 1-butene in ethylene copolymer.

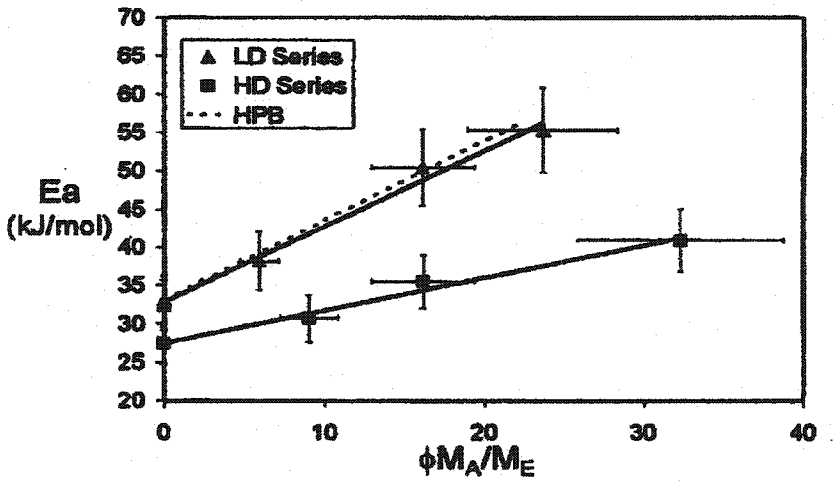

Figure 2.2 Relationship between branching level and flow activation energy for polyethylene

Since long chain branched mPE can be considered as a mixture of linear, T-shaped and H-shaped molecules, the authors defined the fraction of branched molecules ϕ as:[5]

$$\phi = 1 - \frac{\beta + 1}{(2\beta + 1)^2} \qquad [2.2]$$

where β is the average branches per molecule:

$$\beta = \frac{M_N \lambda}{14 \times 10^3} \qquad [2.3]$$

and λ is the number of long chain branches per 10^4 carbon atoms.

The experimental data of mPE also agree with Eq.2.1, in Fig.2.2. Yan et al.[19] also reported that the apparent flow activation energy of mPE is a linear function of the LCB density, (LCB/10^4).

For thermorheologically simple materials, E_a can be determined by Eq.1.17. In the case of thermorheologically complex materials, such as long chain branching polyethylene, the temperature sensitivity factor, a_T, is time-dependent. Wood-Adams and Costeux[10] suggested the concept of an activation energy spectrum, $E_a(\lambda)$, to describe the thermorheologically complexity. In the generalized Maxwell model, we consider that each element has its own time shift factor and activation energy, $E_{a,i}$, as show as Eq.2.4.

$$\lambda_{i,T} = \lambda_{i,0} \exp\left[\frac{E_{a,i}}{R}\left(\frac{1}{T} - \frac{1}{T_0}\right)\right] \qquad [2.4]$$

The zero shear viscosity can be described in terms of the temperature-dependent relaxation spectrum as in Eq.2.5.

$$\eta_0(T) = \sum_{i=1}^{N} G_i \lambda_{i,T} \qquad [2.5]$$

By combining Eq.1.17, 2.4 and 2.5, and making use of a truncated Taylor series expansion of the exponential terms ($e^x \cong 1+x$), we can get:

$$\frac{\hat{E}_a}{R} = \frac{\sum G_i \lambda_{i,0} \frac{E_{a,i}}{R}}{\eta_0(T_0)} \qquad [2.6]$$

where $\hat{E}_a$ is the apparent activation energy. It can alternatively be written in terms of continuous relaxation spectrum H(λ):

$$\frac{\hat{E}_a}{R} \cong \frac{\int_0^\infty \lambda_0 \frac{E_a(\lambda_0)}{R} H(\lambda_0) d(\ln \lambda_0)}{\eta(T_0)} \qquad [2.7]$$

Wood-Adams and Costeux also found that the activation energy spectra $E_a(\lambda)$ calculated from G'(ω) and G"(ω) are different, as shown in Fig 2.3. This can also be seen in Mavridis' research[20] on LDPE. By using an artificial discrete relaxation spectrum, they demonstrated that the flow activation energy spectrum calculated from the shift factor a_T for G'(ω) is closer to the real flow activation energy spectrum than from the shift factor a_T for G"(ω). The results show that the $E_a(\lambda)$ of long chain branched mPE at small relaxation time is closer to the E_a of linear mPE, and increases with the relaxation time. HPBD and HPI three-arm stars have similar behavior[11, 14].

Graessley [21] qualitatively suggested that two mechanisms lead to thermorheological complexity for long chain branched polymers. One is that the entanglement density depends on temperature. Another is that long chain branches rearrange by free-end arm retraction with different energies, depending on the temperature coefficient of chain dimensions in the species. The temperature coefficient for thermorheologically complex

materials, $k = d\ln C_\infty / dT$, should be negative. Both mechanisms lead to thermorheological complexity, and it is not clear how to distinguish them experimentally.

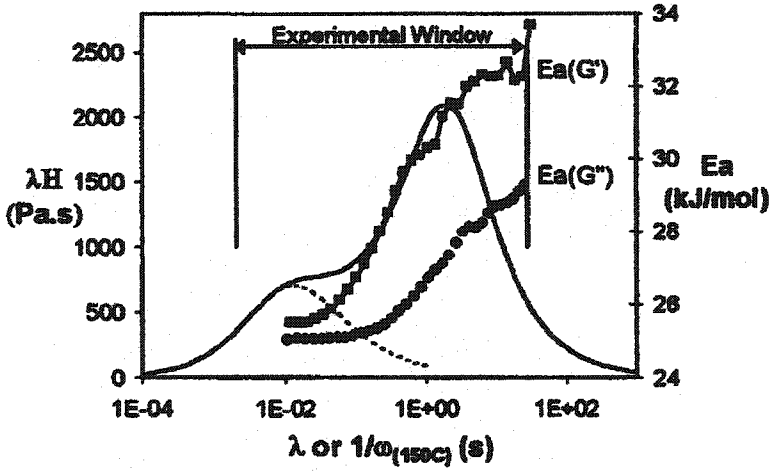

Figure 2.3 Continuous relaxation spectrum and time-dependent activation energy. HDB1 at 150 °C.

Thermorheological complexity of star polymers is not only dependent on long chain branching structure, but also on chemical structure. Some three-arm star polybutadienes and polyisoprenes have the same activation energy for flow as their linear polymers, and are thermorheologically simple, that is because the temperature coefficients of these materials are positive.[14, 22-23]

2.1.4 Short Chain Branching

Carella et al[13] studied the effect of short chain branching level on thermorheological behavior of linear HPBD. The HPBD samples corresponded to copolymers of ethylene and 1-butene with mole fraction of 1-butene ranging from 0.04 to 0.99. They found that the time-temperature superposition principle was obeyed in all cases. The effect of short

chain branching could be explained by the change in glass transition temperature (T_g). The variation of the shift factor with temperature followed the WLF equation[7], even at very high temperatures relative to T_g. Although none of the samples followed the Arrhenius behavior, the deviation from Arrhenius behavior decreased as the degree of short chain branching decreased.

In long chain branched polymers, the short chain branching level (in other words, chain structure) only affects the activation coefficient, $\wedge$ in Eq.2.1, shown in Figure 2.1.

2.1.5 Problem Statement

For thermorheologically simple materials, if we combine the Arrhenius equation, the activation energy of flow and the viscoelastic properties at a reference temperature, the viscoelastic properties at different temperatures can easily be calculated.

However for thermorheologically complex materials, time-temperature superposition is not valid. The time shift factor a_T is not only dependent on the relaxation time, but also on the viscoelastic properties[10, 20]. Wood-Adams and Costeux[10] suggested a concept of the activation energy spectrum. The problem now is how to find the real activation energy spectrum, and then to use this spectrum to predict the viscoelastic properties at different temperatures just as in the case of the thermorheologically simple materials.

The relaxation spectrum is a characteristic spectrum of materials, the viscoelastic properties can directly be calculated from this spectrum, for example Eq.1.5, 1.10 and 1.11. We assume that the relaxation spectrum $H(\lambda)$ at different temperature T and T_0 can be superimposed by a time shift factor $a_T(\lambda)$, $a_T(\lambda)=\lambda/\lambda_0$.

$$H(\lambda,T)=H\left[\frac{\lambda}{a_T(\lambda)},T_0\right] \qquad [2.8]$$

and the shift factor can be calculated from the activation energy spectrum:

$$a_T(\lambda) = \exp\left[\frac{E_a(\lambda_0)}{R}\left(\frac{1}{T}-\frac{1}{T_0}\right)\right] \qquad [2.9]$$

Now, if we know the relaxation spectrum and the activation energy spectrum at temperature T_0, $H(\lambda_0)$ and $E_a(\lambda_0)$, we can reach the goal of prediction for viscoelastic properties at different temperatures.

In Eq.1.5, the shear relaxation modulus G(t,T) at temperature T becomes:

$$\begin{aligned} G(t,T) &= \int_0^\infty H(\lambda,T)\exp(-t/\lambda)d\ln\lambda \\ &= \int_0^\infty H\left(\frac{\lambda}{a_T},T_0\right)\exp\left(-\frac{t/a_T}{\lambda/a_T}\right)d\left[\ln\left(\frac{\lambda}{a_T}\right)+\ln a_T\right] \\ &= \int_0^\infty H(\lambda_0,T_0)\exp\left(-\frac{t/a_T}{\lambda_0}\right)d\ln(\lambda_0) \\ &+ \int_0^\infty H(\lambda_0,T_0)\exp\left(-\frac{t/a_T}{\lambda_0}\right)d\ln a_T \end{aligned} \qquad [2.10]$$

In the case of thermorheologically simple material, the a_T is a constant, and $d(\ln a_T)=0$, then becomes Eqs.2.11

$$G(t,T) = G\left(\frac{t}{a_T},T_0\right) \qquad [2.11]$$

So the time shift factor for the relaxation spectrum is the same as the time shift factor for the other rheological properties

In the case of thermorheologically complex materials, the a_T is a function of the relaxation time λ, $a_T(\lambda)$, then $d(\ln a_T)\neq 0$. From Eq.2.10, we can see that the relaxation modulus G(t,T) at different temperatures can not be superimposed by a simple time-shift factor. Similarly, the storage modulus $G'(\omega,T)$ and the loss modulus $G''(\omega,T)$, Eq.1.3 and 1.4 can be expressed as:

$$G'(\omega,T)=\int_0^\infty\left[H(\lambda_0,T_0)\frac{(a_T\omega)^2(\lambda_0)^2}{1+(a_T\omega)^2(\lambda_0)^2}\right]d\ln(\lambda_0)$$
$$+\int_0^\infty\left[H(\lambda_0,T_0)+\frac{(a_T\omega)^2(\lambda_0)^2}{1+(a_T\omega)^2(\lambda_0)^2}\right]d\ln a_T \qquad [2.12]$$

$$G''(\omega,T)=\int_0^\infty\left[H\left(\frac{\lambda}{a_T},T_0\right)\frac{(a_T\omega)(\lambda/a_T)}{1+(a_T\omega)^2(\lambda/a_T)^2}\right]d\ln\left(\frac{\lambda}{a_T}\right)$$
$$+\int_0^\infty\left[H\left(\frac{\lambda}{a_T},T_0\right)\frac{(a_T\omega)(\lambda/a_T)}{1+(a_T\omega)^2(\lambda/a_T)^2}\right]d\ln a_T \qquad [2.13]$$

The $a_T(\lambda)$ has different effects on the storage modulus G'(ω,T) and the loss modulus G"(ω,T). This can explain that the flow activation energy spectrums, $E_a(\lambda)$, calculated from the shift factor a_T for G'(ω) and G"(ω) are different.[10]

2.2 Theory for Stress Relaxation in Polymer Melts

2.2.1 Reptation Theory for Linear Polymers

The reptation theory (the tube model) is a well-known molecular theory to describe the molecular motion in entangled polymer system[24, 25]. In an entangled polymer system, a polymer molecule is undergoing Brownian motion in a fixed network, as in Figure 2.5 (a)[25]. The dots in the figure represent the network (one dot corresponds to an entanglement segment), and the polymer cannot cut through these. Since the polymer is not allowed to cut through the network points, we can assume that the polymer effectively undergoes motion in a tube as in Figure 2.5 (b) and (c). The viscoelastic properties of polymer are dependent on how the polymer molecule escapes from the tube.

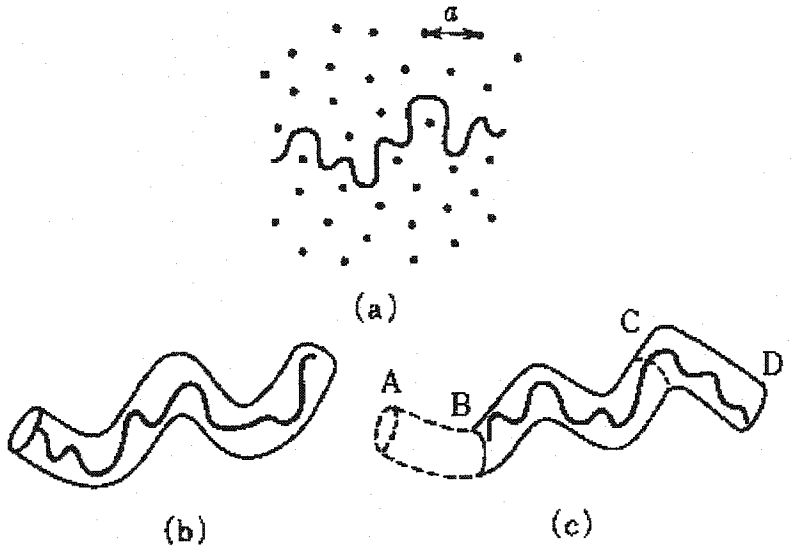

Figure 2.4 (a) A polymer moving in a fixed network; (b) the tube model; (c) the situation depicted in (b) after some time has passed.

There are the two main improvements to the reptation theory. The first is contour-length fluctuations (CLF). Since the tube diameter is much wider that the diameter of the molecular chain, and the chain wanders about within the tube, the chain can "wrinkle up" within the tube. The tube itself fluctuates in length when the chain wrinkles and unwrinkles. This is due to Brownian motion of the polymer molecule, and stress is thereby relaxed.

The second is constraint release (CR), because the tube is made from other chains which are moving around, the tube must also move.

Likhtman A. E. and McLeich[26] reported a theoretical model which includes CLF and CR. This model is:

$$G(t)=G_e\left(\frac{4}{5}\mu(t)R(t,c_v)+\frac{1}{5Z}\sum_{p=1}^{Z}\exp\left(-\frac{p^2t}{\tau_R}\right)+\frac{1}{Z}\sum_{p=Z}^{N}\exp\left(-\frac{2p^2t}{\tau_R}\right)\right) \quad [2.14]$$

where μ(t) is the tube-segment occupation function, it includes reptation and CLF, R(t) is constraint release, the second is longitudinal modes relaxation and the third is fast Rouse motion inside the tube.

2.2.2 Arm Retraction Theory for Star Polymers

The star structure is the simplest LCB structure with a single branch point. In star polymer melts, just as for linear chains, the entanglement network prevents motion of the chain except along the confining tube, but the branch point prevents reptation. Stress in star polymers relaxes by arm retraction instead of reptation, as Figure 2.5. Star arms explore new configurations by retreating along their tubes and poking out again in a new direction. This motion is called arm retraction, and it is the same motion as contour-length fluctuation.

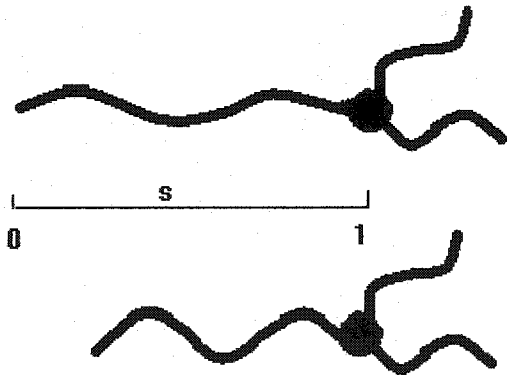

Figure 2.5 Arm retraction of star polymer

Pearson and Helfand [27] reported a theory of arm retraction. To relax all the stress held by the strained conformations of the arm, the free end of the arm must retract all the way

back to the branch point of the star. The free end arm retracts back along the tube with a barrier potential U(s):

$$U(s) = \frac{15Ns^2}{8N_e} \qquad [2.15]$$

where s is a fractional distance to arm length, it equals 0~1 from the free end to branch point; shown in Figure 2.5, N is the arm length, and N_e is the entanglement segment length. The relaxation time $\tau(s)$ is:

$$\tau(s) = \tau_R \exp[U(s)] \qquad [2.16]$$

τ_R is the Rouse time $\tau_R = \tau_e(N/N_e)^2$, where τ_e is the Rouse time of an entanglement segment.

Ball and McLeish [28] considered dynamic dilution. At the time $\tau(s)$, the relaxed chain segments can be thought as completely mobile, and the effective entangled network is diluted. The effective entangled network is only built with unrelaxed chain segments. The concentration of entangling chains is reduced by a factor $\phi = 1-s$ (ϕ is the volume fraction of unrelaxed chains), the entanglement length in such a diluted network is given by:

$$N(\phi) = \frac{N_e}{\phi}, \quad N(s) = \frac{N_e}{1-s} \qquad [2.17]$$

The potential U(s) becomes:

$$U(s) = \frac{15N}{8N_e}\left(s^2 - \frac{2}{3}s^3\right) \qquad [2.18]$$

The relaxation modulus function, G(t), can be expressed in terms of $\tau(s)$, as:

$$G(t) = 2G_0 \int_0^1 (1-s)\exp[-t/\tau(s)]ds \qquad [2.19]$$

The results agreed well with experimental data of HPBD star polymers especially in the low frequency range.

Milner and McLeish [29, 30] improved Ball and McLeish's model. In their model, arm retraction for small s such as $U(s) < k_BT$ is not active. The motion of the free end for such small s and hence short times is that of the end of a long Rouse chain. The relaxation time at early times, τ_{ealy}, is given by:[24]

$$\tau_{early} = \frac{225\pi^3}{256}\left(\frac{N}{N_e}\right)^2 \tau_R s^4 \qquad [2.20]$$

At longer times, the arm retraction is active. The relaxation time becomes:

$$\tau_{late}(s) \approx \frac{15\pi^2}{8}\left(\frac{N}{N_e}\right)^3 \tau_e \frac{\exp[U(s)]}{\left[U'(s)^2 + 2s^2\left|U''(1)\right|/\pi\right]^{1/2}}\left(\frac{\pi}{2U''(0)}\right)^{1/2} \qquad [2.21]$$

To construct a second crossover from τ_{ealy} to τ_{late}, $\tau(s)$ is given by:

$$\tau(s) = \frac{\tau_{early}(s)\exp[U(s)]}{1+\exp[U(s)]\tau_{early}(s)/\tau_{late}(s)} = p(s)\exp[U(s)] \qquad [2.22]$$

and :

$$p(s) = \frac{\tau_{early}(s)\tau_{late}(s)}{\tau_{late}(s)+\tau_{early}(s)\exp[U(s)]} \qquad [2.23]$$

This model improves the agreement in the high frequency range compared to Ball & McLeish's model.

Milner et al.[31] reported a model for star-linear polymer blends. Because the arm retraction is nearly the same as contour-length fluctuation, linear chains can be seen as a "two-arm" star chain before the reptation time τ_d of the linear chains, and are considered to be undergoing arm retraction the same as star arms. The effective potential becomes:

$$U(s)=\frac{15}{8}n_a\left[s^2-\frac{2}{3}\left(\phi_s+\phi_l\sqrt{\frac{2n_a}{n_l}}\right)s^3\right] \qquad [2.24]$$

where n_a is the length of star arm, n_l is the length of linear chain, ϕ_s is star volume fraction, ϕ_l is linear volume fraction.

At the reptation time scale τ_d of linear chain, dynamic dilution will fail because all of the linear chains finish relaxation at the same time, the tubes of entangled chains (only star arm chain) undergo constraint-release Rouse motion, and stress is relaxed as the tubes are able to expand their diameters. The constraint-release Rouse motion ends at time τ_C. τ_d and τ_C are found by solving Eq.2.25 and 2.26. In this time range, the effective entangled volume fraction, $\Phi(t)$, is given Eq.2.27. Then the relaxation modulus G(t) is expressed as Eq.2.28.

$$\tau(s_d)=\frac{15}{4}n_l{}^3\left(1-s_d\sqrt{2n_a/n_l}\right)^2\tau_e \qquad [2.25]$$

$$\tau_C=\tau_d\left(\frac{\Phi(\tau_d)}{\phi_s(1-s_d)}\right)^2 \qquad [2.26]$$

$$\Phi(t)=\Phi(\tau_d)\left(\frac{\tau_d}{t}\right)^{1/2} \qquad [2.27]$$

$$G(t)=G_0\phi_s(1-s_d)\Phi(t) \qquad [2.28]$$

When $t > \tau_C$, dynamic dilution recovers, and only star arms have entangled segments, the effective potential U(s) and relaxation time $\tau(s)$ are given by Eq.2.29 and 2.30:

$$U(s)=\frac{15}{8}n_a\phi_s\left[s^2-\frac{2}{3}s^3\right] \qquad [2.29]$$

$$\tau(s)=\frac{\tau_C p(s)}{p(s_d)}\exp[U(s)-U(s_d)] \qquad [2.30]$$

Based on the arm retraction theory,[26-29] Levine and Milner [32] developed a model for thermorheological complexity of star polymers, and verified it with rheological data of star-branched hydrogenated polybutadiene. The idea is that the effective entanglement length, N_e, is temperature dependent, shown as Eq.2.31:

$$\frac{N_e(T)}{N_e(T_0)} = \exp\left[-\Delta\left(\frac{1}{T}-\frac{1}{T_0}\right)\right] \qquad [2.31]$$

Where Δ is an energy, they found Δ=380 K for HPBD. Then they apply this temperature dependent effective entanglement length to the Ball & Mcleish model (Eq.2.15, 2.18 and 2.19) the results agree with experiment data of HPBD at 160 °C and 190 °C, especially in the low frequency range.

2.2.3 Comment

Wood-Adams and Costeux[10] suggested that there is a characteristic activation energy spectrum for thermorheologically complex materials. Thermorheological complexity of star polymers can be explained by Levine & Milner's model. So the activation energy spectrum should be calculated by using arm retraction theory.

Metallocene polyethylene can be simply considered as a blend of linear and long chain branched polyethylene,[5] therefore we will use Milner & McLeish model and Levine & Milner model to qualitatively study the effect of LCB level on the activation energy spectrum.

Also, contour-length fluctuations(CLF) of linear chain is the same as arm retraction of star polymers. If we can measure the CLF of a linear chain, then we should observe thermorheological complexity with a linear polymer in the time range affected by the

CLF. Part of this work will be to use a very high molecular weight linear hydrogenated polybutadiene to test this theory.

3 Objectives of This Work

The primary objective of this project is to evaluate the activation energy spectrum proposed by Wood-Adams and Costeux [10] and to test their approximation technique for inferring the activation energy spectrum.

The secondary objective is to develop a technique for de-convoluting the various temperature sensitivities in long chain branched metallocene polyethylene in terms of relevant structural elements.

The third is to use a very high molecular weight linear HPBD sample to test the arm retraction theory, by measuring the effect of CLF.

The final objective is to use arm retraction theory to analysis the effective factors on the activation energy spectrum.

4 Experiments

4.1 Experiment Materials

The long chain branched metallocene polyethylenes (HDB set) and the linear hydrogenated 1,4-polybutadiene (HPBD) sample are listed in Table 4-1.

All samples for rheological testing were prepared by compression molding on a Caver Laboratory Press (Model 2114). The size of the sample is 1.2 mm thick with a 25mm diameter. The HDB samples were molded at 140 °C and HPBD samples at 150 °C. In all cases the molds were heated in the press at the molding temperature for 5 minutes to allow the material to melt. A pressure less than 10 000 psi was applied and then released to minimize air bubble formation, this procedure was repeated 5 times. Finally the pressure was increased to 15 000 psi and held for 5 minutes, after which the mold was cooled down to room temperature, while the pressure was maintained.

Table 4.1 mPE and HPBD Samples

Sample	HDB1	HDB5	HDB6	HDB7	HPBD
M_W, g/mol	77,000	79,000	68,000	70,000	334,000
M_W/M_N *	2.13	2.42	2.69	3.07	1.19
$M_{W,S}$ **	63,639	45,993	29,994	21,962	167,000
β***	0.067	0.21	0.34	0.54	0

*: $M_W/M_N = 2(\beta+1)$. [5]

**: $M_{W,S}$ is the weight-average segment molecular weight. [5] It also is the weight-average arm molecular weight for branched molecules, M_a.

***: β is the average number of branches per molecule

4.2 Oscillatory Shear Test

Oscillatory shear tests of the HDB series were performed using a Rheometric Scientific ARES strain-controlled rheometer (ARES). Osillatory shear tests of the HPBD sample were performed using a Rheometric Dynamic stress-controlled rheometer 5000 (SR-5000).

The main test parameters of oscillatory shear measurements are temperature, strain or stress, frequency and points per decade.

The principles of setting test conditions are:

a. The deformation of the samples should be in the liner viscoelasticity (LVE) range throughout the test.
b. The samples should be thermally stable while they are being tested.
c. The torques should be in the test range of the ARES or SR-5000.

Dynamic strain or stress sweep tests are used to determine the linear viscoelastic range. Figure 4.1 is a strain sweep test of HDB5 at frequency 5 rad/s and temperature 170 °C, the complex viscosity decreases with increasing of strain when strain is more than 10 %, and it is a constant in the region of the strain smaller than 10%, so the LVE region at this frequency is the strain < 10 %.

Figure 4.2 is a stress sweep test of the HPBD at frequency 1 rad/s and temperature 190 °C. The HPBD has a very high viscosity because of its high molecular weight, therefore at low stresses the response strain is too small relative to the noise level of the instrument. In the stress range from 800 to 3000 Pa, the complex viscosity is a constant. So the test stress should be in this range at this frequency.

According to the test results of strain or stress sweep at different frequencies, we can divide the frequency sweep ranges and the amplitudes of strain or stress.

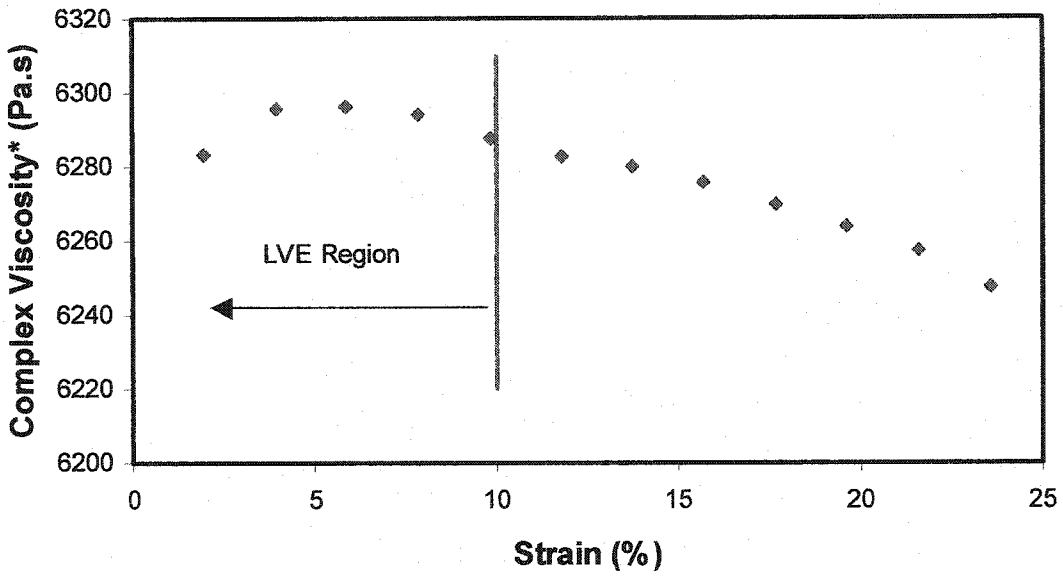

Figure 4.1 Strain Sweep of HDB5 at Frequency 5 rad/s and Temperature 170 °C

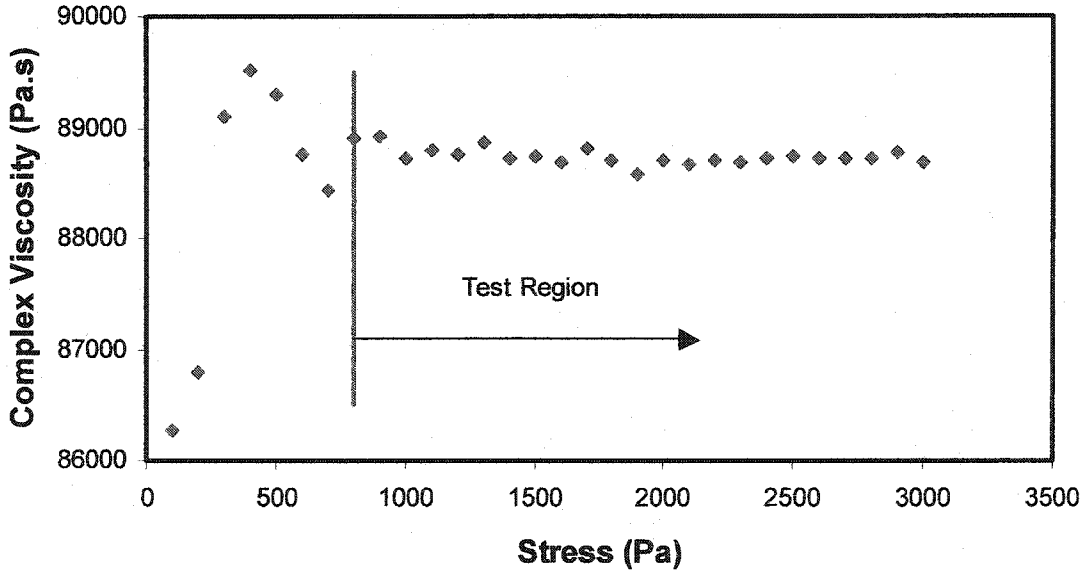

Figure 4.2 Stress Sweep of HPBD at Frequency 1 rad/s and Temperature 190 °C

Dynamic time sweeps at testing temperatures are used to test the thermal stability of the sample. Figure 4.3 is a time sweep test of HDB5 at temperature 190 °C and frequency 1 rad/s. The complex viscosity decreases after 6000s, this means the sample degraded after 6000s at temperature 190 °C. The dynamic time sweep test results of HDB5, 6 and 7 show that their thermally stable time regions in the temperature range 150-190 °C are less than 2 hours, so the whole test time of these sample should be under two hours. Figure 4.4 is a time sweep test of the HPBD at temperature 190 °C and frequency 1 rad/s. The results show that the thermally stable time region of the HPBD is about 10 hours.

The final test conditions of HDB samples and HPBD sample are shown in Table 4.2 and 4.3.

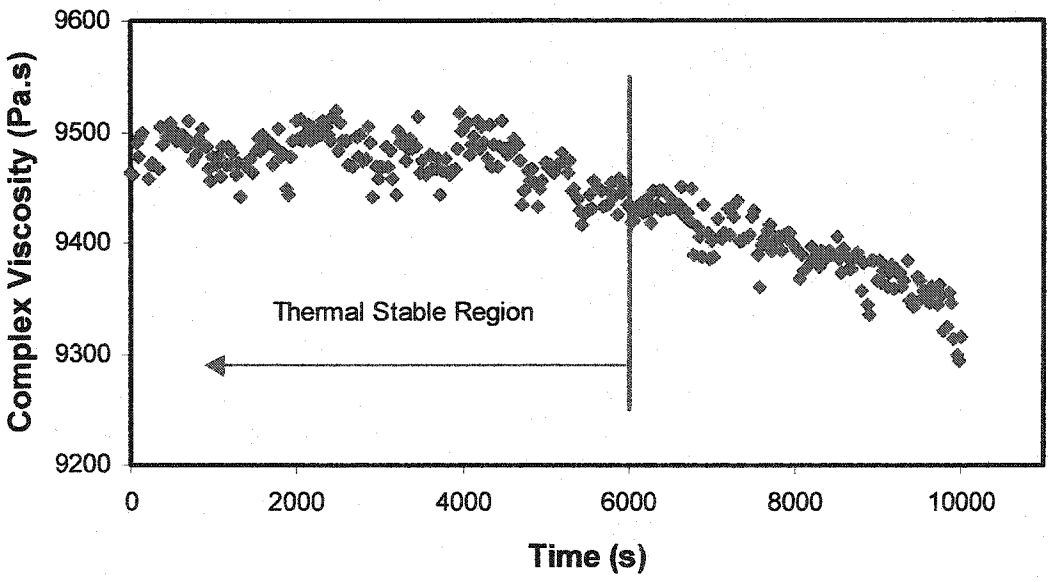

Figure 4.3 Time Sweep Test of the HDB5 at Temperature 190 °C and Frequency 1 rad/s

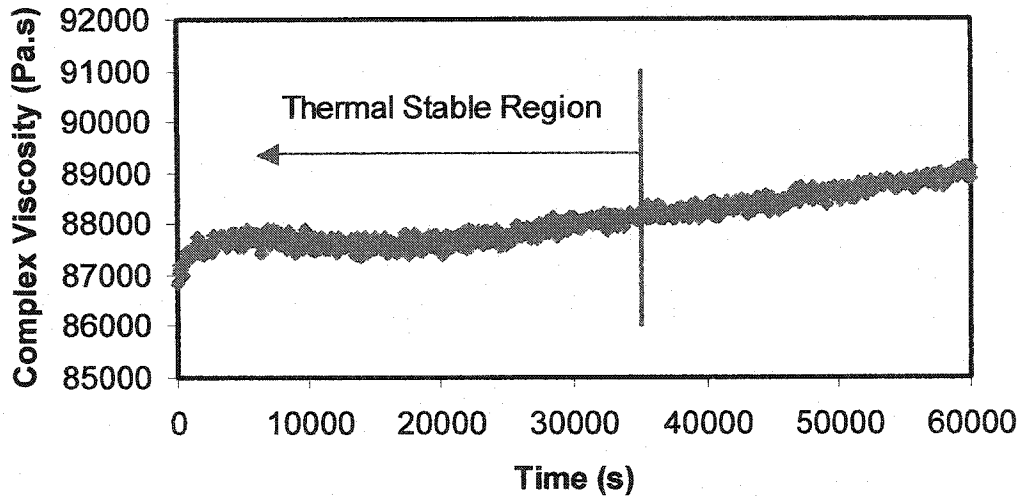

Figure 4.4 The time sweep test of the HPDB at 190 °C and frequency 1 rad/s

Each test was repeated with 5 samples at every temperature for the HDB series. Because of the limitation of the HPBD material, the tests for the HPBD were only repeated with two samples.

Table 4.2 Oscillatory Shear Test Conditions for the HDB Series

Sample	HDB5, HDB6, HDB7							
Frequency, rad/s	500-5		5-0.5	0.5-0.005				
Temperature, °C	150, 160, 170	180, 190	150~190	150	160	170	180	190
Strain, %	3	5	10	20	25	30	35	40
Points per Decade	9		9	5				
Gap, mm	1							

Table 4.3 Oscillatory Shear Test Conditions of HPBD

Sample	HPBD						
Frequency, rad/s	50~0.5		0.5~0.05		0.05~0.005		
Temperature, °C	150, 170	190	150	170, 190	150	170	190
Stress, Pa	2000	4000	2000	1000	500	400	300
Points per Decade	10		5		5		
Gap, mm	1.1~1.2						

4.3 Creep and Recovery Test

The branch arms of the HDB series materials have long relaxation times, and the oscillatory shear test might not reach the terminal zone and directly get the zero shear viscosity. The same is observed with the HPBD sample, because it has a large molecular weight, and the reptation time of this material is much longer than the frequency range accessible with the SR-5000.

Kraft et al.[33, 34] reported a technique of creep and recovery to obtain the creep compliance up to very long times while keeping the maximum strain in the LVE region. According to the Boltzmann superposition principle, the shear strain in a creep experiment can be described as:

$$\gamma(t) = \int_{-\infty}^{t} J(t-t')d\sigma(t') \qquad [4.1]$$

In a creep and recovery experiment, the creep under a stress σ_0 is ended at t_1 and recovery is started. The recovery period can be seen a second creep under a negative stress of $-\sigma_0$. From Eq.4.1, the resulting shear strain, $\gamma(t)$, is:

$$\gamma(t) = J(t)\sigma_0 + J(t-t_1)(-\sigma_0) \qquad [4.2]$$

then:

$$J(t) = \gamma(t)/\sigma_0 + J(t-t_1) \qquad [4.3]$$

Using Eq.4.3, we can extend J(t) time range from t_1 to 2 t_1, and then to 3 t_1 untill the steady state is reached.

In the creep measurement, if the deformation is in the LVE range, the creep compliance is independent of stress. Figure 4.5 shows the J(t) of HDB5 at 190 °C at different stresses. This test is used to determine the LVE region. The optimal stress for creep should be small enough within the LVE region and large enough to provide satisfactory resolution. The recovery time should be large enough to reach the steady state.

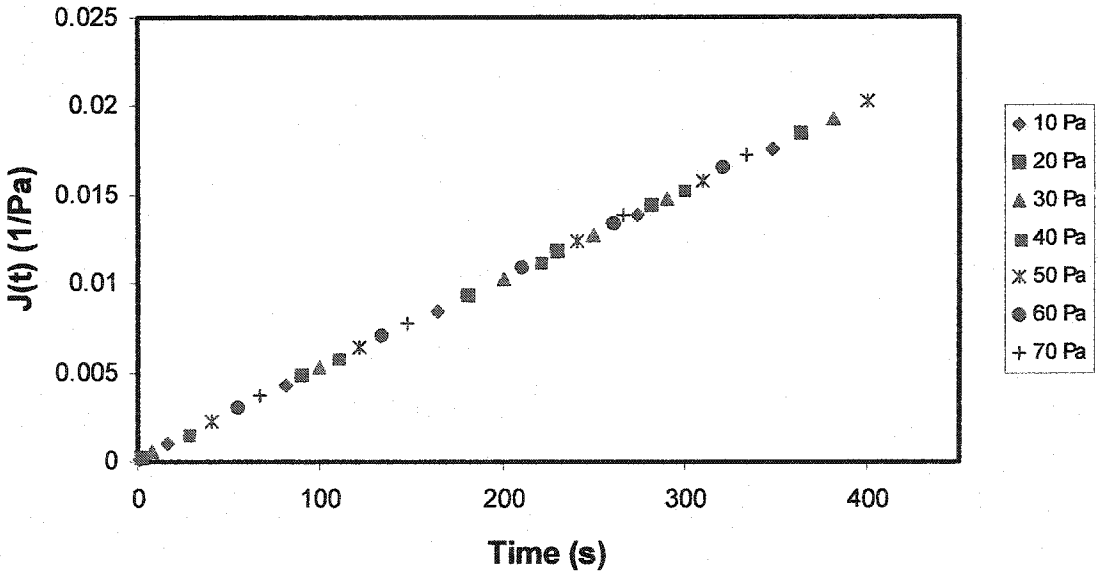

Figure 4.5 Creep Compliance of HDB5 at 190 °C Tested at Different Stress

Table 4.4 is the test conditions for HDB5 and HPBD samples.

Table 4.4 Creep and Recovery Test Conditions of HDB5 and HPBD

Temperature, °C		150	170	190
HDB5	Stress, Pa	20	15	10
	Creep Time, s	1000		
HPBD	Stress, Pa	500	400	300
	Creep Time, s	900		

4.4 Optimization of Experiment Data

In the oscillatory experiment, sometimes air bubbles will be introduced in the sample while loading the sample, and you cannot see them. This can significantly affect the experimental data especially at lower frequencies. Also the HDB series samples have poor thermal stability, and experimental data will change dramatically at lower frequencies as thermal degradation happens. To control the quality of experimental data, the Shewhart control technique[35] is used.

There are k samples, Y_i is the observation of *i*th sample. The average moving range is:

$$AMR = \frac{1}{k-1}\sum_{i=1}^{k}\left|Y_i - Y_{i-1}\right| \qquad [4.4]$$

An estimated standard deviation is

$$s_{AMR} = AMR/1.128 \qquad [4.5]$$

The upper (UCL) and lower (LCL) control limits are

$$UCL = \overline{Y} + 3s_{AMR}, LCL = \overline{Y} - 3s_{AMR} \qquad [4.6]$$

where $\overline{Y}$ is the average value.

Only Y_i in the range UCL > Y_i > LCL are collected.

5 Experimental Results and Discussion

5.1 Experimental Data

All experimental data and calculated relaxation spectra of the HDB series and the HPBD samples are tabulated in Appendix I.

The experimental data of the HDB series is an average value of more than four samples. The coefficients of variation, defined as the value of standard deviation divided by the average value, mostly are smaller than 3%. For few points at lower frequencies, the coefficients of variation are between 3% and 5%.

Because the samples of the HPBD are limited, each set of experimental data of the HPBD is an average of only two samples. The coefficients of variation are smaller than 5% except for a few points at lower frequencies.

Figure 5.1 and 5.2 show the storage modulus, G'(ω), and loss modulus, G"(ω), of the HDB series at 170 °C. Figure 5.3 and 5.4 show the storage modulus and loss modulus of the HPBD at 150 °C, 170 °C and 190°C. Figure 5.5 shows the strain in a creep and recovery test of the HPBD at 170 °C. Figure 5.6 shows the compliance, J(t), of HPBD at 170 °C. In creep and recovery experiment, the compliance at long times equals:

$$J(t) = J_S^0 + t/\eta_0 \qquad [5.1]$$

where J_S^0 is the steady state compliance. This equation is used to determine the zero shear viscosity. It is shown in Figure 5.6.

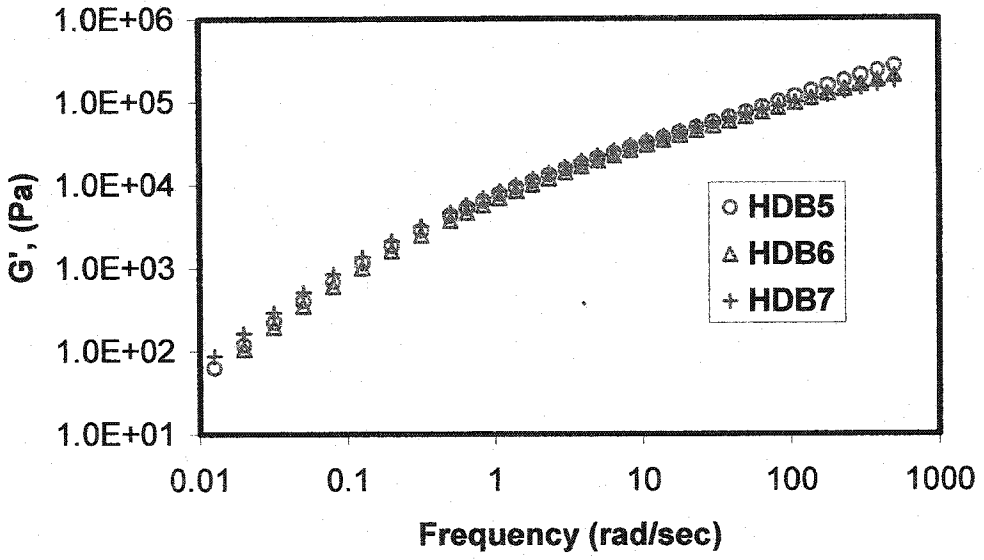

Figure 5.1 The storage modulus of the HDB5, 6 and 7 at 170 °C

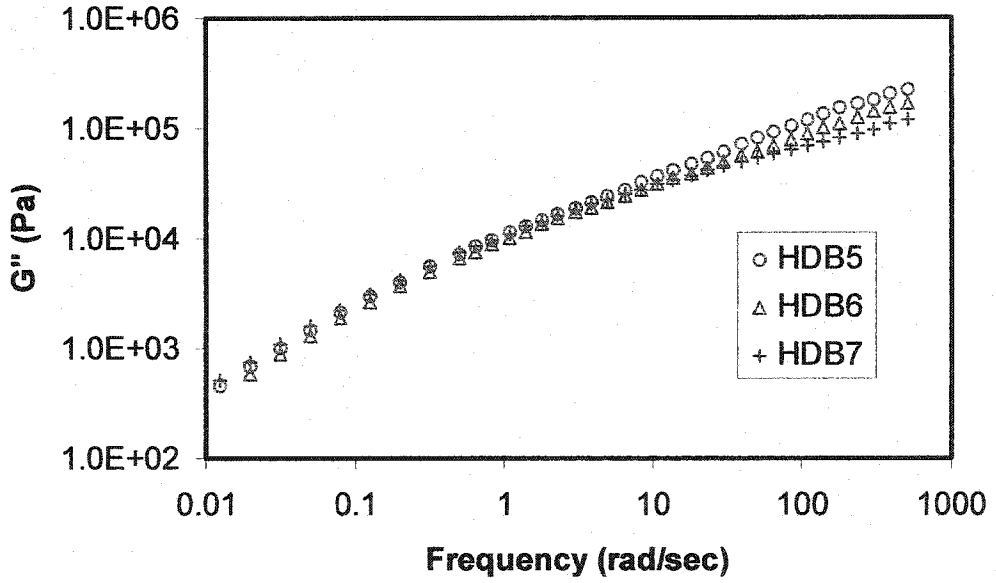

Figure 5.2 The loss modulus of the HDB5, 6 and 7 at 170 °C

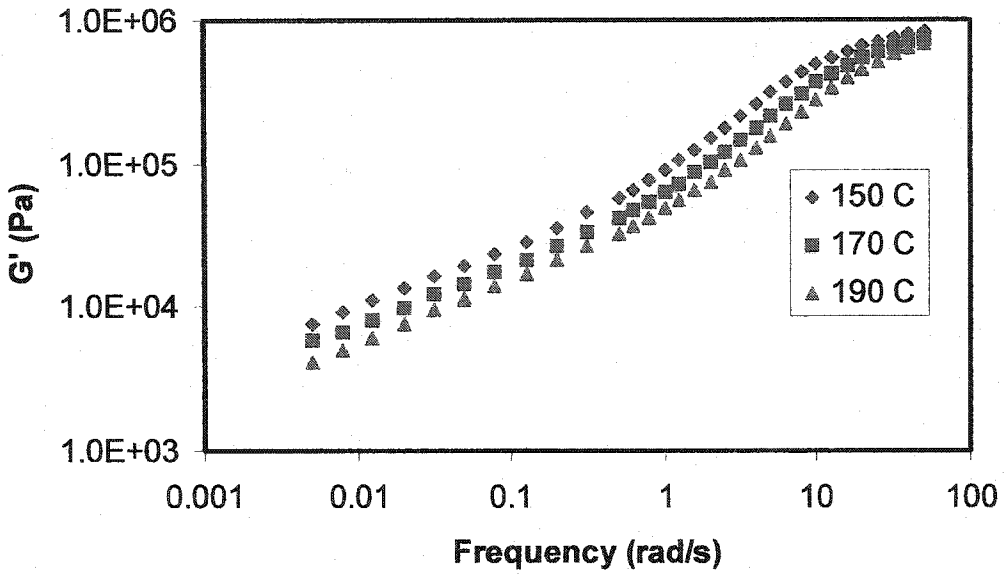

Figure 5.3 The storage modulus of the HPBD at 150 °C, 170 °C and 190 °C

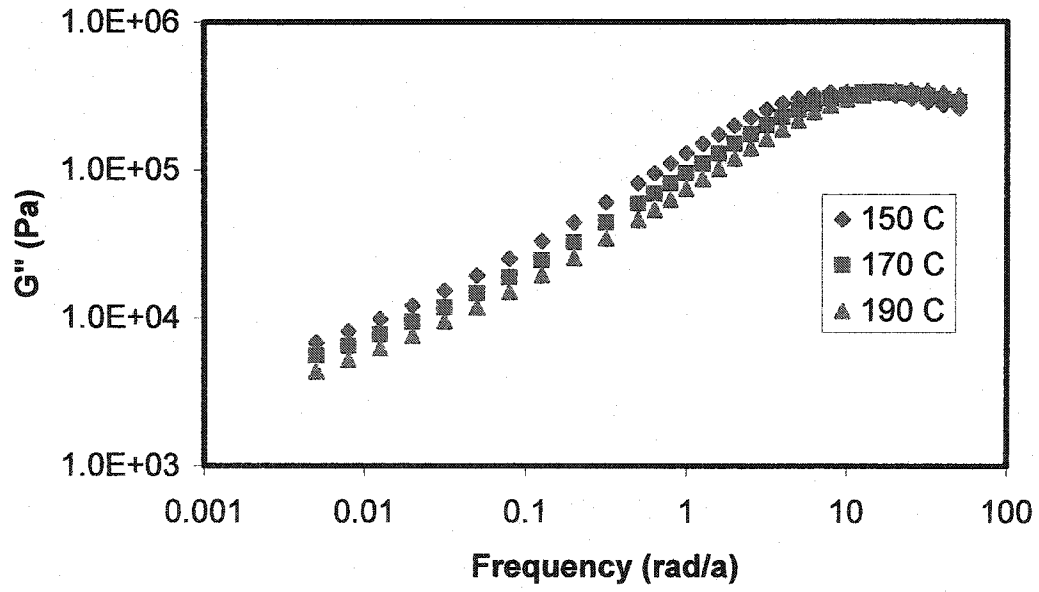

Figure 5.4 The loss modulus of the HPBD at 150 °C, 170 °C and 190 °C

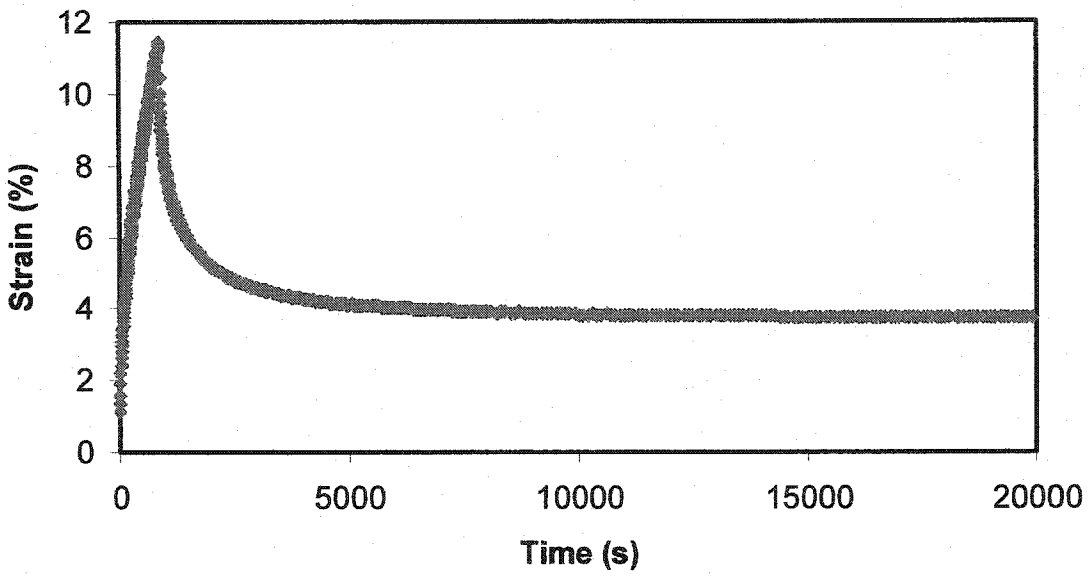

Figure 5.5 The creep and recovery test results of HPBD at 170 °C

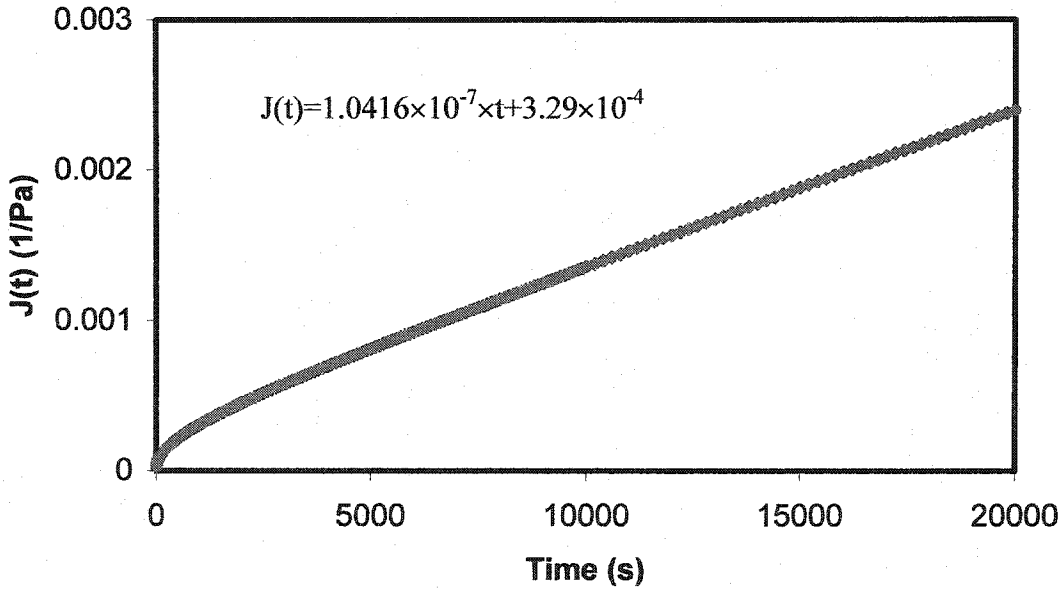

Figure 5.6 The compliance of the HPBD at 170 °C

5.2 Relaxation Spectrum

The relaxation spectrum, H(λ), was calculated from experimental G'(ω) and G"(ω) data, by using a nonlinear regularization technique (NLRG)[9]. Figure 5.7 shows the H(λ) of HDB5 at 150 °C, 170 °C and 190 °C. The area under the curve corresponds to the zero shear viscosity, which decreases with increasing temperature. The peak position also moves to shorter times when temperature increases.

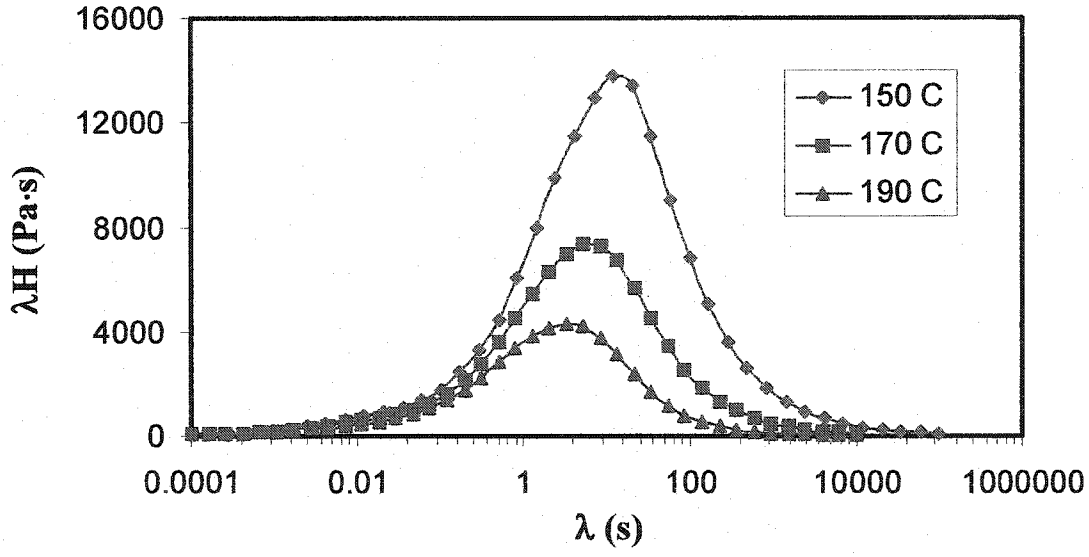

Figure 5.7 The relaxation spectrum of the HDB5 at 150, 170 and 190°C

Figure 5.8 shows the G'(ω) and G"(ω) of HDB5 at 170 °C, the points are experimental data, the lines were calculated from H(λ), they agree very well. Figure 5.9 is the difference between experimental complex viscosity data and those calculated from H(λ) for HDB5 at 170 °C. For most points the difference is less than ±1 %. The same results were observed for every material at each temperature. Therefore the H(λ) from

NLRG can be used to accurately calculate the rheological properties in the experimental window.

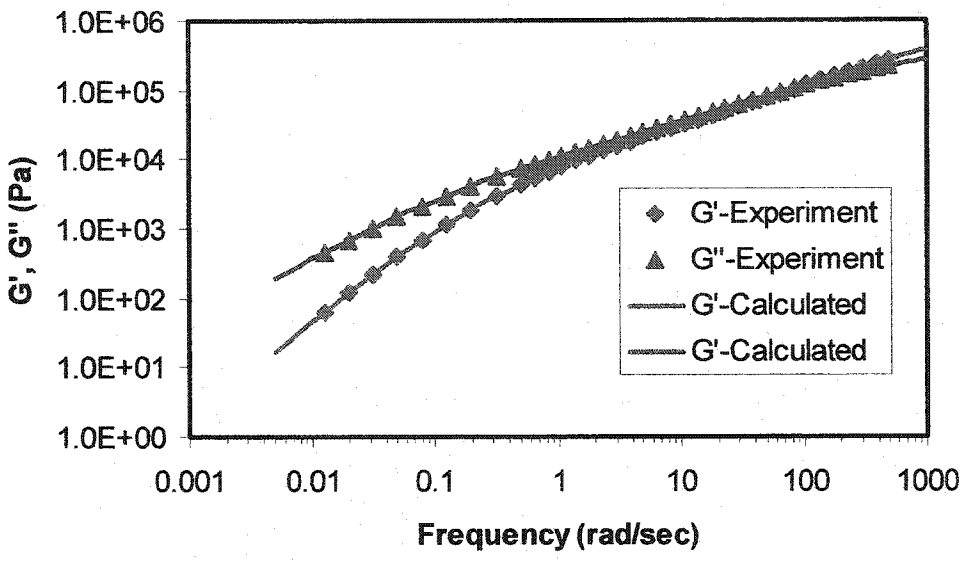

Figure 5.8 The experimental and calculated storage and loss modulus, HDB5 at 170 °C

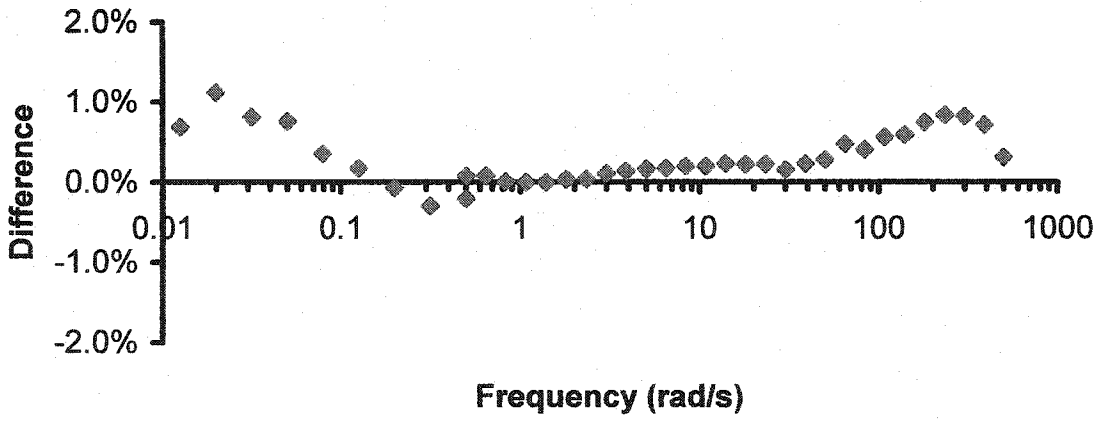

Figure 5.9 The difference of complex viscosity between experimental data and calculated from relaxation spectrum, HDB5 at 170 °C

5.3 Zero Shear Viscosity and the Apparent Activation Energy

The zero shear viscosity, η_0, can be determined from creep and recovery experiment (Eq.5.1) or calculated from H(λ) (Eq.1.6). Figure 5.10 shows the complex viscosity of HBD5 at 170 °C, the points are the experimental data and the line was calculated from H(λ). We can see that the lowest frequency experimental point is close to the steady state. Table 5.1 contains the zero shear viscosity and the apparent activation energy of HDB5 determined from the creep and recovery experiments (SR-5000), and the oscillatory shear experiments (ARES). The η_0 from H(λ) are higher than those from creep and recovery experiments by more than 10%. This difference is likely due to two instrument differences. Figure 5.11 shows the complex viscosities measured by the ARES and the SR-5000. At lower frequencies, the complex viscosities from the ARES are obviously higher than those from the SR-5000, this difference is also more than 10%. However the difference of the apparent activation energies from the two methods is less than 3%, in Table 5.1. We chose to use the η_0 from H(λ) (ARES) for the HDB series.

For HPBD, the oscillatory shear and creep and recovery experiments were both performed with the SR-5000. Because of its high molecular weight, we cannot reach the Newtonian plateau in the oscillatory test range (see Figure 5.12), therefore we use the η_0 from the creep and recovery experiments.

Table 5.2 presents the zero shear viscosity and the apparent activation energy of the HDB series and the HPBD. The experimental data of the HDB1 were provided by Dr. Wood-Adams[10]. The apparent activation energy based on η_0 is calculated by fitting the linearized form of Eq.1.18.

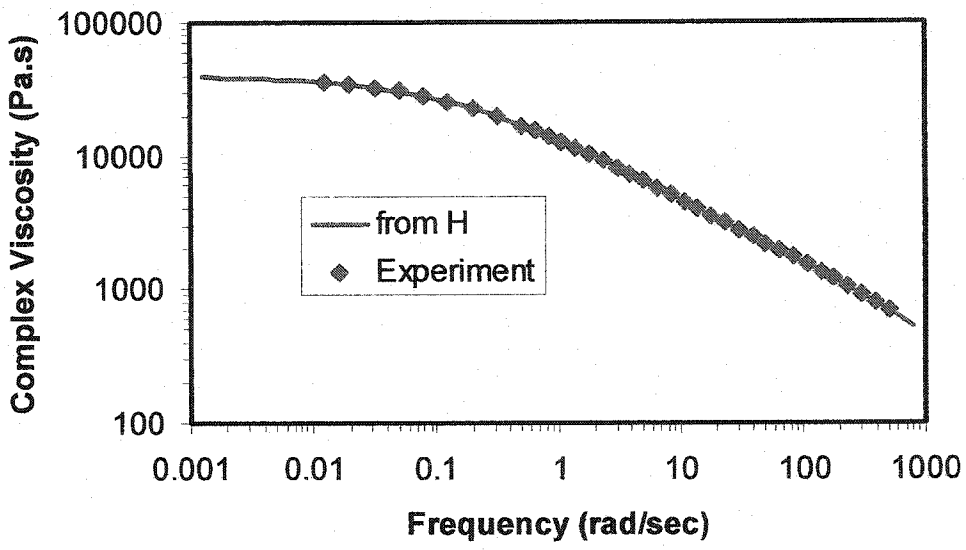

Figure 5.10 The complex viscosity of the HDB5 at 170 °C

Table 5.1 The zero shear viscosity and the apparent activation energy of the HDB5

	η_0, Pa.s					$\hat{E}_a$ (KJ)
Temp., °C	150	160	170	180	190	
ARES *	73503	51609	39558	29033	22638	47.76
SR-5000 **	61800		33850		19700	46.54
Difference	15.9%		14.4%		13.0%	2.6%

*: η_0 was calculated from H(λ).

**: η_0 was determined from creep and recovery test results.

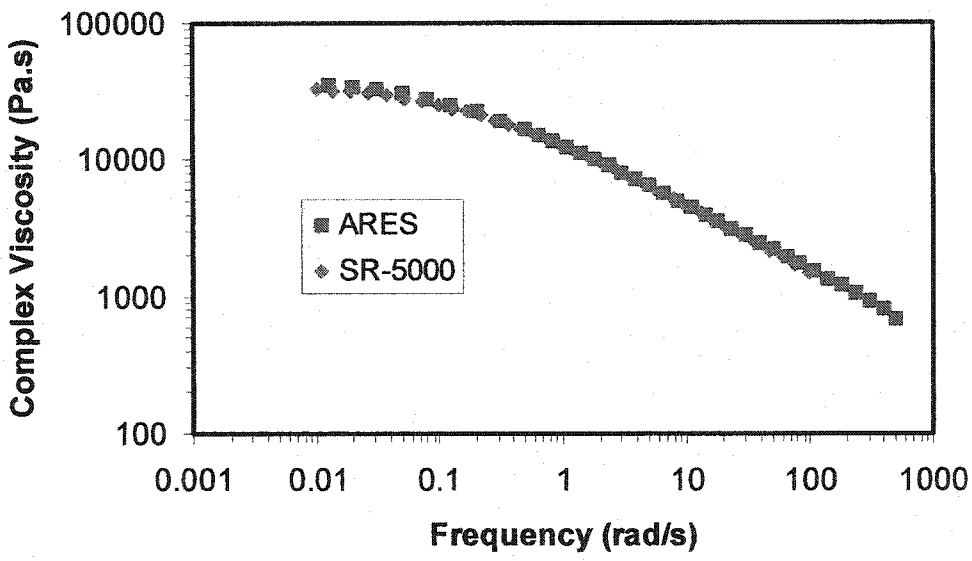

Figure 5.11 The complex viscosity of HDB5 measured with two different instruments.

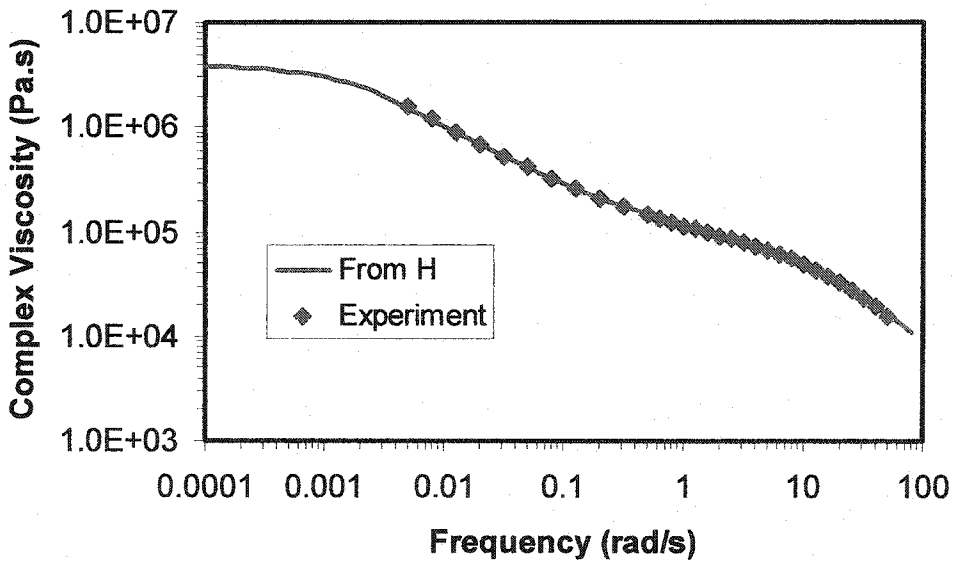

Figure 5.12 The complex viscosity of the HPBD at 170 °C

Table 5.2 The zero shear viscosity and the apparent activation energy of the HDB series and HPBD

	η_0, kPa.s					$\hat{E}_a$ (KJ)
Temp., °C	150	160	170	180	190	
HDB1*	11.30				5.30	30.7
HDB5	73.50	51.61	39.56	29.03	22.64	47.76
HDB6	68.08		34.07		18.90	52.19
HDB7	97.71	66.67	46.75	36.70	24.68	54.55
HPBD**	15,733		8,914		5,186	45.16

*: The data of HDB1 were provided by Dr. Wood-Adams.[10]

**: η_0 came from creep and recovery experiment.

5.4 Thermorheological Complexity of the HDB Series

A plotting method for detecting thermorheologically complex behavior was suggested by Wood-Adams and Costeux.[10]. A plot of the complex modulus vs a product of zero shear viscosity and frequency is temperature independent for thermorheologically simple materials and temperature dependent for thermorheologically complex materials. Figure 5-13 is the plots of $G^*(\omega)$ vs $\eta_0 \times \omega$ for a linear mPE (HDL1) data provided by Dr. Wood-Adams[10], it is temperature independent. Figure 5.14 to 5.16 are such plots for HDB5, 6 and 7. These three materials are obviously thermorheologically complex.

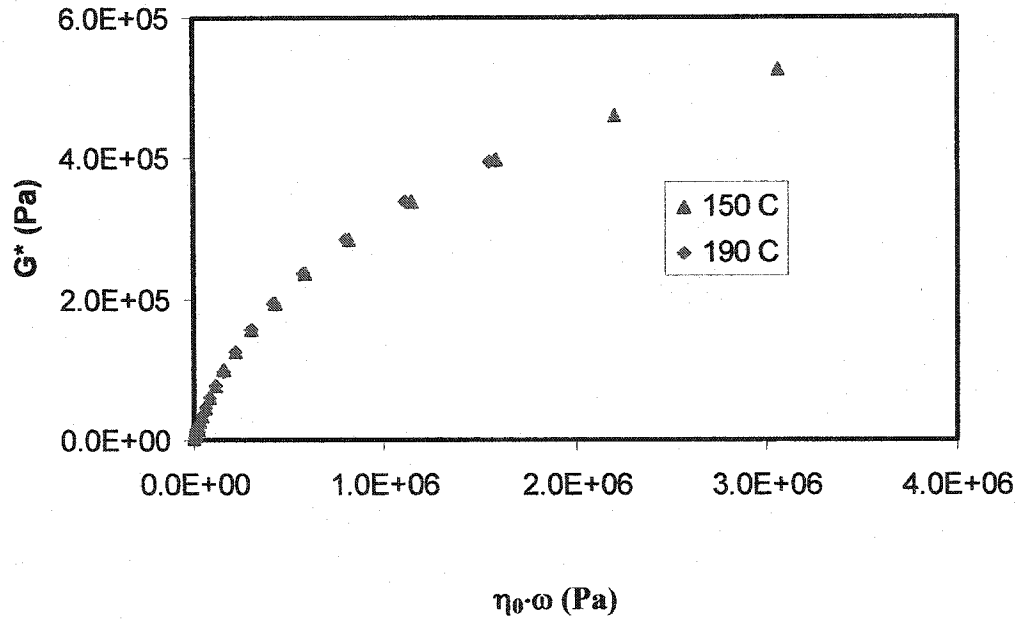

Figure 5.13 Plot of G* vs $\eta_0 \cdot \omega$ for the HDL1

Note: Data is provided by Dr. Wood-Adams.

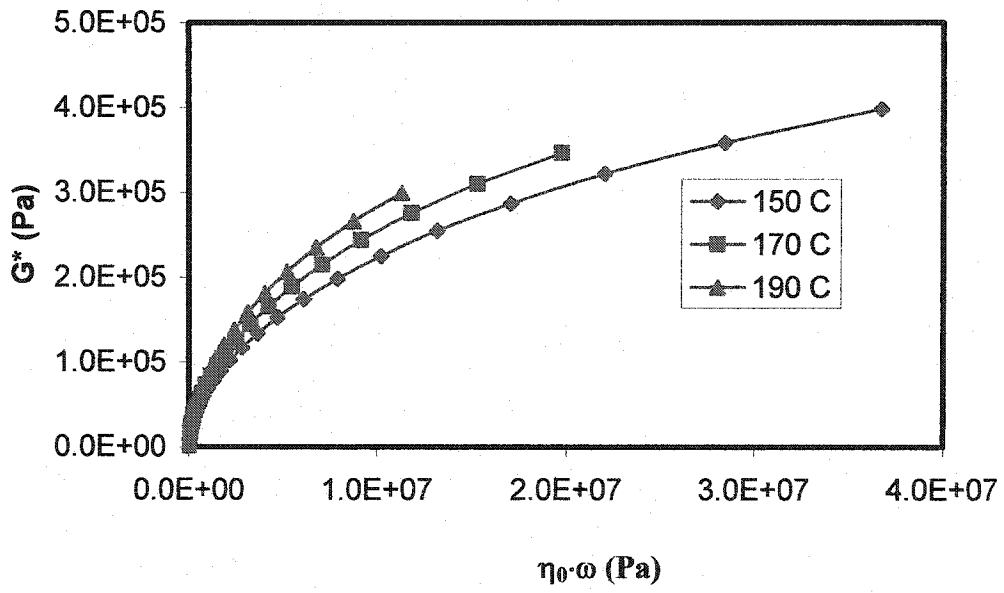

Figure 5.14 Plot of G* vs $\eta_0 \cdot \omega$ for the HDB5

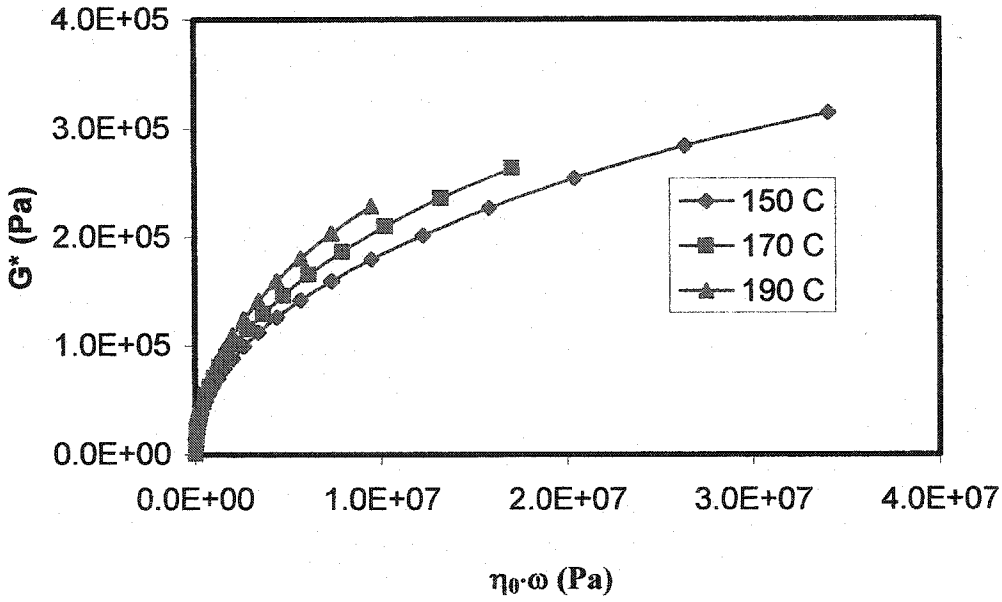

Figure 5.15 Plot of G* vs $\eta_0 \cdot \omega$ for the HDB6

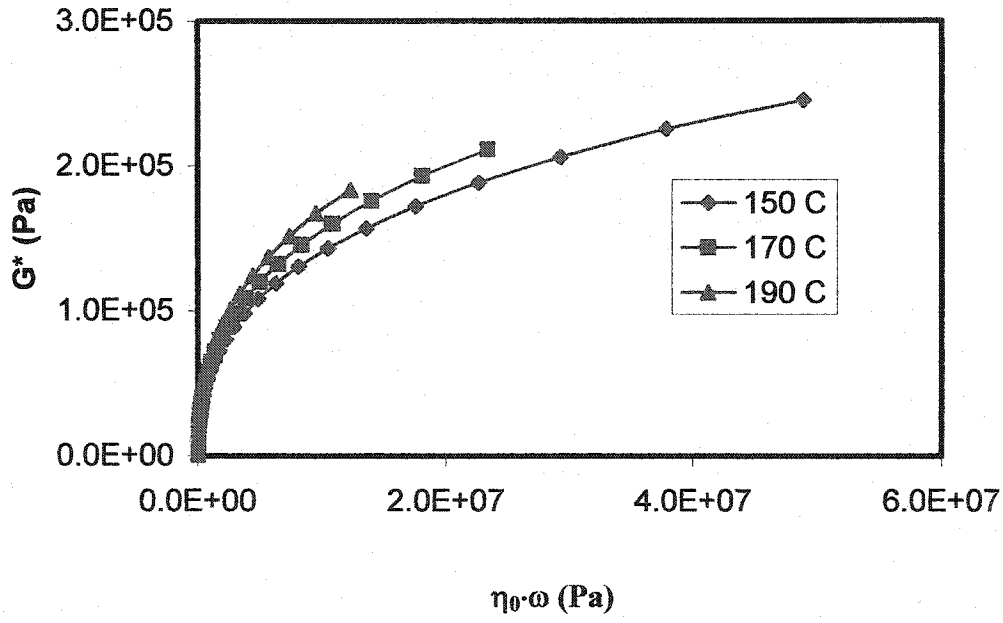

Figure 5.16 Plot of G* vs $\eta_0 \cdot \omega$ for the HDB7

5.5 Activation Energy Spectrum, $E_a(\lambda_0)$ of HDB Series

The calculation of the activation energy spectrum, $E_a(\lambda_0)$, is shown in Figure 5.17 and Eq.5.2. The relaxation modulus, G(t), is used to determine the $E_a(\lambda_0)$, it is calculated from the H(λ) which was found from the complex modulus.

$$\frac{t(T)}{t(T_0)} = \exp\left[\frac{E_a(\lambda_0)}{R}\left(\frac{1}{T} - \frac{1}{T_0}\right)\right] \qquad [5.2]$$

where $\lambda_0 = t(T_0)$.

Wood-Adams and Costeux[10] found that the activation energy spectrum $E_a(\lambda_0)$ calculated from the time shift factors of G'(ω) and G"(ω) are different, as shown in Fig 2.3. By using an artificial discrete relaxation spectrum, they demonstrated that the activation energy spectrum calculated from the shift factor a_T for G'(ω) is closer to the real flow activation energy spectrum than that from the shift factor a_T for G"(ω). They also tried to determine the $E_a(\lambda_0)$ directly from the relaxation spectrum, H(λ), but the resulting spectrum was oscillatory because the calculation is very sensitive to small inaccuracies in the H(λ).

The same phenomenon is observed for the HDB series samples, as shown in Figure 5.18. In this work the $E_a(\lambda_0)$ from the time shift factor of G(t) is also considered and found that it is little higher than that from G'(ω).

Figure 5.19 is the $Ea(\lambda_0)$ of the HDB5 at 170 °C. They were calculated from the time shift factor of G(t) between 170 °C and 190 °C, and 170 °C and 150 °C, the third spectra is the average. At short times, the $E_a(\lambda_0)$ is close the activation energy of linear high-density mPE (27.5 kJ/mol, HDL1 in reference 10), the $E_a(\lambda_0)$ is higher than the apparent

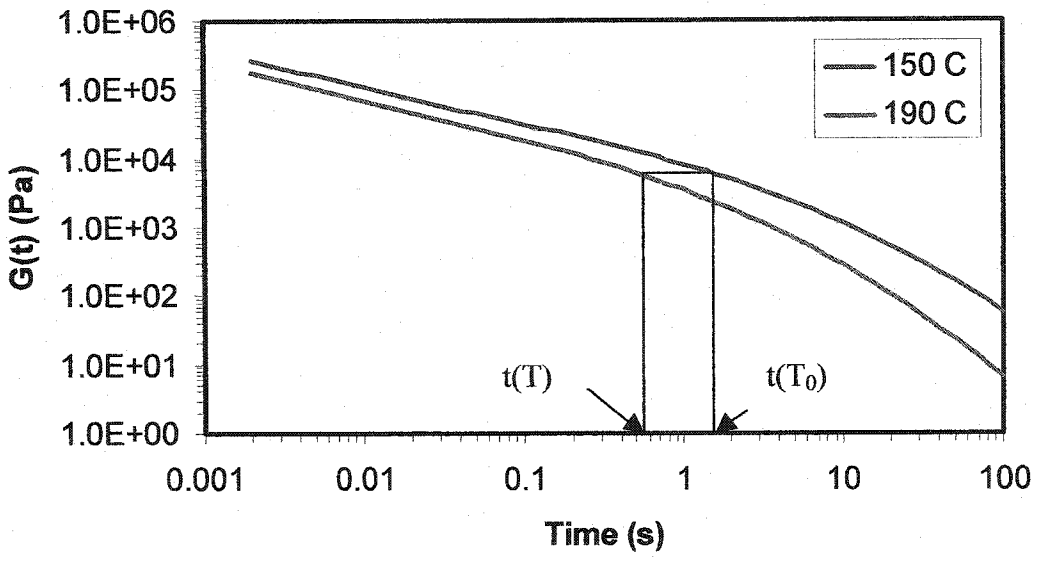

Figure 5.17 The calculation of the $E_a(\lambda_0)$

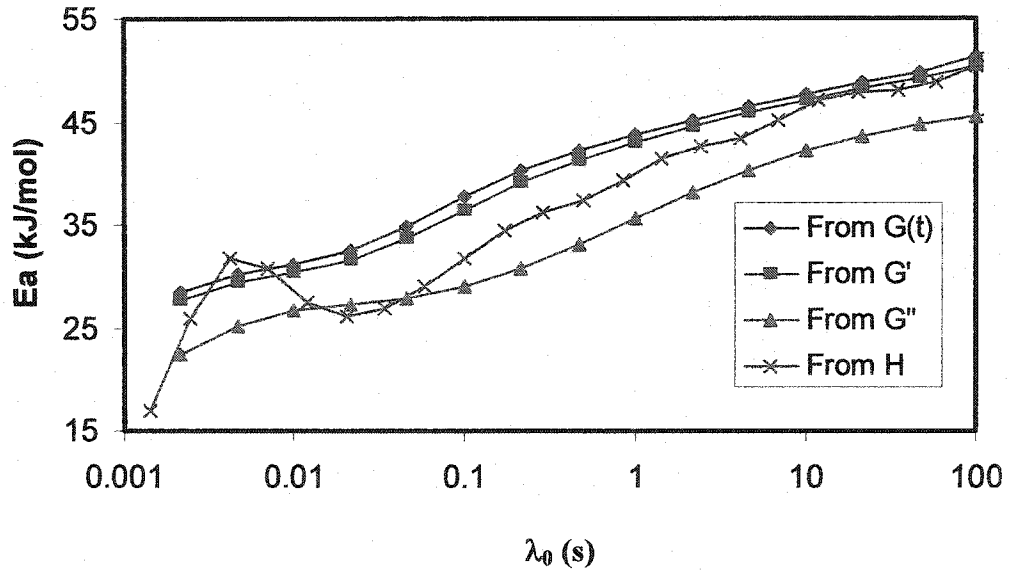

Figure 5.18 $E_a(\lambda_0)$ calculated from G(t), G'(ω), G" (ω) and H(λ), HDB5 at 170 °C

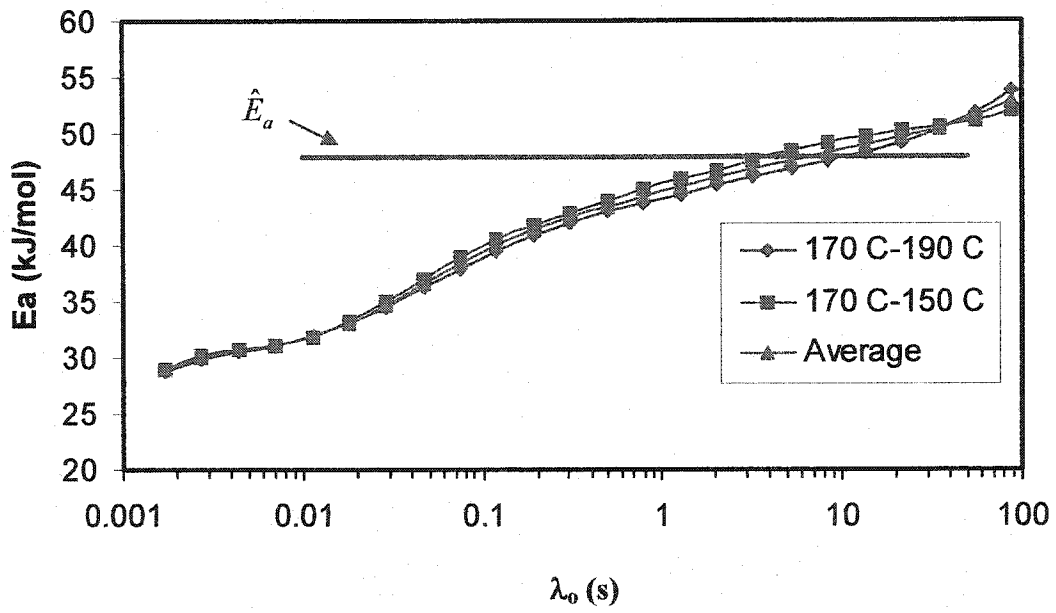

Figure 5.19 The activation energy spectrum, $E_a(\lambda_0)$, of HDB5 at 170 °C

activation energy, $\hat{E}_a$, at longer times. In the experimental window, the $E_a(\lambda)$ calculated from different temperatures agree very well, the accuracy decreases outside the experimental window. Fortunately, the most important time region of the relaxation spectrum is located in the experimental window, see Figures 5.7, 5.20 and 5.21.

The relaxation spectra of HDB5 at 150 °C and 190 °C were calculated from the $E_a(\lambda_0)$ and the $H(\lambda_0)$ at 170 °C. Compared to the $H(\lambda)$ calculated from experimental data at these temperatures, they agree very well, Figure 5.20. The same results were obtained for HDB7 (Figure 5.21). This means that the time shift factor of the $H(\lambda)$ is the same as the time shift factor of the G(t). In other words, the $E_a(\lambda_0)$ calculated from the time shift factor of G(t) is the same as that from $H(\lambda_0)$, and this activation energy spectrum should be the real $E_a(\lambda_0)$ of the materials.

To further test the activation energy spectrum from the time shift factor of G(t), we used the $H(\lambda)$ calculated from the $E_a(\lambda_0)$ and the $H(\lambda_0)$ at 170 °C to calculate $G'(\omega)$ and $G''(\omega)$ at other temperatures, then compared the results to the experimental data. Figure 5.22 and 5.23 show $G'(\omega)$ and $G''(\omega)$ of HDB5 at 150 °C, 160 °C, 180 °C and 190 °C, the points are the experimental data, and the lines are the calculated results. We can see they also agree very well, the average difference between calculation and experimental data is less then 3%. The same results were obtained for HDB7, Figure 5.24 and 5.25.

For thermorheologically complex materials, the time shift actors of G(t), $G'(\omega)$ and $G''(\omega)$ are different, but G(t) and $H(\lambda)$ have a same time shift factor. Therefore the activation energy spectrum, $E_a(\lambda_0)$, can be determined from G(t). Using this activation energy spectrum, $E_a(\lambda_0)$, and the relaxation spectrum, $H(\lambda_0)$, at the reference temperature T_0, we can predict the rheological properties at other temperatures.

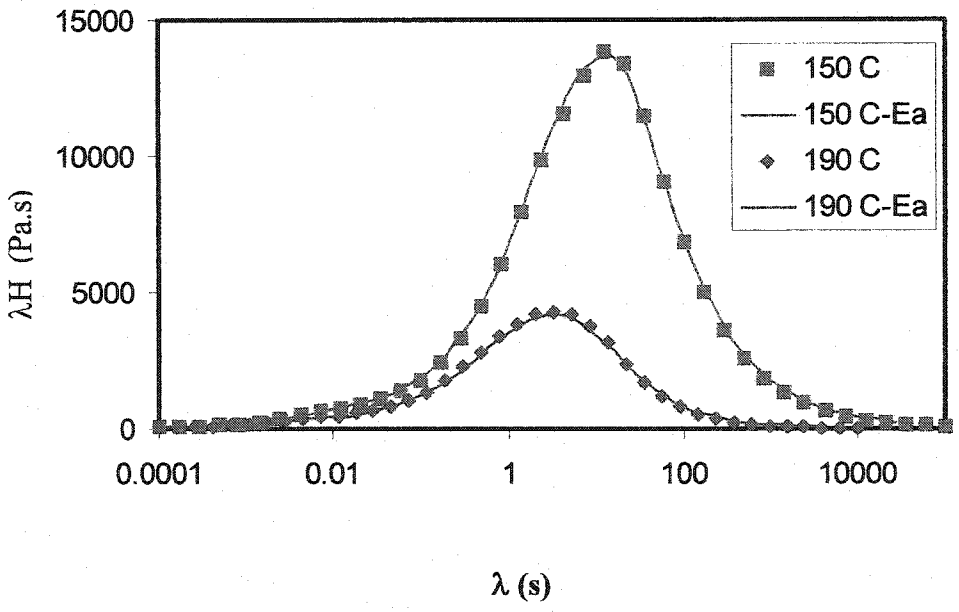

Figure 5.20 The H(λ) of the HDB5 at 150 °C and 190 °C, lines were calculated from $E_a(\lambda_0)$ and $H(\lambda_0)$ at 170 °C, points were calculated from experimental G'(ω) and G"(ω).

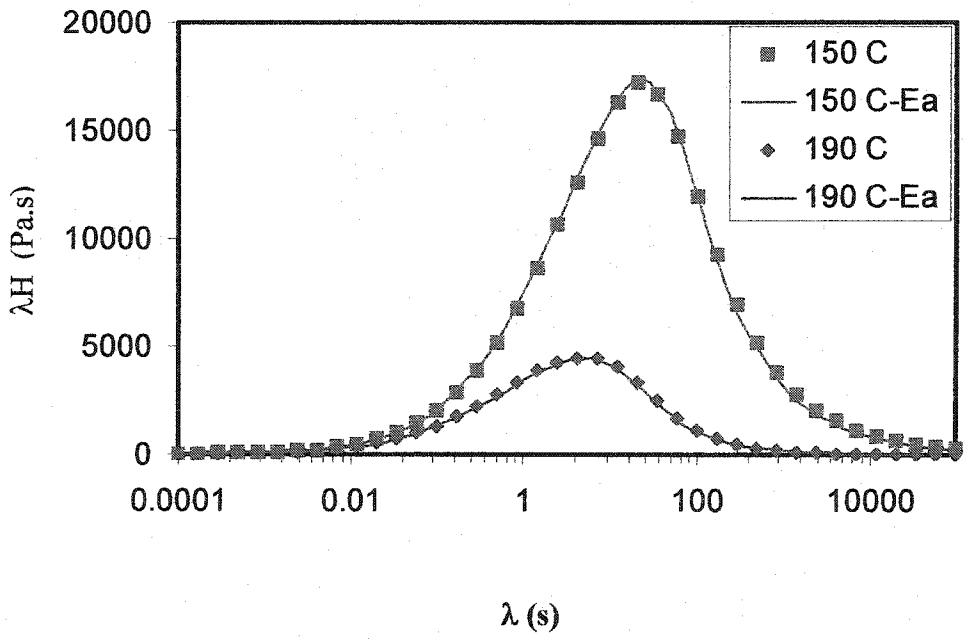

Figure 5.21 The H(λ) of the HDB7 at 150 °C and 190 °C, lines were calculated from $E_a(\lambda_0)$ and $H(\lambda_0)$ at 170 °C, points were calculated from experimental G'(ω) and G"(ω).

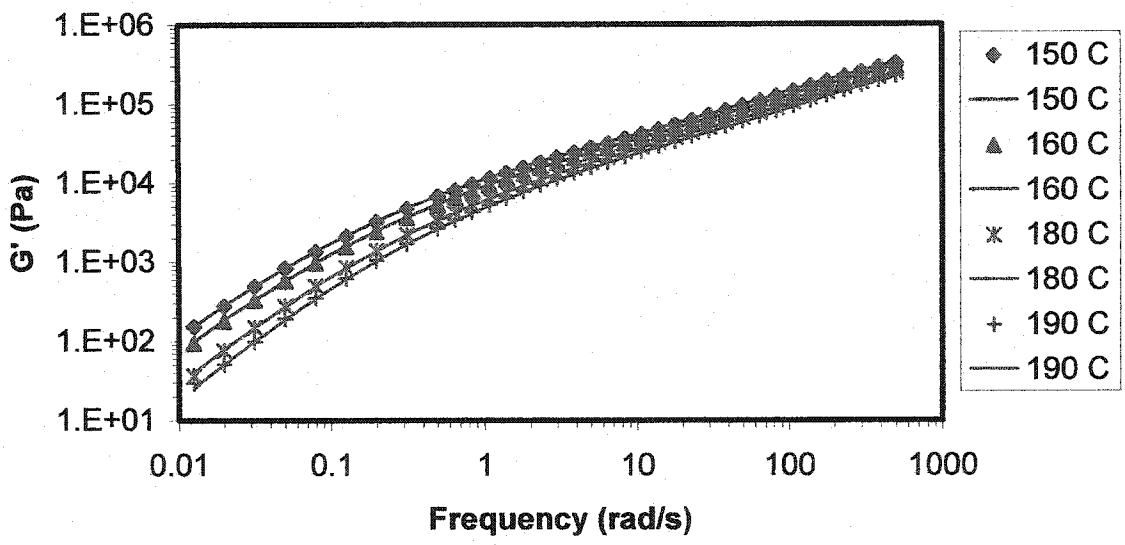

Figure 5.22 The storage modulus of HDB5 at 150 °C, 160 °C, 180 °C and 190 °C, points are the experimental data, and lines were calculated from $E_a(\lambda_0)$ and $H(\lambda_0)$ at 170 °C.

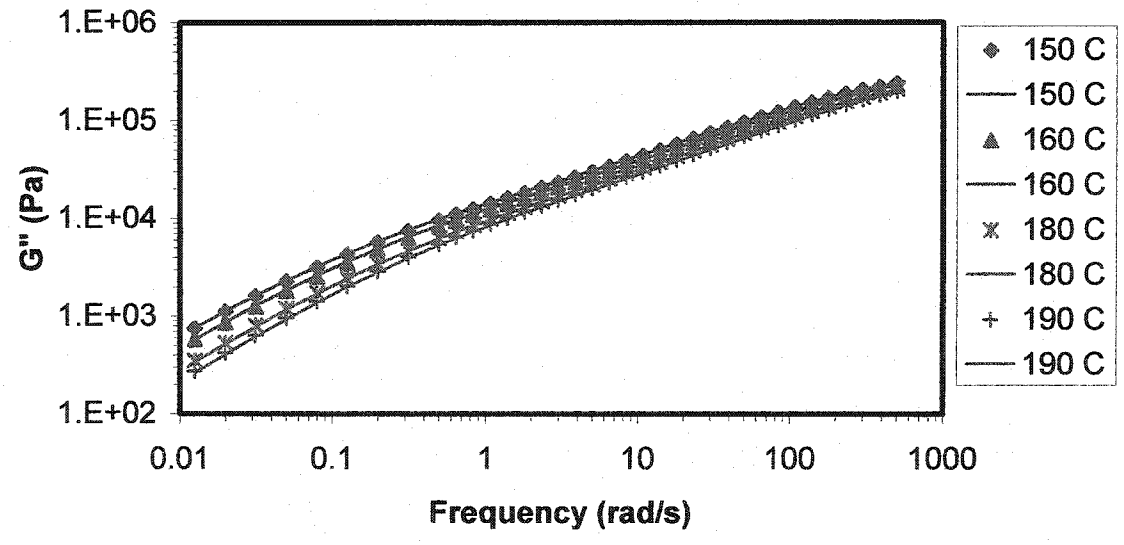

Figure 5.23 The loss modulus of HDB5 at 150 °C, 160 °C, 180 °C and 190 °C, points are the experimental data, and lines were calculated from $E_a(\lambda_0)$ and $H(\lambda_0)$ at 170 °C.

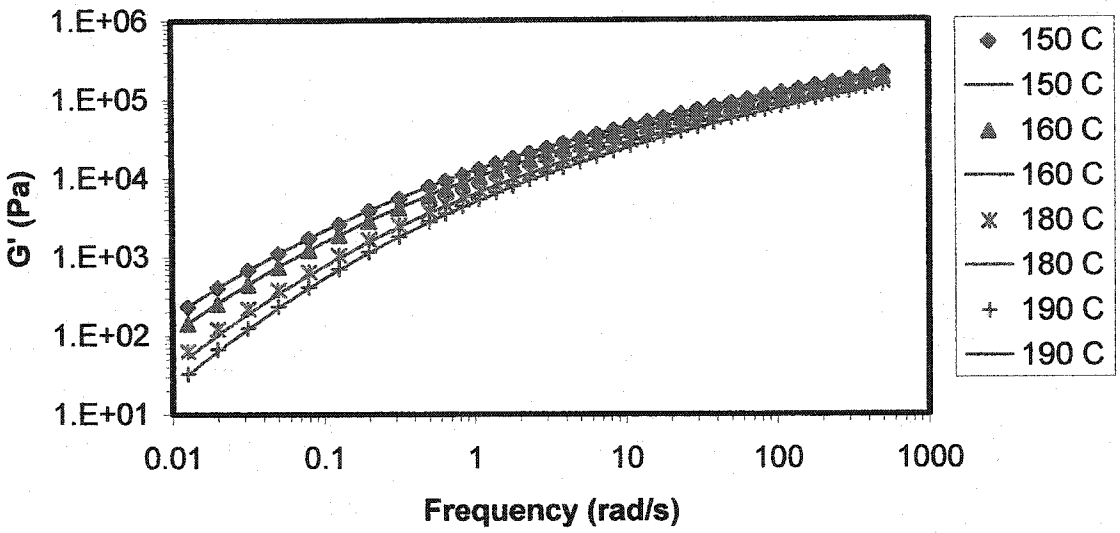

Figure 5.24 The storage modulus of HDB7 at 150 °C, 160 °C, 180 °C and 190 °C, points are the experimental data, and lines were calculated from $E_a(\lambda_0)$ and $H(\lambda_0)$ at 170 °C.

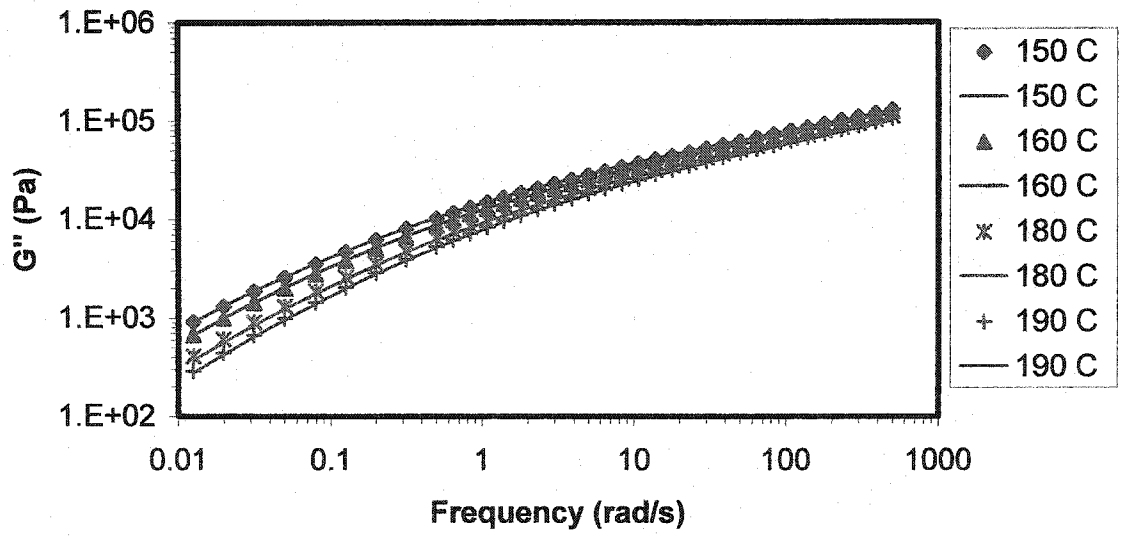

Figure 5.25 The loss modulus of HDB7 at 150 °C, 160 °C, 180 °C and 190 °C, points are the experimental data, and lines were calculated from $E_a(\lambda_0)$ and $H(\lambda_0)$ at 170 °C.

5.6 Effect of Long Chain Branching Level

Based on studies of hydrogenated polybutadiene stars (HPBD), Raju, Graessley and Carella et al.[11-14] reported that the apparent flow activation energy, $\hat{E}_a$, increases linearly with the product of the volume fraction of branched molecules and the arm molecular weight, see Eq.2.1.

The $\hat{E}_a$ of the HDB series is also affected by the long chain branching level and the branch length. Figure 5.26 is a plot of the $\hat{E}_a$ and a product of the average number of branches per molecule, β, and the weight-average segment molecular weight, $M_{W,S}$, i.e., the weight-average arm molecular weight. The data of HDB3 and 4 comes from ref 10. The apparent activation energy increases with the $\beta M_{W,S}$, except for HDB4.

Repeat experiments for HDB3 and 4 were attempted in order to verify previous results. Unfortunately, the materials are not stable at high temperatures now.

Figure 5.27 shows the activation energy spectra, $E_a(\lambda_0)$, for HDB1, HDB5, HDB6 and HDB7 at temperature 170 °C. The average number of branches per molecule, β, increases from HDB1 ($\beta = 0.067$) to HDB7 ($\beta = 0.54$), see Table 4.1. The activation energy spectrum, $E_a(\lambda_0)$, shifts up as the long chain branching level increases. At short times, $E_a(\lambda_0)$ is close to the activation energy of linear high-density mPE, 27.5 kJ/mol, for all branched materials.

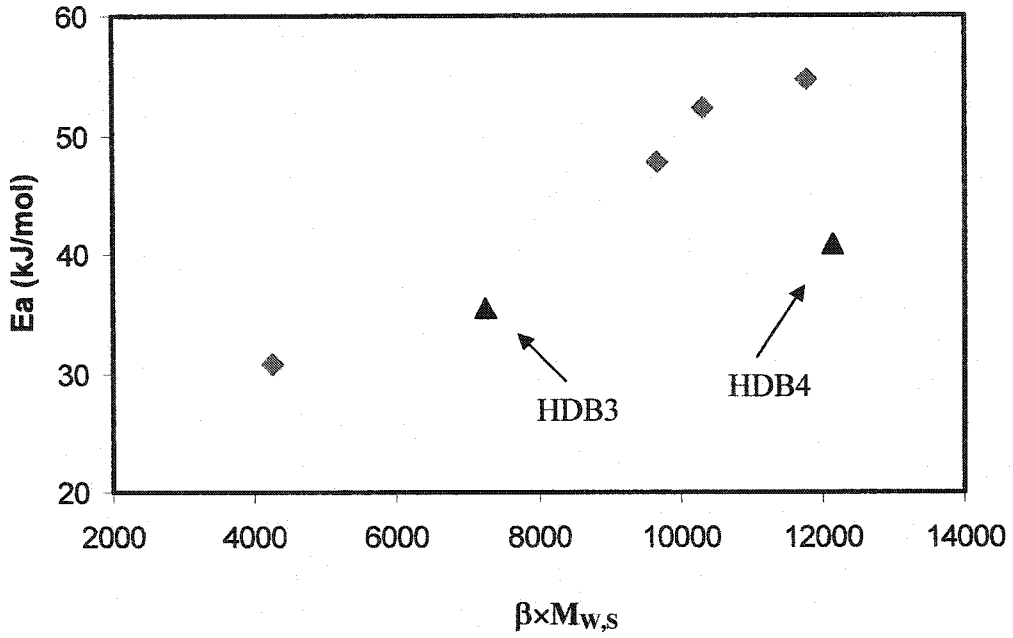

Figure 5.26 Relationship between $\hat{E}_a$ of the HDB series and $\beta \times M_{W,S}$

Note: the data of HDB3 and 4 comes from ref 10.

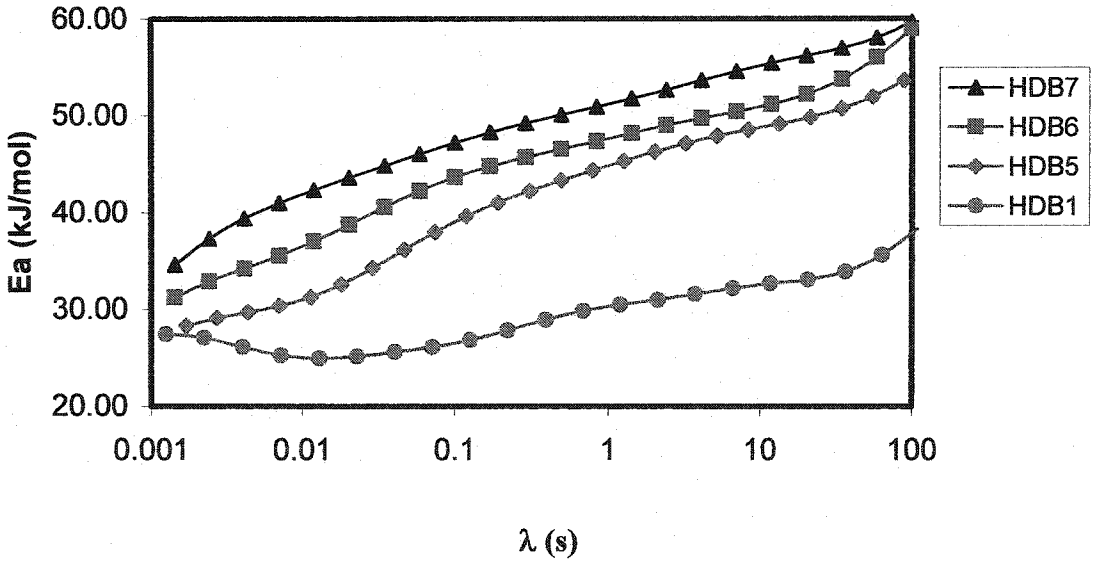

Figure 5.27 The activation energy spectrum of the HDB series at 170 °C

Wood-Adams[36], Koopmans[37] and Kim[38] reported that the zero shear viscosity of mPEs increased with long chain branching level. Figure 5.28 shows the complex viscosities of HDB5, 6 and 7 at 150 °C. Because the materials have different molecular weights, the effect of LCB on η_0 is not clear in Figure 5.28. Figure 2.29 is a plot in terms of $\eta_0/\eta_{0,L}$ to β, where $\eta_{0,L}$ is the zero shear viscosity of a linear material which has the same molecular weight as the branched material, it was calculated from the equation[36]:

$$\eta_{0,L} = 6.8\times10^{-15} M_W^{\,3.6} \qquad [5.2]$$

The ratio of $\eta_0/\eta_{0,L}$ increases with β in Figure 5.29, i.e. the degree of long chain branching enhances the zero shear viscosity, the data of HDB1,3 and 4 were provided by Dr. Wood-Adams[10]. This result is the same as that reported by Wood-Adams et al.[36]

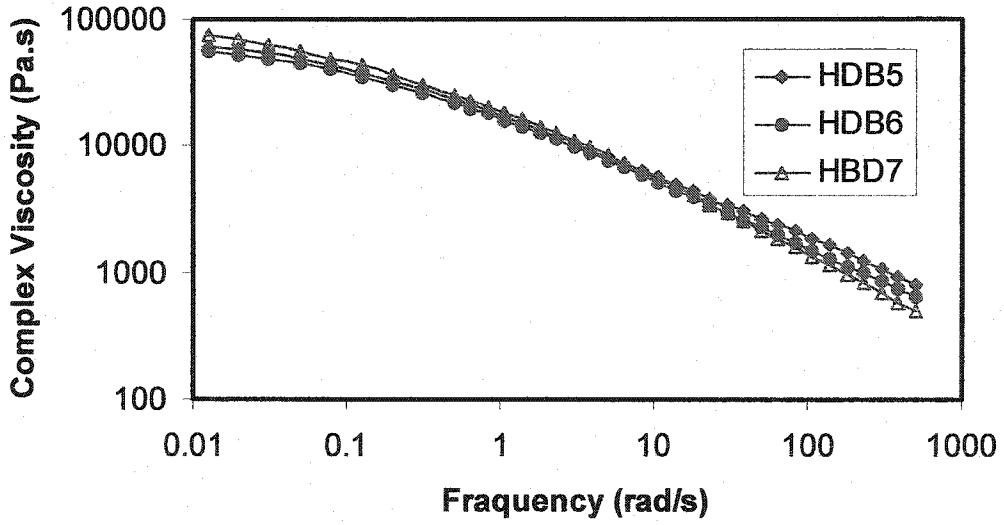

Figure 5.28 The complex viscosity of HDB5, 6 and 7 at 150 °C.

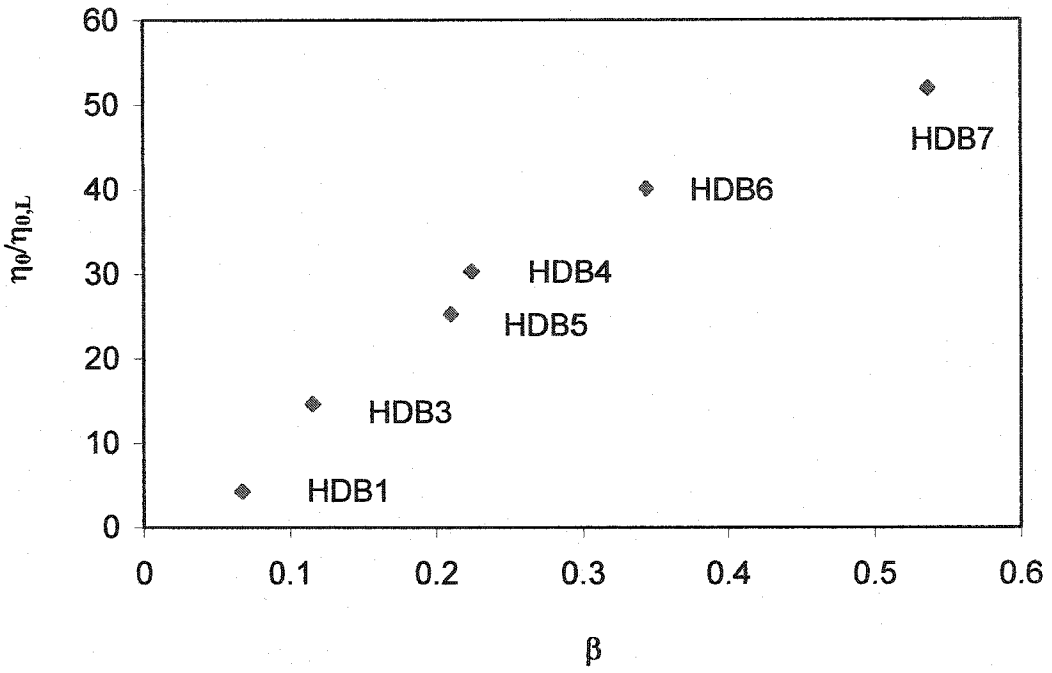

Figure 5.29 A plot of $\eta_0/\eta_{0,L}$ vs β for the HDB series at 150 °C, the data of HDB1,3 and 4 were provided by Dr. Wood-Adams[10].

5.7 Thermorheological Complexity of High Molecular Weight Linear Hydrogenated Polybutadiene

Graessley[21]and Levin and Milner[32] suggested a mechanism leading to thermorheological complexity for long chain branched polymers. For long chain branched polymers, the branches rearrange by arm retraction, and the entanglement length for molecular arm is temperature dependent according to these authors. The temperature coefficient, $k = d\ln C_\infty / dT$, is negative for thermorheologically complex materials.

Linear polymers are thermorheologically simple materials, and until now thermorheological complexity of linear polymers at timescales other than glassy scales has not been reported.

According the relaxation mechanism of linear molecules,[24-26] stress is relaxed first by Rouse motion, than by contour-length fluctuations and finally by reptation. Contour-length fluctuations for linear molecules is the same mechanism as the arm retraction of long chain branched molecules.

HPBD has a negative temperature coefficient,[21] therefore a linear HPBD material should be thermorheologically complex in the time range that is affected by contour-length fluctuations.

If a linear HPBD sample has a large enough molecular weight, the effect of the contour-length fluctuations would be visible in the experimental window of the rheometer. We chose a HPBD sample with molecular weight of 334,000 g/mol and a polydispersity, $M_W/M_N = 1.19$.

Figure 5.30 is a plot of the complex modulus vs the product of zero shear viscosity and frequency, at 150 °C, 170 °C and 190 °C. The zero shear viscosities were determined with the creep and recovery experiments (Table 5.2). Figure 5.30 is temperature dependent, this means that the HPBD sample is thermorheologically complex as we expected.

Figure 5.31 shows the relaxation spectrum of the HDPB at 190 °C, calculated from the complex modulus. Unfortunately, the main peak of the spectrum is outside the experimental window.

A technique for combining oscillatory data and creep and recovery data was used to extend the experimental window.[34] The retardation spectra from the complex modulus and the creep compliance are used as an intermediate tool to combine the data from the oscillatory and creep and recovery experiments. The spectra were calculated by the nonlinear regularization (NLRG) computational technique[9].

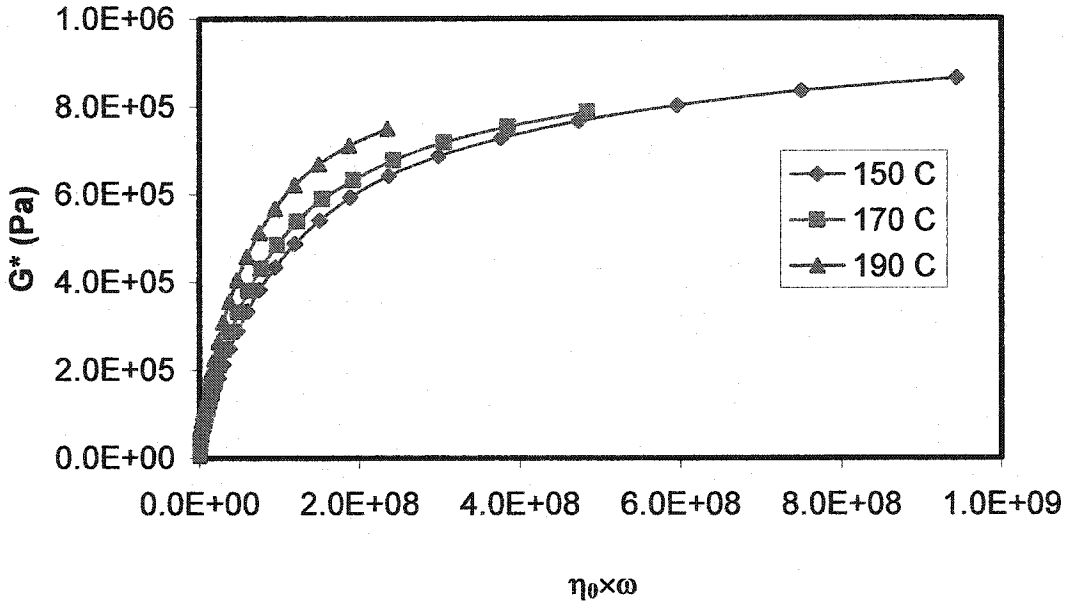

Figure 5.30 Plot of G* vs $\eta_0 \cdot \omega$ for the HPBD at 150 °C, 170 °C and 190 °C.

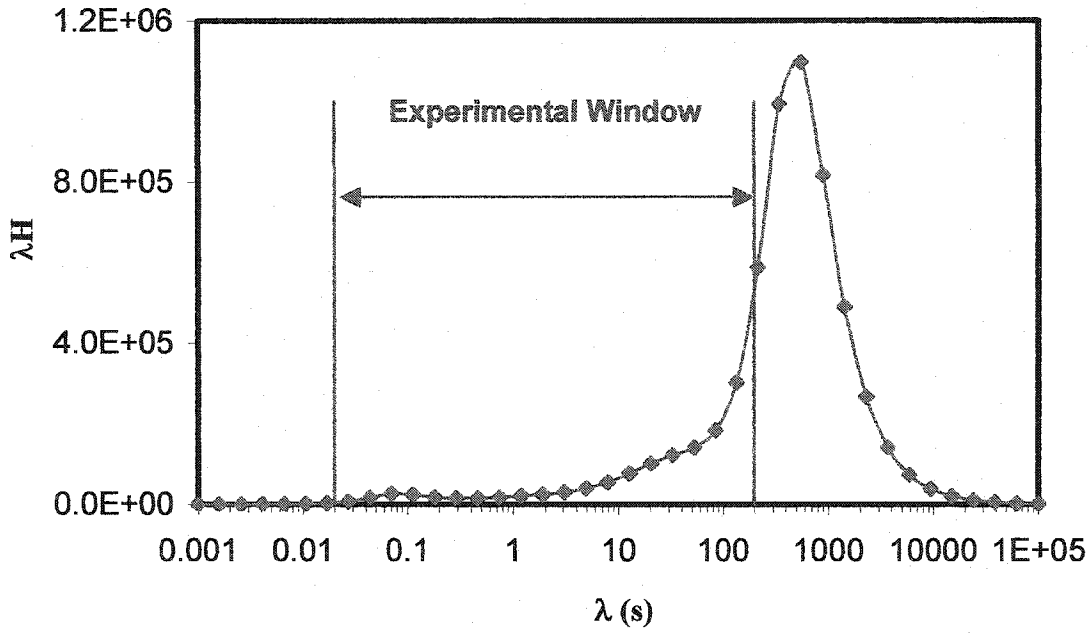

Figure 5.31 The relaxation spectrum of the HPBD at 190 °C, calculated from G*(ω)

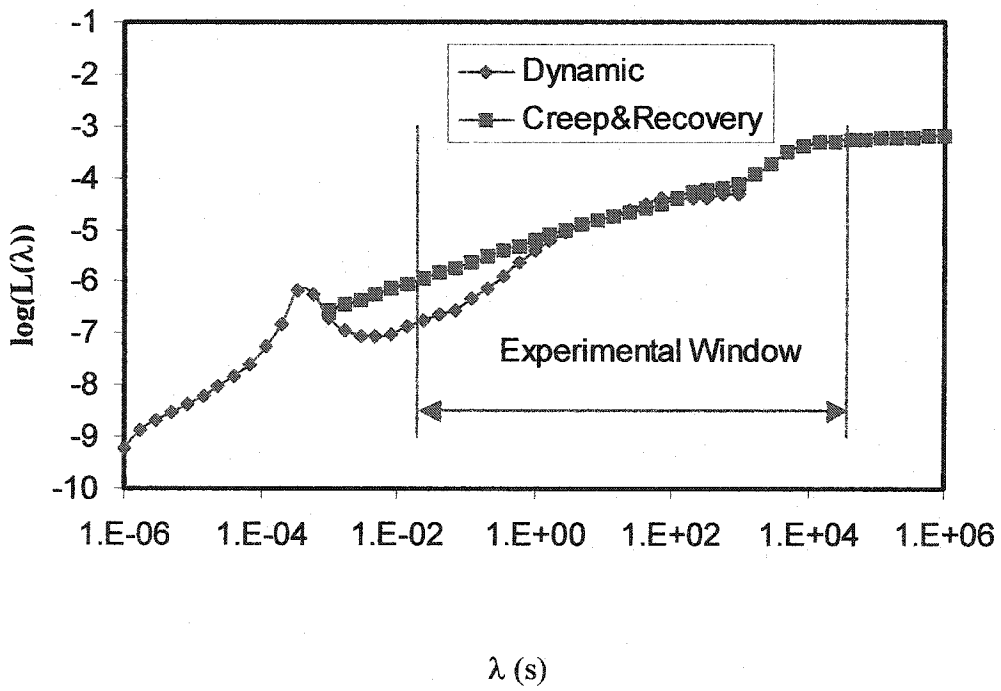

Figure 5.32 Retardation spectra from complex modulus and creep compliance, HPBD at 190 °C.

Figure 5.32 shows the retardation spectra from the complex modulus and creep compliance. There is a superposition of the spectra with in the region of overlapping experimental windows (10s to 100s). Therefore, a combined retardation spectrum is taken by the short time part of L(λ) from the complex modulus and the long time part from the creep compliance. Then the combined retardation spectrum is used to calculate the complex compliance and the complex modulus, from Equation 5.3 to 5.6.

$$J'(\omega) = \int_{-\infty}^{\infty} L(\lambda) \frac{1}{1+\omega^2\lambda^2} d\ln\lambda \qquad [5.3]$$

$$J''(\omega) = \frac{1}{\omega\eta_0} + \int_{-\infty}^{\infty} L(\lambda) \frac{\omega\lambda}{1+\omega^2\lambda^2} d\ln\lambda \qquad [5.4]$$

$$G'(\omega) = \frac{J'(\omega)}{J'(\omega)^2 + J''(\omega)^2} \qquad [5.5]$$

$$G''(\omega) = \frac{J''(\omega)}{J'(\omega)^2 + J''(\omega)^2} \qquad [5.6]$$

This technique can extend the complex modulus to the long time end of the creep and recovery experimental window. Figure 5.33 shows the complex modulus, the points are from oscillatory shear experiment and the line is from the combined retardation spectrum. They agree well.

Figure 5.34 shows the relaxation spectrum from the extended complex modulus. Compared to the spectrum from the experimental complex modulus, there is one more peak at long times in the spectrum from the combined data.

There are three peaks in the combined relaxation spectrum. Peak 1 is at 0.1 s, peak 2 is at 200 s, and peak 3 is at 3000 s

The Rouse time of an entanglement segment, τ_e, can be expressed as:

$$\tau_e = \frac{\zeta N_e^{\ 2} b^2}{3\pi^2 k_B T} \qquad [5.7]$$

HPBD has the same molecular structure as polyethylene. The data of PE can be used to estimate the τ_e of HPBD. From reference 39, for polyethylene at 413 K, the chain end-to-end radius squared per chain mass $\langle R^2 \rangle / M$ equals 1.25 $\text{Å}^2 \text{mol g}^{-1}$. With a monomer molecular weight, M_0=28, this implies a value of $b = (M_0 \langle R^2 \rangle / M)^{1/2} = 5.9$ Å. The entanglement molecular weight of PE from ref 11 is $M_e = 1000$.

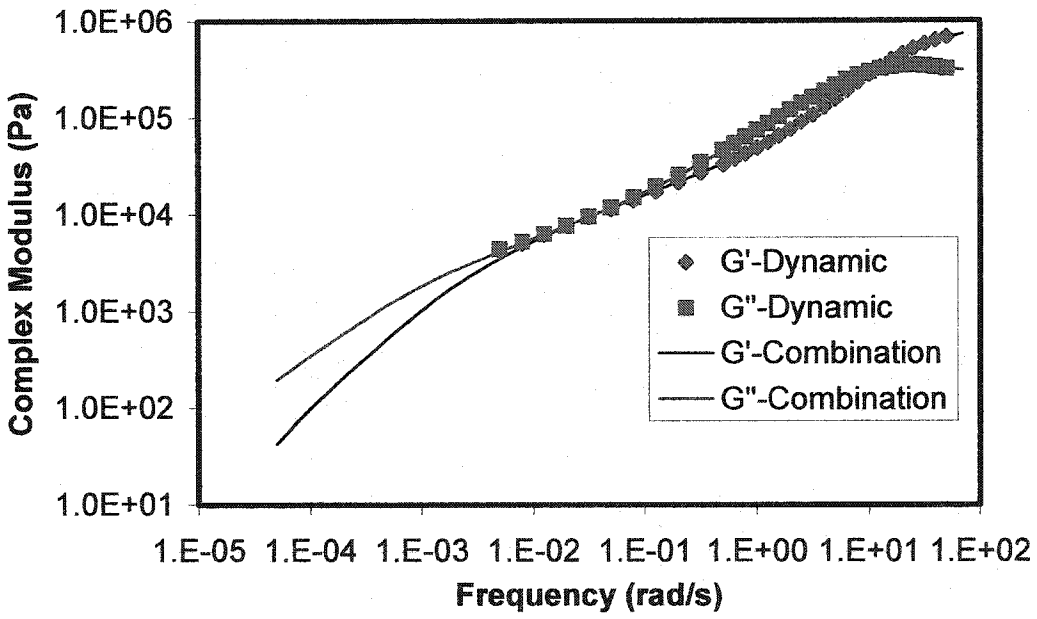

Figure 5.33 Complex modulus from L(λ) and oscillatory experiment, HPBD at 190 °C

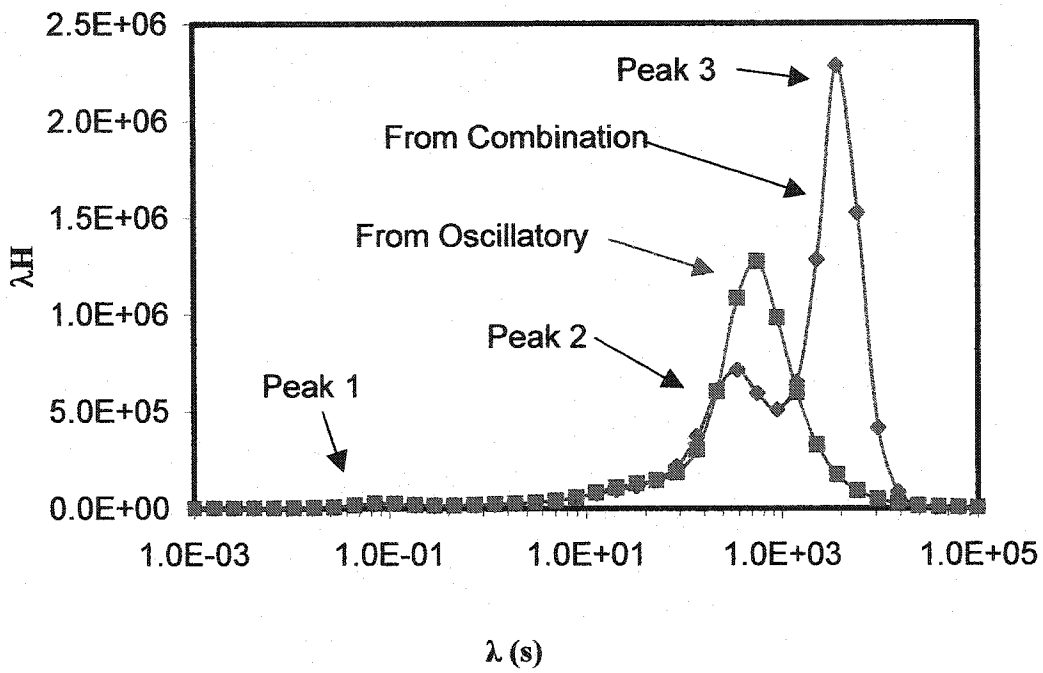

Figure 5.34 The relaxation spectrum of HPDB at 190 °. One was calculated from complex modulus of oscillatory experiment, another was calculated from combined complex modulus.

The monomeric friction coefficient ζ is temperature dependent. Jutta [40] reported that the temperature dependent ζ could be expressed in terms of WLF form:

$$\log[\zeta(T)] = \log[\zeta(T_{ref})] - \frac{C_1(T - T_{ref})}{C_2 + T - T_{ref}} \qquad [5.8]$$

Jutta also gave the data of PE at 413 K, $\log(\zeta) = -8.554$ poise^{-1}cm^{-1}, $C_1 = 2.018$, $C_2 = 253$ K.

So the Rouse time of an entanglement segment for HPBD at 463 K (190 °C) is $\tau_e = 4.77 \times 10^{-6}$ s. Then the Rouse time is $\tau_R = \tau_e(M_W/M_e)^2 = 0.53$ s. This is the same scale as peak 1 in Figure 5.34. The reptation time [24] is $\tau_d = \tau_e(M_W/M_e)^3 = 178$ s. From Likhtman

and Mcleish paper,[26] the renormalized reptation time (after to contour-length fluctuations) is

$$\tau_{df} = \tau_d\left(1 - \frac{2C_1}{\sqrt{Z}} + \frac{C_2}{Z} + \frac{C_3}{Z^{3/2}}\right) \qquad [5.9]$$

where $C_1 = 1.69$, $C_2 = 4.17$, $C_3 = -1.55$ and $Z = M_W/M_e$, therefore $\tau_{df} = 147$ s.

Peak 2 in Figure 5.34 has the same time scale as τ_{df}. The contour-length fluctuations occur in the time range from τ_R to τ_{df}, in other word the contour-length fluctuations of HPBD happen in the time range from peak 1 (0.1s) to peak 2 (200 s). The manifestation of the CLF in the spectrum is the broad shoulder between the first peak and second peak.

Peak 3 in Figure 5.34 is located at a time about 3000 s, it is much longer that the reptation time τ_d. This peak could not be well explained to data, further work is necessary. For now we will neglect this peak, as we are only interested in the behavior until reptation (peak 2).

Figure 5.35 shows the activation energy and relaxation spectra of HPBD at 190 °C. The $E_a(\lambda_0)$ was calculated from the G(t) at 190 °C and 150 °C. In Figure 5.35, the $E_a(\lambda_0)$ changes from the time of peak 1 to peak 2 of the relaxation spectrum, in other word, from τ_R to τ_{df}. It approaches the activation energy of the linear HPBD (30.1 kJ, in ref 11) before the time of the peak 1. After the time of peak 2, the $E_a(\lambda_0)$ remains at a constant higher value. This time range, peak 1 to peak 2, is the same as that of occurrence of the contour-length fluctuations. It means that contour-length fluctuations causes the thermorheological complexity of this linear polymer.

The apparent activation energy, $\hat{E}_a$, of HPBD is 45.2 kJ/mol, see Table 5.2. The zero shear viscosity came from the creep and recovery experiments.

The thermorheological complexity of the linear high molecular weight HPBD which is caused by the contour-length fluctuations experimentally proves that arm retraction of long chain branches leads to the thermorheological complexity for long chain branched materials.

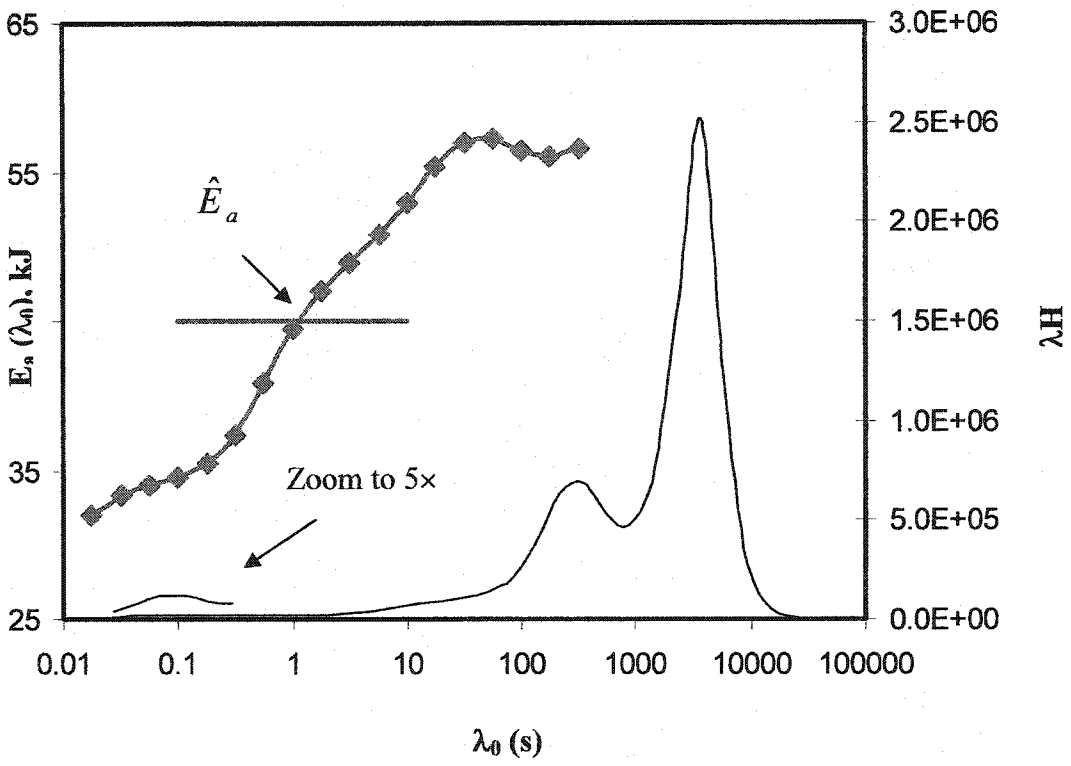

Figure 5.35 The activation energy and relaxation spectrum of the HPBD at 190 °C

6 Theoretical Analysis of Activation Energy Spectrum

6.1 Arm Retraction Theory of Star Polymers

The star structure is the simplest LCB structure with a single branch point. The arm retraction theory quantitatively describes the stress relaxation in star polymers.[26-31] Because of the branch point, star polymers cannot relax stress by reptation as linear polymers do, instead they undergo arm retraction again an energy barrier, U(s). Note that s is a fractional distance along the arm, it goes from 0 to 1 from the free end to the branch point; see Figure 2.5. Considering dynamic dilution, at the time $\tau(s)$, the relaxed chain segments can be thought as completely mobile, and the effective entangled network is diluted. The effective entangled network is only built with unrelaxed chain segments. The fraction of unrelaxed chains is 1-s, therefore the relaxation time, energy barrier and the relaxation modulus can be expressed as:

$$\tau(s) = \tau_R \exp[U(s)] \qquad [6.1]$$

$$U(s) = \frac{15N}{8N_e}\left(s^2 - \frac{2}{3}s^3\right) \qquad [6.2]$$

$$G(t) = 2G_0 \int_0^1 (1-s)\exp[-t/\tau(s)]ds \qquad [6.3]$$

where τ_R is the Rouse time $\tau_R = \tau_e(N/N_e)^2$, where τ_e is the Rouse time of an entanglement segment; N is the arm length, and N_e is the entanglement segment length.

Graessley [21] suggested that the entanglement segment length was temperature dependent for thermorheologically complex materials. According to Graessley's suggestion and the arm retraction theory, Levine and Milner [32] developed a model for thermorheological complexity of star polymers, and verified it with rheological data of

star-branched hydrogenated polybutadiene. They modified the arm retraction model (Eq.6.1-6.3) by incorporating a temperature dependent entanglement length:

$$\frac{N_e(T)}{N_e(T_0)} = \exp\left[-\Delta\left(\frac{1}{T}-\frac{1}{T_0}\right)\right] \qquad [6.4]$$

In this equation Δ is an energy, they found Δ=380 K for HPBD stars.

A stress relaxation model of linear-star blends was also developed by Milner and McLeish et al.[31] In this work we incorporate Levine and Milner's temperature dependent entanglement length into the theory for linear-star blends.

Long chain branched metallocene polyethylene can be simply considered as a blend of linear and long chain branched polyethylene[5]. We can use the arm retraction theory to qualitatively study the thermrheological complexity of long chain branched polyethylene.

To simplify the study, we first used the Levine and Milner model to study the effect of molecular weight on the apparent activation energy and the activation energy spectrum, and secondary we used the Milner and McLeish model to study the effect of the volume fraction of branched molecules.

Levine and Milner [32] fitted the experimental data of HPBD stars, a model of polyethylene, with different arm lengths at different temperatures. They found that the fitted entanglement length at 190 °C for HPBD stars in their model was 2.2 times that of linear molecule. They called this fitted value the apparent entanglement length of star arms. For example, the apparent entanglement molecular weight of HPBD stars, M_e, is 2056 g/mol at 190 °C. This value is larger than that Raju et al [11-14] reported and the generally accepted value (M_e is 1250 g/mol for HPBD and HDPE at 190 °C).

In the Levine and Milner model, the input parameters are M_a, M_e, τ_e, Δ and T. In this work, the parameters from Levine and Milner's paper, Δ=380 K, $M_{e,\,190\,^\circ C}$ = 2056 g/mol were used.

The Rouse time of the entanglement segment was calculated with Eq.5.7, using literature data described in chapter 5, resulting in $\tau_e = 4.77 \times 10^{-6}$ s at 190 °C.

The τ_e is temperature dependent as in Eq.6.5.

$$\tau_e(T) = \tau_e(T_0)\exp\left[\frac{E_a}{R}\left(\frac{1}{T}-\frac{1}{T_0}\right)\right] \qquad [6.5]$$

The E_a should be the activation energy of the linear polymer, for HPBD E_a = 30.1 kJ/mol.

Raju and Graessley and Carella [11-14] reported a linear relationship between the apparent activation energy and a product of the arm molecular weight and the volume fraction of star for star and linear blends of HPBD (Eq.2.1). The activation energy for linear HPBD is 30.1 kJ/mol, and the activation coefficient[14] $\wedge$ is 1.05 kJ/mol. Then Eq.2.1 becomes:

$$\left(\hat{E}_a\right)_B = 30.1 + 1.05\phi\frac{M_a}{M_e} \qquad [6.6]$$

where the entanglement molecular weight in Eq.6.6 is , M_e = 1250.

Figure 6.1 shows the activation energy spectrum of HPBD stars with M_a = 37000 at 190 °C calculated from the Levine and Milner model, and τ_e(T) calculated from Eq.6.5 with E_a = 30.1 kJ. The spectrum at shorter times approaches 38 kJ/mol, this value is much higher than the activation energy of linear HPBD (30.1 kJ/mol). The apparent activation energy from the model is 70.6 kJ/mol, is also much higher than that from Eq.6.6 (61.2 kJ/mol). From the experimental results of HDB series (Figure 5.27) and Wood-Adams

and Costeux's[10] report, the activation energy spectrum of long chain branched polymers at shorter times should approaches to the activation energy of the linear material.

Milner, McLeish and Levin et al.[29-32] also reported that the arm retraction theory could simulate the rheological properties very well at longer times, but could not at shorter times. The inaccuracies of the arm retraction theory model at shorter times cause the inaccuracies of the apparent activation energy and the amplitude of the activation energy spectrum. The shape of the activation energy spectrum from the model is similar to the experimental results (Figure 6.1).

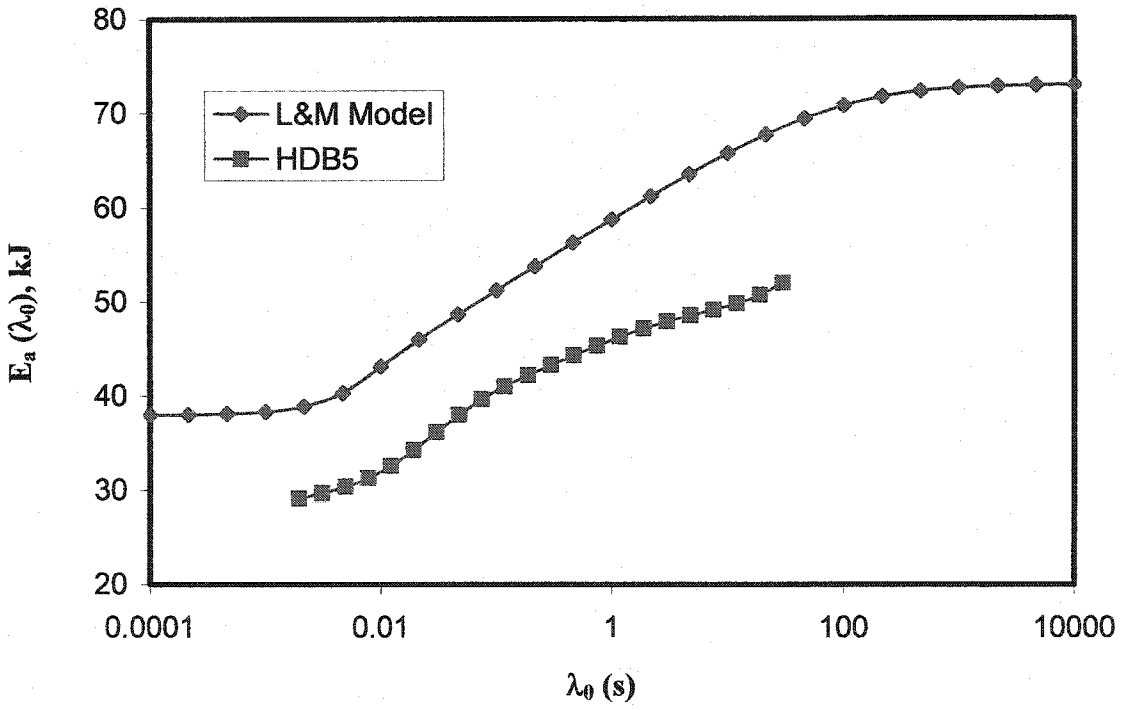

Figure 6.1 The activation energy spectra of HPBD stars with M_a = 37000 calculated from the Levine and Milner model, and the HDB5 at 190 °C.

The apparent activation energy of HPBD stars with different arm molecular weights calculated from the Levine and Milner model and from Eq.6.6 are presented in Table 6.1

and Figure 6.2. The relationship between $\hat{E}_a$ and M_a from the model is linear. The $\hat{E}_a$ from the model is higher than that from Eq.6.6.

Table 6.1 The apparent activation energy of HPBD stars from the L&M model and Eq.6.6, kJ.

ϕMa	50000	37000	25000	15000
L&M Medol	84	70.6	58.2	47.6
Eq.6.2	72.1	61.2	51.1	42.7

Note: the volume fraction of star polymers, ϕ, is 1.

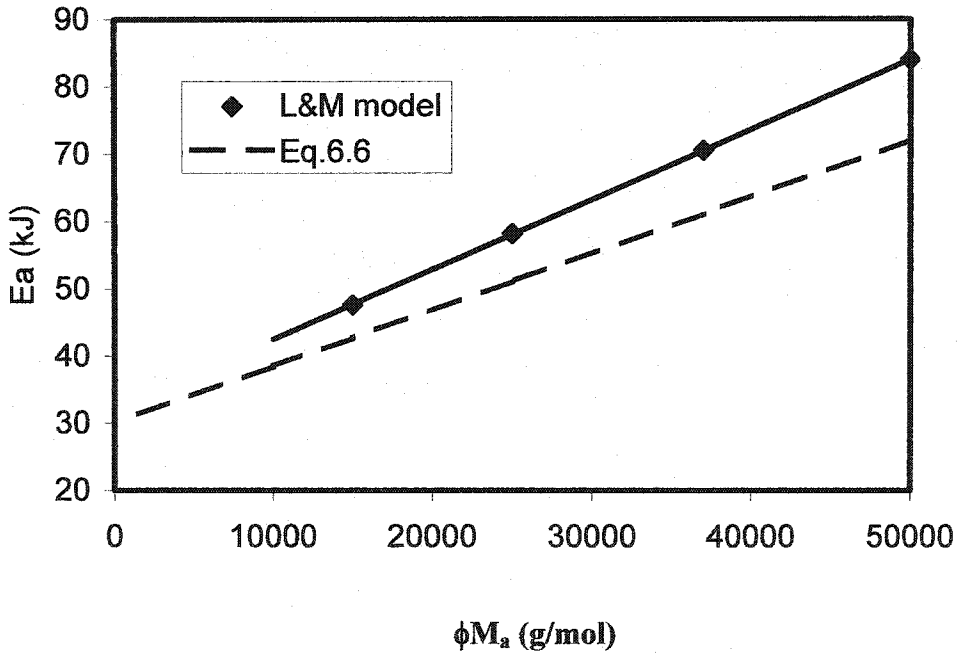

Figure 6.2 The apparent activation energy of star HPBD with different M_a, from Levine and Milner model and Eq.6.6

Figure 6.3 is the activation energy spectra for stars of different arm molecular weights at 190 °C. At shorter times, the activation energy spectra of star HPBD of different arm molecular weights converge to a constant (38 kJ/mol). This constant should be the activation energy of the linear material. Because of the inaccuracies of the model at shorter times, that constant is higher than the activation energy of the linear polymer (30.1 kJ/mol).

After the Rouse times (see Table 6.2), the activation energy spectrum increases with time until the arm is relaxed.

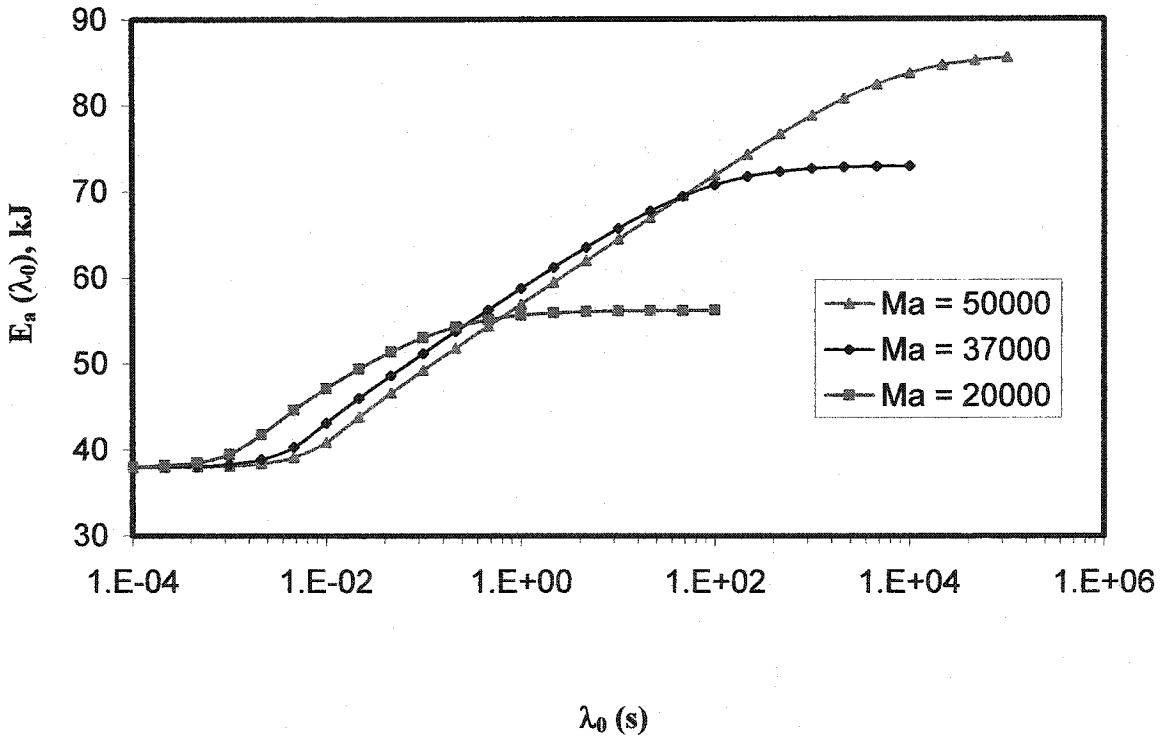

Figure 6.3 The activation energy spectra of HPBD stars of different arm molecular weights, at 190 °C, calculated from the Levine and Milner model.

Table 6.2 The relaxation time of whole arm, $\tau(1)$, and the Rouse time, τ_R, from the model of Levine and Milner.

Ma		20000	37000	50000
$\tau(1)$, s	190 °C	0.20	118.5	11257
	160 °C	0.54	440.7	52765
τ_R, s	190 °C	4.51E-4	1.55E-3	2.82E-3
	160 °C	8.69E-4	2.98E-3	5.43E-3

Note: The $\tau(1)$ is the relaxation time, $\tau(s)$, at $s = 1$ in Eq.6.1. It is the time when the stress is totally relaxed.

The τ_R is the Rouse time, $\tau_R = \tau_e (M_a/M_e)^2$.

The molecular weight not only affects the magnitude of the activation energy spectrum, but also its breadth, which ranges from the Rouse time to the time that the stress is totally relaxed.

6.2 Linear and Star Blends

Milner and McLeish et al.[31] used the arm retraction theory to develop a model of linear and star blends, Eq.2.24-2.30. The final result is:

$$\begin{aligned}\frac{G(t)}{G_0} &= 2\phi_s \int_0^{s_d} \Phi_<(s)\exp[-t/\tau_{s<}(s)]ds + \\ &2\phi_l \int_0^{s_d} \Phi_<(s')\exp[-t/\tau_{s<}(s')]ds' + \\ &\phi_s \int_{s_d}^{s_c} \frac{\Phi(\tau)}{2\tau}\exp[-t/\tau]d\tau + \\ &2\phi_s \int_{s_d}^{1} \Phi_>(s)\exp[-t/\tau_{s>}(s)]ds + \\ &\Phi_d[\Phi_d - \phi_s(1-s_d)]\exp(-t/\tau_d)\end{aligned} \qquad [6.7]$$

The first two terms correspond to arm retraction of stars and contour-length fluctuations of linear chains before reptation time τ_d. ϕ_s and ϕ_l are the volume fraction of star and linear polymers, s is the fraction length of star arm, Φ is the fraction of unrelaxed chains; s_d is the fraction length of star arm chain at reptation time τ_d. The symbol " ' " corresponds to the linear chain. The linear chain can be looked as a two-arm star before the reptation time τ_d. The third term accounts for stress relaxed during the constraint-release regime, it starts at the reptation time τ_d, and ends at a time τ_C. The τ_C and $\Phi(\tau)$ are obtained from Eq.2.26 and Eq.2.27. The fourth term comes from star arm retraction after the constraint-release regime. The final term is the stress lost by reptation of the linear chains, Φ_d is the volume fraction of entangled chains at the reptation time.

We used this model with a temperature dependent entanglement molecular weight for the stars to study the effect of the volume fraction of stars on the thermorheological complexity of star-linear blends.

In order to compare the results of this study to those of the Levine and Milner model, we used the same parameters ($M_e = 2056$, $\tau_e = 4.77 \times 10^{-6}$ s) that were used with the Levine and Milner model, and chose a star-linear blend system with an arm molecular weight $M_a = 37000$ g/mol for stars and a molecular weight $M_L = 74000$ g/mol for linear chains.

Table 6.3 and Figure 6.4 present the apparent activation energy of star-linear blends with different volume fractions of stars. The apparent activation energy from the modified Milner and McLeish model increases linearly with increasing of the volume fraction of stars. The same reason of the inaccuracies of the model at shorter times as the

Levine and Milner model, the apparent activation energy from the modified Milner and McLeish model is higher than that from Eq.6.6.

Table 6.3 Apparent activation energy of star-linear blends of HPBD with M_a = 37000 g/mol for stars and M_L = 74000 g/mol for linear chains, kJ.

ϕ_S	0.25	0.5	0.75
Model	44.9	52.5	61.2
Eq.6.2	37.9	45.6	53.4

Note: ϕ_S is a volume fraction of stars.

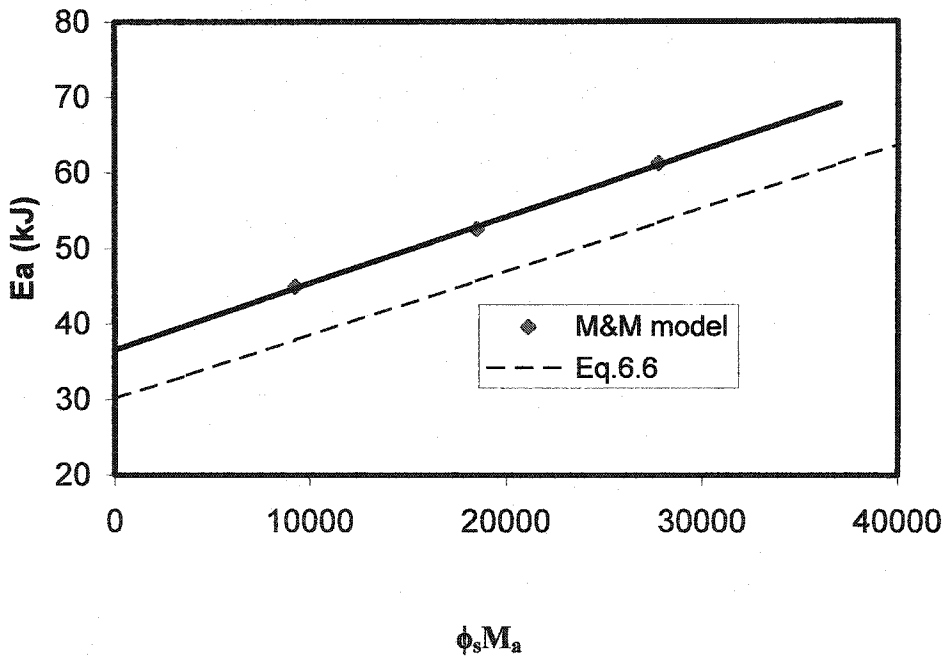

Figure 6.4 Apparent activation energy of star-linear blends of HPBD with M_a = 37000 g/mol for stars and M_W = 111000 g/mol for linears.

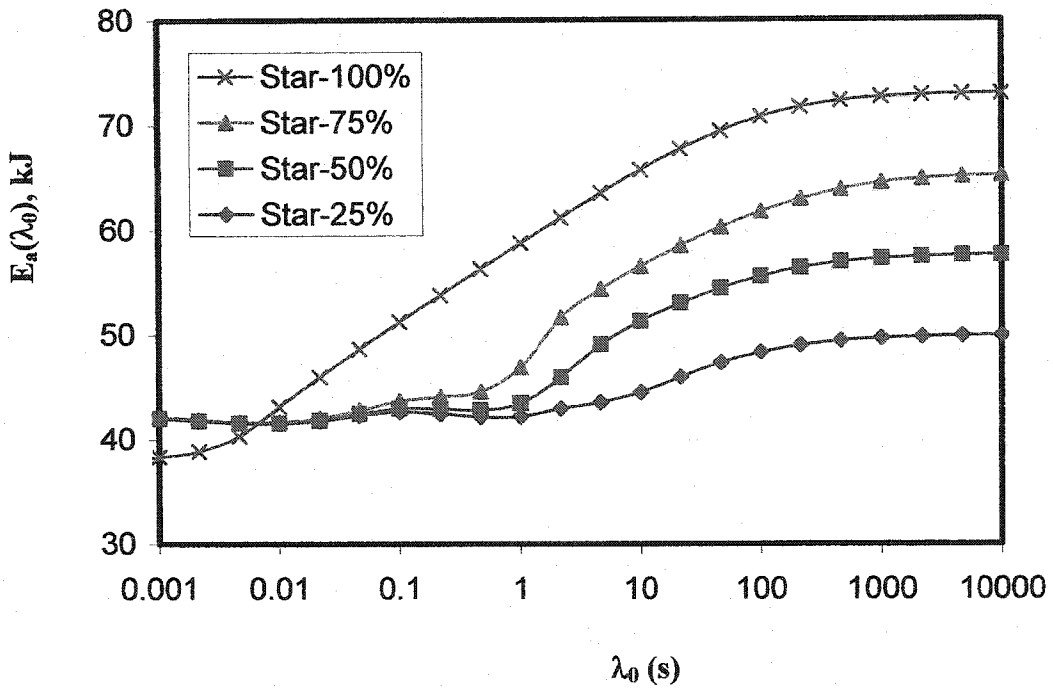

Figure 6.5 Activation energy spectra of star-linear blends of HPBD with M_a = 37000 g/mol, M_L = 74000 g/mol, at 190 °C, calculated from Milner and McLeish model. The spectrum of pure star was calculated from the Levine and Milner model.

Table 6.4 The constraint-release regime of star-linear blends of HPBD.

ϕ_s		0.25	0.5	0.75
τ_d, s	190 °C	0.29	0.29	0.29
	160 °C	0.61	0.61	0.61
τ_c, s	190 °C	4.64	1.16	0.52
	160 °C	9.72	2.43	1.08

Note: τ_d, the reptation time, was calculated from Eq.2.25.

τ_C, the constraint-release end time, was calculated from Ea.2.26.

Figure 6.5 shows the activation energy spectra of star-linear blends of HPBD at 190 °C calculated with the modified Milner and McLeish model, the spectrum of pure stars, $\phi_S = 1$, comes from the Levine and Milner model. All spectra were calculated from G(t) at 190 °C and 160 °C. In the time range from 0.1 s to 10 s, the spectra from the Milner and McLeish model do not increase with time as dose the spectrum from the Levine and Milner model. This time range corresponds to the constraint-release time range, from τ_d to τ_C (see Table 6.4), which should not be thermorheologically complex.

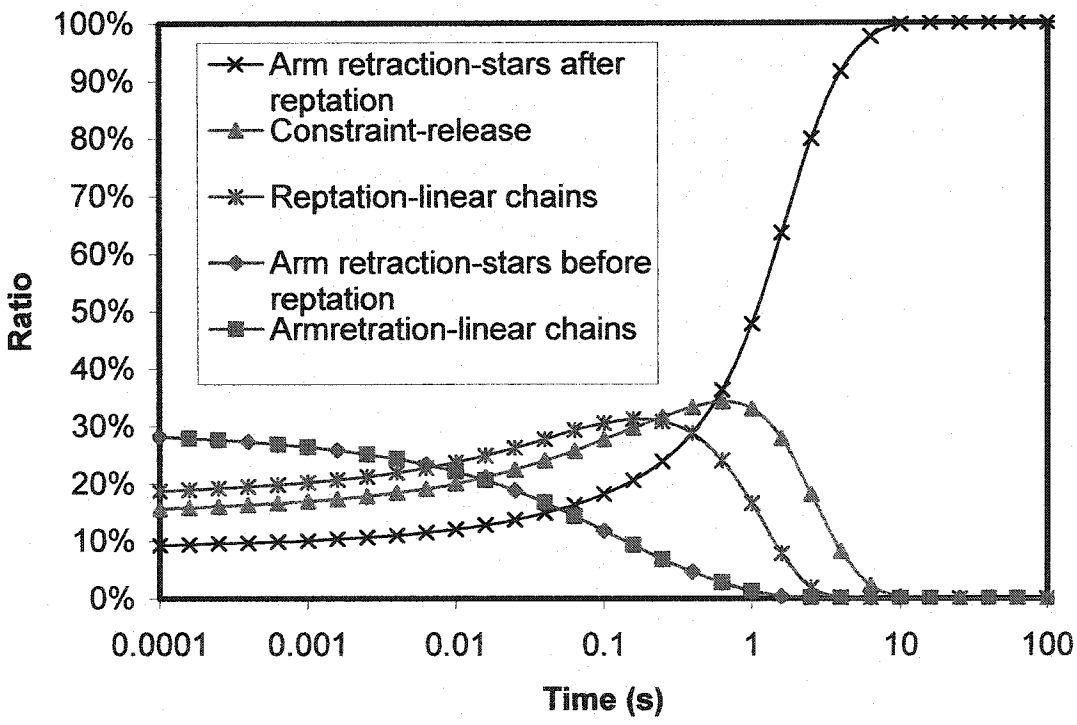

Figure 6.6 The contributions to G(t) of each term in Eq.6.7.

Figure 6.6 shows the contributions to G(t) of each term in Eq.6.7 for $\phi_S = 0.5$ at 190 °C. In the time range from 0.1 s to 10 s, constraint-release and reptation of linear chains

give the main contributions to the relaxation modulus. Constraint-release and reptation of linear chains are not thermorhoelogically complex processes, thus the activation energy spectrum from the modified Milner and McLeish model has a plateau in this time regime.

In Figure 6.5, the activation energy spectra of different volume fraction of stars converge to a constant (41 kJ/mol) at shorter times. This value is littler high than that from the Levine and Milner model (38 kJ/mol). This is because of the difference of the two models at shorter times. In the Levine and Milner model, $\tau(s) = \tau_R \exp[U(s)]$, τ_R is the reptation time. In the Milner and McLeish model, $\tau(s) = p(s)\exp[U(s)]$, p(s) is defined by Eq.2.23, they reported that using p(s) instead of τ_R improved the data agreement at shorter times[29, 30]. At longer times, the magnitude of the spectrum increases with increasing the star fraction. The star fraction does not affect the breadth of the activation energy spectrum.

6.3 Results of Theoretical Analysis

According the Levine and Milner model and the modified Milner and McLeish model, the apparent activation energy of long chain branched PE increases linearly with a product of the volume fraction of stars and the arm molecular weight, agreeing with experimental results of Raju et al [11-14] and Wood-Adams and Costex [10].

The activation energy spectrum converges to the activation energy of the linear material at short times, this also agrees with the experimental results of this work and Wood-Adams and Costex's [10].

The arm molecular weight not only affects the magnitude of the activation energy spectrum, but also affects the breadth of the spectrum. The volume fraction of stars only affects the magnitude of the activation energy spectrum.

7 Conclusions

- For thermorheologically complex materials, the time shift factors of the relaxation modulus, storage and loss modulus are different, but the relaxation modulus and relaxation spectrum have the same time shift factor. Therefore the activation energy spectrum can be determined from the relaxation modulus. This activation energy spectrum is a characteristic material function. Therefore, by combining it with the relaxation spectrum at the reference temperature, viscoelastic properties at different temperatures can be predicted.
- The activation energy spectrum of long chain branched metallocene polyethylene is close to the activation energy of the linear material at short times, it increases as long chain branching level increases at longer times.
- The apparent activation energy of metallocene polyethylene increases with a product of the branching level and the arm molecular weight.
- Linear hydrogenated polybutadiene is thermorheologically complex. Thus contour-length fluctuations of linear hydrogenated polybutadiene leads to the thermorheological complexity of this linear polymer. It proves that the arm retraction mechanism, which is equivalent to contour-length fluctuations of linear chains, leads to the thermorheological complexity of long chain branched polyethylene.
- The theoretical analysis based on the arm retraction theory verified that the apparent activation energy of long chain branched polyethylene increases linearly with a product of the volume fraction of long chain branches and the arm molecular weight.

- Based on the theoretical analysis, the activation energy spectrum of star polymers converges to the activation energy of the linear material before the Rouse time, then it increases until the arm is relaxed. The arm molecular weight not only affects the magnitude of the spectrum, but also affects the breadth of the spectrum. The volume fraction of stars in star-linear blends only affects the magnitude of the activation energy spectrum.

References

1. Wood-Adams, P. Ph.D. Thesis. *The Effect of Long Chain Branching on the Rheological Behavior of Polyethylenes Synthesized Using Constrained Geometry and Metallocene Catalysts.* McGill University, **1998.**
2. Scheirs, J. and Kaminsky, W. Ed. *Metallocene-Based Polyolefins: Preparation, Properties and Technology.* John Wiley & Sons Inc., New York, **2000.**
3. Kaminsky, W., *New Polymers by Metallocene Catalysis,* Macromol. Chem. Phys. **1996**, 197, 3907-3945.
4. Hamielec, A. E. and Soares, J. B. P., *Polymerization reaction engineering -- metallocene catalysts.* Prog. Polym. Sci. **1996**, 21, 651-706.
5. Costeux, S. and Wood-Adams, P. M., *Molecular Structure of Metallocene-Catalyzed Polyethylene: Rheologically Relevant Representation of Branching Architecture in Single Catalyst and Blended Systems.* Macromolecules, **2002**, 35, 2514-2528.
6. Dealy, J. M. and Wissbrun, K. F., *Melt Rheology and Its Role in Plastics Processing Theory and Applications,* Kluwer Academic Publishers, **1990**
7. Ferry, J. D. *Viscoelastic Properties of Polymers*, John Wiley & Sons Inc., **1980**
8. Gupta, R. K. *Polymer and Composite Rheology*, Second Edition, Revised and Expanded, Marcel Dekker, Inc. **2000**
9. Honerkamp, J. and Weese, J., *A Nonlinear regularization Method for the Calculation of Relaxation Spectra,* Rheol. Acat, **1993**, 32, 65-73.
10. Wood-Adams, P. M.; Costeux, S., *Thermorhological Behavior of Polyethylene: Effects of Microstructure and Long Chain Branching,* Macromolecules **2001**, 34, 6281-6290.

11. Raju, V. R.; Rachapudy, H., and Graessley, W. W., *Properties of Amorphous and Crystallizable Hydrocarbon Polymers. IV. Melt Rheology of Linear and Star-Branched Hydrogenated Polybutadiene*, J. Polym. Sci., Polym. Phys. Ed., **1979**, 17, 1223-1235.

12. Graessley, W. W. and Raju, V. R., *Some Rheological Properties of Solution and Blend of Hydrogenated Polybutadiene,* J. Polym. Sci., Polym. Symp., **1984,**71, 77-93.

13. Carella, J. M., and Graessley, W. W., *Effects of Chain Microstructure on the Viscoelastic Properties of Linear Polymer Melts: Polybutadiene and Hydrogenated Polybutadiene,* Macromolecules, **1984**, 17, 2775-2786.

14. Carella, J. M., and Graessley W. W.,, *Thermorheological Effects of Long-Chain Branching in Entangled Polymer Melts,* Macromolecules, **1986**, 19, 659-667.

15. Raju, V. R.; Smith, G. G.; Marin, G., Knox, J. R. and Graessley, W. W., *Properties of Amorphous and Crystallizable Hydrocarbon Polymers. I. Melt Rheology of Fractions of Linear Polyethylene,* J. Polym. Sci. Polym. Phys. Ed., **1979**, 17, 1183-1195.

16. Gabriel, C.; Kaschta, J. and Münstedt, H., *Influence of Molecular Structure on Rheological Properties of Polyethylenes*, Rheol. Acta. **1998**, 37, 7-20.

17. Gabriel, C. and Münstedt, H., *Creep Recovery Behavior of Metallocene Linear Low-Density Polyethylenes,* Rheol. Acta. **1999**, 38, 393-403.

18. Malmberg, A.; Liimatta, J.; Lehtinen, J. and Löfgren, B., *Characteristics of Long Chain Branching in Ethylene Polymerization with Single Site Catalysts,* Macromolecules, **1999**, 32, 6687-6696

19. Yan, D.; Wang, W. J. and Zhu, S., *Effect of Long Chain Branching on Rheological Properties of Metallocene Polyethylene,* **Polymer**, 1999, 40, 1737-1744.

20. Marvidis, H. and Shroff, R. N., *Temperature Dependence of Polyolefin Melt Rheology,* Ploym. Eng. and Sci., **1992**, 32, 1778-1791

21. Graessley, W. W., *Effect of Long Branches on the Temperature Dependence of Viscoelastic Properties in Polymer Melt,* Macromolecules, **1982**, 15, 1164-1167

22. Kasehagen, L. J.; Macosko, C. W.; Trowbridge, D. and Magnus, F., *Rheology of Long-Chain Randomly Branched Polybutadiene*, J. Rheol., **1996**, 40, 689-709

23. Bero, C. A. and Roland, C. M., Macromolecules, **1996**, 29, 1911-1913

24. Doi, M. and Edwards, S. F., *The Theory of Polymer Dynamics,* Oxford University Press, Oxford, **1986**.

25. Doi, M., *Introduction to Polymer Physics,* Clarendon Press, Oxford, **1996**.

26. Likhtman, A. E. and McLeish, T. C. B., *Quantitative theory for linear dynamics of linear entangled Polymers,* Macromolecules, **2002**,

27. Pearson, D. S. and Helfand, E., *viscoelastic Properties of Star-Shaped Polymers,* Maromolecules, **1984**, 17, 888-895.

28. Ball, R. C. and McLeish, T. C. B., *Dynamic Dilution and the Viscosity of Star Polymer Melts,* Macromolecules, **1989**, 22, 1911-1913.

29. Milner, S. T. and McLeish, T. C. B., *Parameter-Free Theory for Stress Relaxation in Star Polymer Melts,* Macromolecules, **1997**, 30, 2159-2166.

30. Milner, S. T. and McLeish, T. C. B., *Arm-Length Dependence of Stress Relaxation in Star Polymer Melts,* Macromolecules, **1998**, 31, 7479-7482.

31. Milner, S. T.; McLeish, T. C. B.; Young, R. N.; Hakiki, A. and Johnson, J. M., *Dynamic Dilution, Constraint-Release, and Star-Linear Blend,* Macromolecules, **1998**, 31, 9345-9353.

32. Levine A. J. and Milner S. T., *Star Polymers and the Failure of Time-Temperature Superposition,* Macromolecules, **1998**, 31, 8623-8637.

33. Kraft, M.; Meissner, J.; Kaschta Macromolecules **1999**, 32, 751-757.

34. Chunxia, H.; Wood-Adams, P. M.; John, M. D.; Robert, L. S. and Teresa, P. K., *Linear Viscoelastic Characterization of High-Melt-Strength Polypropylenes over a Broad Range of Frequencies,* **2002**

35. Mason, R. T., *Statistical Design and Analysis of Experiments,* John Wiley & Sons Inc., **1989**.

36. Wood-Adams, P. M.; Dealy, J. M.; DeGroot, A. W. and Redwine, O.D., *Effect of Molecular Structure on the Linear Viscoelastic Behavior of Polyethylene,* Macromolecules **2000**, 33, 7489-7499.

37. Malmberg, A., Kokko, E., Lehmus, P., Löfgren, B., and Seppälä, J. V., *Long-Chain Branched Polyethylene Polymerized by Metallocene Catalysts*, Macromolecules, **1998**, 31, 8448-8454.

38. Kim, Y. S.; Chung, C. I.; Lai, S. Y. and Hyun, K. S., J. Appl. Polym. Sci. **1996**, 59, 125.

39. Fetters L. J., Lohse, D. J., Richter D., Witten T. A. and Zirkel A. *Connection Between Polymer Molecular Weight, Density, Chain Dimensions, and Melt Viscoelastic Properties,* Macromolecules, 1994, 27, 4639-4647.

40. Jutta, L. *Effect of Small-scale Architecture on Polymer Mobility,* Journal of Chemical Physics, 2002, 112, 5473-5479.

Nomenclature

ROMAN LETTERS

a_T Time shift factor

E_a Activation energy for flow

$\hat{E}_a$ Apparent activation energy for flow

$E_a(\lambda)$ Activation energy spectrum

$E_a(\lambda)$ Activation energy spectrum at reference temperature

$G(t)$ Shear stress relaxation modulus

G_0 Plateau modulus

G_N^0 Plateau modulus

$G'(\omega)$ Storage modulus

$G''(\omega)$ Loss modulus

$G^*(\omega)$ Complex modulus

$H(\lambda)$ Relaxation spectrum

$H(\lambda_0)$ Relaxation spectrum at reference temperature

$J(t)$ Shear creep compliance

J_S^0 Steady state compliance

$J'(\omega)$ Storage compliance

$J''(\omega)$ Loss compliance

$J^*(\omega)$ Complex compliance

$L(\lambda)$ Retardation spectrum

M_a Arm molecular weight

M_e Average molecular weight between entanglements

Mn Number average molecular weight

M_W Weight average molecular weight

n_a Length of star arm

n_l Length of linear chain

N Arm length

N_e Entanglement segment length

PI Polydispersity index

s Fraction distance of star arm

s_d Fraction distance at reptation time

t Time

T Temperature

T_0 Reference temperature

U(s) Barrier potential for arm retraction

GREEK LETTERS

γ Shear strain

γ_0 Strain amplitude in oscillatory shear

δ Mechanical loss angle

η Viscosity

η_0 Zero shear viscosity

$\eta^*(\omega)$ Complex viscosity

λ Relaxation time

ρ Density

σ Shear stress

σ_0 Stress amplitude in oscillatory shear

τ Relaxation time

τ_C Constraint-release ends time

τ_d Reptation time

τ_e Rouse time for entanglement segment

τ_R Rouse time

ϕ_l Volume fraction of linear chains

ϕ_s Volume fraction of stars

$\Phi(t)$ Effective entangled volume fraction

$\Phi(\tau_d)$ Entangled volume fraction at reptation time

Appendix

Oscillatory Shear Experimental Data and the Relaxation Spectrum

Table A 1 Oscillatory Shear Experimental Data of the HDB5

Temp.	150 °C				160 °C			
Frequency	G'		G"		G'		G"	
rad/s	Pa	CV	Pa	CV	Pa	CV	Pa	CV
5.00E+02	3.19E+05	1.4%	2.38E+05	1.4%	2.88E+05	0.7%	2.25E+05	0.6%
3.87E+02	2.83E+05	1.4%	2.20E+05	1.4%	2.54E+05	0.7%	2.07E+05	0.6%
3.00E+02	2.49E+05	1.3%	2.03E+05	1.3%	2.23E+05	0.7%	1.90E+05	0.6%
2.32E+02	2.18E+05	1.4%	1.86E+05	1.3%	1.95E+05	0.7%	1.73E+05	0.7%
1.80E+02	1.90E+05	1.4%	1.69E+05	1.3%	1.69E+05	0.7%	1.56E+05	0.7%
1.39E+02	1.65E+05	1.4%	1.52E+05	1.3%	1.47E+05	0.7%	1.40E+05	0.7%
1.08E+02	1.43E+05	1.4%	1.37E+05	1.3%	1.27E+05	0.7%	1.25E+05	0.7%
8.34E+01	1.24E+05	1.4%	1.22E+05	1.3%	1.10E+05	0.7%	1.11E+05	0.7%
6.46E+01	1.08E+05	1.4%	1.08E+05	1.3%	9.49E+04	0.7%	9.82E+04	0.7%
5.00E+01	9.35E+04	1.4%	9.54E+04	1.4%	8.22E+04	0.7%	8.64E+04	0.7%
3.87E+01	8.12E+04	1.4%	8.40E+04	1.4%	7.13E+04	0.7%	7.58E+04	0.7%
3.00E+01	7.06E+04	1.4%	7.37E+04	1.4%	6.20E+04	0.8%	6.64E+04	0.7%
2.32E+01	6.16E+04	1.4%	6.46E+04	1.3%	5.39E+04	0.7%	5.81E+04	0.7%
1.80E+01	5.38E+04	1.4%	5.66E+04	1.4%	4.70E+04	0.8%	5.08E+04	0.7%
1.39E+01	4.70E+04	1.4%	4.96E+04	1.3%	4.10E+04	0.8%	4.46E+04	0.7%
1.08E+01	4.11E+04	1.4%	4.36E+04	1.4%	3.58E+04	0.9%	3.91E+04	0.8%
8.34E+00	3.60E+04	1.4%	3.83E+04	1.4%	3.12E+04	0.8%	3.43E+04	0.7%
6.46E+00	3.15E+04	1.4%	3.37E+04	1.4%	2.72E+04	0.8%	3.02E+04	0.8%
5.00E+00	2.75E+04	1.4%	2.96E+04	1.4%	2.36E+04	0.8%	2.65E+04	0.8%
5.00E+00	2.75E+04	1.4%	2.97E+04	1.4%	2.36E+04	0.8%	2.66E+04	0.8%
3.87E+00	2.39E+04	1.4%	2.62E+04	1.4%	2.05E+04	0.8%	2.34E+04	0.7%
3.00E+00	2.08E+04	1.4%	2.31E+04	1.3%	1.77E+04	0.8%	2.06E+04	0.8%
2.32E+00	1.80E+04	1.4%	2.04E+04	1.4%	1.52E+04	0.8%	1.82E+04	0.8%
1.80E+00	1.55E+04	1.4%	1.80E+04	1.4%	1.30E+04	0.9%	1.60E+04	0.8%
1.39E+00	1.33E+04	1.4%	1.59E+04	1.4%	1.10E+04	0.9%	1.41E+04	0.8%
1.08E+00	1.13E+04	1.4%	1.40E+04	1.4%	9.26E+03	0.9%	1.24E+04	0.8%
8.34E-01	9.56E+03	1.4%	1.24E+04	1.4%	7.76E+03	0.9%	1.08E+04	0.8%
6.46E-01	8.03E+03	1.4%	1.09E+04	1.4%	6.43E+03	1.0%	9.44E+03	0.8%
5.00E-01	6.68E+03	1.4%	9.50E+03	1.4%	5.30E+03	0.9%	8.20E+03	0.8%
5.00E-01	6.68E+03	1.4%	9.52E+03	1.4%	5.28E+03	1.0%	8.21E+03	0.9%
3.15E-01	4.69E+03	1.4%	7.40E+03	1.5%	3.61E+03	1.0%	6.30E+03	0.9%
1.99E-01	3.20E+03	1.4%	5.67E+03	1.4%	2.41E+03	1.1%	4.75E+03	0.9%
1.26E-01	2.11E+03	1.4%	4.26E+03	1.4%	1.55E+03	1.0%	3.51E+03	0.9%
7.92E-02	1.35E+03	1.4%	3.14E+03	1.3%	9.60E+02	1.1%	2.54E+03	0.9%
5.00E-02	8.28E+02	1.6%	2.26E+03	1.4%	5.70E+02	1.5%	1.80E+03	0.9%
3.15E-02	4.89E+02	1.5%	1.60E+03	1.4%	3.27E+02	1.0%	1.25E+03	0.9%
1.99E-02	2.77E+02	2.2%	1.10E+03	1.1%	1.78E+02	2.0%	8.57E+02	0.9%
1.26E-02	1.52E+02	3.2%	7.48E+02	0.9%	9.36E+01	4.1%	5.78E+02	0.6%

Note: CV is the coefficient of variation, it equals the standard deviation divided by the average.

Continues Table A1

Temp.	170 °C				180 °C			
Frequency	G'		G"		G'		G"	
rad/s	Pa	CV	Pa	CV	Pa	CV	Pa	CV
5.00E+02	2.68E+05	0.3%	2.20E+05	0.2%	2.45E+05	1.6%	2.09E+05	1.5%
3.87E+02	2.36E+05	0.3%	2.01E+05	0.4%	2.15E+05	1.6%	1.91E+05	1.5%
3.00E+02	2.06E+05	0.3%	1.83E+05	0.4%	1.87E+05	1.6%	1.73E+05	1.5%
2.32E+02	1.79E+05	0.3%	1.66E+05	0.4%	1.62E+05	1.6%	1.56E+05	1.5%
1.80E+02	1.55E+05	0.3%	1.49E+05	0.3%	1.40E+05	1.6%	1.39E+05	1.5%
1.39E+02	1.34E+05	0.3%	1.33E+05	0.3%	1.21E+05	1.6%	1.24E+05	1.4%
1.08E+02	1.16E+05	0.3%	1.18E+05	0.2%	1.04E+05	1.6%	1.10E+05	1.5%
8.34E+01	9.98E+04	0.3%	1.04E+05	0.2%	8.96E+04	1.6%	9.65E+04	1.5%
6.46E+01	8.64E+04	0.6%	9.19E+04	0.3%	7.73E+04	1.7%	8.47E+04	1.6%
5.00E+01	7.46E+04	0.3%	8.07E+04	0.3%	6.68E+04	1.7%	7.42E+04	1.6%
3.87E+01	6.46E+04	0.3%	7.06E+04	0.3%	5.78E+04	1.7%	6.48E+04	1.6%
3.00E+01	5.60E+04	0.3%	6.18E+04	0.3%	5.01E+04	1.7%	5.67E+04	1.6%
2.32E+01	4.87E+04	0.3%	5.41E+04	0.2%	4.34E+04	1.7%	4.95E+04	1.6%
1.80E+01	4.23E+04	0.3%	4.73E+04	0.3%	3.76E+04	1.7%	4.32E+04	1.6%
1.39E+01	3.68E+04	0.3%	4.14E+04	0.3%	3.26E+04	1.7%	3.78E+04	1.6%
1.08E+01	3.20E+04	0.3%	3.62E+04	0.3%	2.82E+04	1.7%	3.30E+04	1.6%
8.34E+00	2.78E+04	0.3%	3.18E+04	0.3%	2.44E+04	1.7%	2.90E+04	1.6%
6.46E+00	2.41E+04	0.3%	2.79E+04	0.2%	2.10E+04	1.8%	2.54E+04	1.6%
5.00E+00	2.08E+04	0.3%	2.45E+04	0.2%	1.80E+04	1.8%	2.22E+04	1.7%
5.00E+00	2.08E+04	0.3%	2.45E+04	0.2%	1.80E+04	1.8%	2.22E+04	1.7%
3.87E+00	1.79E+04	0.4%	2.15E+04	0.3%	1.54E+04	1.9%	1.95E+04	1.7%
3.00E+00	1.53E+04	0.3%	1.89E+04	0.3%	1.31E+04	1.9%	1.71E+04	1.7%
2.32E+00	1.30E+04	0.3%	1.66E+04	0.3%	1.11E+04	1.8%	1.49E+04	1.7%
1.80E+00	1.10E+04	0.3%	1.46E+04	0.3%	9.28E+03	1.8%	1.30E+04	1.7%
1.39E+00	9.28E+03	0.3%	1.28E+04	0.3%	7.72E+03	1.8%	1.14E+04	1.7%
1.08E+00	7.74E+03	0.3%	1.11E+04	0.3%	6.38E+03	1.8%	9.86E+03	1.7%
8.34E-01	6.41E+03	0.3%	9.68E+03	0.3%	5.22E+03	1.8%	8.52E+03	1.7%
6.46E-01	5.26E+03	0.4%	8.39E+03	0.3%	4.23E+03	1.8%	7.34E+03	1.7%
5.00E-01	4.27E+03	0.5%	7.23E+03	0.4%	3.40E+03	1.8%	6.28E+03	1.7%
5.00E-01	4.23E+03	0.5%	7.23E+03	0.4%	3.35E+03	1.8%	6.27E+03	1.7%
3.15E-01	2.83E+03	0.5%	5.46E+03	0.4%	2.19E+03	1.8%	4.67E+03	1.7%
1.99E-01	1.84E+03	0.6%	4.06E+03	0.4%	1.39E+03	1.9%	3.42E+03	1.8%
1.26E-01	1.15E+03	0.6%	2.95E+03	0.4%	8.44E+02	2.1%	2.45E+03	1.8%
7.92E-02	6.89E+02	0.8%	2.10E+03	0.4%	4.95E+02	2.1%	1.72E+03	1.9%
5.00E-02	4.00E+02	0.6%	1.47E+03	0.5%	2.77E+02	1.9%	1.18E+03	2.0%
3.15E-02	2.21E+02	1.2%	1.00E+03	0.8%	1.48E+02	1.9%	7.99E+02	1.8%
1.99E-02	1.19E+02	3.3%	6.74E+02	0.4%	7.56E+01	2.5%	5.31E+02	1.7%

1.26E-02	6.24E+01	4.2%	4.43E+02	0.8%	3.65E+01	2.3%	3.49E+02	1.7%

Continues Table A1

Temp.	190 °C			
Frequency	G'		G"	
rad/s	Pa	CV	Pa	CV
5.00E+02	2.24E+05	1.2%	1.99E+05	1.2%
3.87E+02	1.96E+05	1.3%	1.80E+05	1.2%
3.00E+02	1.70E+05	1.1%	1.63E+05	1.3%
2.32E+02	1.47E+05	1.3%	1.46E+05	1.2%
1.80E+02	1.26E+05	1.3%	1.30E+05	1.2%
1.39E+02	1.09E+05	1.3%	1.15E+05	1.2%
1.08E+02	9.36E+04	1.3%	1.02E+05	1.2%
8.34E+01	8.05E+04	1.3%	8.91E+04	1.2%
6.46E+01	6.94E+04	1.3%	7.80E+04	1.2%
5.00E+01	5.98E+04	1.3%	6.82E+04	1.3%
3.87E+01	5.17E+04	1.3%	5.96E+04	1.3%
3.00E+01	4.47E+04	1.3%	5.20E+04	1.3%
2.32E+01	3.86E+04	1.3%	4.53E+04	1.3%
1.80E+01	3.34E+04	1.3%	3.95E+04	1.3%
1.39E+01	2.88E+04	1.2%	3.45E+04	1.3%
1.08E+01	2.49E+04	1.3%	3.02E+04	1.2%
8.34E+00	2.14E+04	1.3%	2.64E+04	1.3%
6.46E+00	1.83E+04	1.3%	2.31E+04	1.3%
5.00E+00	1.56E+04	1.3%	2.02E+04	1.3%
5.00E+00	1.56E+04	1.4%	2.02E+04	1.3%
3.87E+00	1.32E+04	1.4%	1.76E+04	1.4%
3.00E+00	1.12E+04	1.4%	1.54E+04	1.4%
2.32E+00	9.33E+03	1.4%	1.34E+04	1.4%
1.80E+00	7.76E+03	1.3%	1.17E+04	1.4%
1.39E+00	6.39E+03	1.4%	1.01E+04	1.4%
1.08E+00	5.22E+03	1.4%	8.70E+03	1.4%
8.34E-01	4.22E+03	1.4%	7.48E+03	1.3%
6.46E-01	3.39E+03	1.4%	6.39E+03	1.4%
5.00E-01	2.68E+03	1.4%	5.43E+03	1.4%
5.00E-01	2.63E+03	1.4%	5.42E+03	1.4%
3.15E-01	1.68E+03	1.4%	3.98E+03	1.4%
1.99E-01	1.04E+03	1.5%	2.87E+03	1.4%
1.26E-01	6.17E+02	1.5%	2.03E+03	1.5%
7.92E-02	3.50E+02	1.7%	1.40E+03	1.5%
5.00E-02	1.91E+02	1.1%	9.54E+02	1.7%
3.15E-02	9.84E+01	2.4%	6.36E+02	1.8%
1.99E-02	5.05E+01	5.8%	4.18E+02	1.4%

Table A 2 Oscillatory Shear Experimental Data of the HDB6

Temp.	150 °C				170 °C			
Frequency	G'		G"		G'		G"	
rad/s	Pa	CV	rad/s	CV	rad/s	CV	rad/s	CV
5.00E+02	2.50E+05	1.3%	1.90E+05	1.2%	2.03E+05	1.6%	1.67E+05	1.8%
3.87E+02	2.24E+05	1.4%	1.75E+05	1.2%	1.80E+05	1.6%	1.52E+05	1.8%
3.00E+02	1.98E+05	1.4%	1.59E+05	1.2%	1.59E+05	1.6%	1.37E+05	1.8%
2.32E+02	1.75E+05	1.4%	1.44E+05	1.2%	1.40E+05	1.6%	1.23E+05	1.7%
1.80E+02	1.55E+05	1.4%	1.30E+05	1.2%	1.24E+05	1.6%	1.10E+05	1.7%
1.39E+02	1.37E+05	1.5%	1.16E+05	1.2%	1.09E+05	1.6%	9.84E+04	1.7%
1.08E+02	1.21E+05	1.5%	1.04E+05	1.3%	9.57E+04	1.6%	8.77E+04	1.6%
8.34E+01	1.07E+05	1.5%	9.33E+04	1.3%	8.42E+04	1.6%	7.80E+04	1.7%
6.46E+01	9.46E+04	1.5%	8.32E+04	1.3%	7.42E+04	1.6%	6.93E+04	1.7%
5.00E+01	8.37E+04	1.5%	7.41E+04	1.2%	6.54E+04	1.6%	6.16E+04	1.7%
3.87E+01	7.42E+04	1.5%	6.61E+04	1.3%	5.76E+04	1.6%	5.48E+04	1.7%
3.00E+01	6.57E+04	1.5%	5.89E+04	1.3%	5.07E+04	1.6%	4.88E+04	1.7%
2.32E+01	5.82E+04	1.5%	5.25E+04	1.3%	4.46E+04	1.6%	4.34E+04	1.7%
1.80E+01	5.15E+04	1.6%	4.69E+04	1.3%	3.91E+04	1.6%	3.87E+04	1.7%
1.39E+01	4.55E+04	1.6%	4.20E+04	1.4%	3.42E+04	1.6%	3.45E+04	1.7%
1.08E+01	4.01E+04	1.6%	3.76E+04	1.3%	2.98E+04	1.6%	3.07E+04	1.7%
8.34E+00	3.53E+04	1.7%	3.37E+04	1.3%	2.59E+04	1.6%	2.74E+04	1.7%
6.46E+00	3.09E+04	1.7%	3.01E+04	1.3%	2.24E+04	1.7%	2.43E+04	1.6%
5.00E+00	2.70E+04	1.8%	2.70E+04	1.3%	1.93E+04	1.7%	2.16E+04	1.7%
5.00E+00	2.70E+04	1.7%	2.70E+04	1.4%	1.93E+04	1.6%	2.16E+04	1.7%
3.87E+00	2.35E+04	1.8%	2.41E+04	1.4%	1.65E+04	1.6%	1.91E+04	1.7%
3.00E+00	2.03E+04	1.8%	2.15E+04	1.4%	1.40E+04	1.6%	1.69E+04	1.7%
2.32E+00	1.74E+04	1.8%	1.92E+04	1.5%	1.18E+04	1.6%	1.50E+04	1.7%
1.80E+00	1.49E+04	2.0%	1.71E+04	1.5%	9.95E+03	1.6%	1.32E+04	1.7%
1.39E+00	1.27E+04	2.0%	1.51E+04	1.6%	8.30E+03	1.6%	1.15E+04	1.6%
1.08E+00	1.07E+04	2.0%	1.34E+04	1.6%	6.86E+03	1.6%	1.00E+04	1.8%
8.34E-01	8.99E+03	2.1%	1.18E+04	1.7%	5.64E+03	1.7%	8.72E+03	1.8%
6.46E-01	7.50E+03	2.2%	1.03E+04	1.7%	4.60E+03	1.7%	7.54E+03	1.8%
5.00E-01	6.19E+03	2.2%	9.03E+03	1.7%	3.71E+03	1.6%	6.47E+03	1.8%
5.00E-01	6.19E+03	2.3%	9.05E+03	1.8%	3.68E+03	1.6%	6.48E+03	1.7%
3.15E-01	4.29E+03	2.5%	6.99E+03	1.9%	2.45E+03	1.5%	4.86E+03	1.8%
1.99E-01	2.91E+03	2.7%	5.31E+03	2.0%	1.58E+03	1.5%	3.59E+03	1.7%
1.26E-01	1.91E+03	2.7%	3.97E+03	2.2%	9.88E+02	1.5%	2.60E+03	1.6%
7.92E-02	1.22E+03	2.7%	2.90E+03	2.2%	5.96E+02	1.4%	1.84E+03	1.7%
5.00E-02	7.48E+02	3.4%	2.09E+03	2.4%	3.45E+02	1.3%	1.28E+03	1.8%
3.15E-02	4.45E+02	3.6%	1.48E+03	2.6%	1.92E+02	2.8%	8.79E+02	1.9%
1.99E-02	2.57E+02	1.2%	1.02E+03	2.7%	1.04E+02	3.0%	5.90E+02	2.2%

Continues Table A2

Temp.	190 C			
Frequency	G'		G"	
rad/s	Pa	CV	Pa	CV
5.00E+02	1.72E+05	0.4%	1.51E+05	0.2%
3.87E+02	1.52E+05	0.5%	1.36E+05	0.3%
3.00E+02	1.33E+05	0.4%	1.22E+05	0.1%
2.32E+02	1.17E+05	0.5%	1.09E+05	0.3%
1.80E+02	1.03E+05	0.5%	9.69E+04	0.3%
1.39E+02	8.99E+04	0.5%	8.61E+04	0.3%
1.08E+02	7.88E+04	0.4%	7.64E+04	0.3%
8.34E+01	6.91E+04	0.5%	6.77E+04	0.3%
6.46E+01	6.05E+04	0.5%	6.00E+04	0.3%
5.00E+01	5.30E+04	0.5%	5.33E+04	0.4%
3.87E+01	4.64E+04	0.6%	4.72E+04	0.4%
3.00E+01	4.05E+04	0.6%	4.19E+04	0.4%
2.32E+01	3.53E+04	0.6%	3.71E+04	0.4%
1.80E+01	3.06E+04	0.6%	3.29E+04	0.5%
1.39E+01	2.65E+04	0.6%	2.92E+04	0.5%
1.08E+01	2.28E+04	0.6%	2.59E+04	0.4%
8.34E+00	1.95E+04	0.6%	2.29E+04	0.5%
6.46E+00	1.66E+04	0.6%	2.02E+04	0.4%
5.00E+00	1.41E+04	0.6%	1.78E+04	0.5%
5.00E+00	1.41E+04	0.6%	1.78E+04	0.4%
3.87E+00	1.19E+04	0.8%	1.56E+04	0.3%
3.00E+00	9.93E+03	0.5%	1.37E+04	0.4%
2.32E+00	8.25E+03	0.7%	1.19E+04	0.4%
1.80E+00	6.79E+03	0.7%	1.04E+04	0.5%
1.39E+00	5.56E+03	0.9%	8.97E+03	0.5%
1.08E+00	4.50E+03	0.6%	7.72E+03	0.5%
8.34E-01	3.62E+03	0.7%	6.61E+03	0.5%
6.46E-01	2.88E+03	0.7%	5.63E+03	0.6%
5.00E-01	2.28E+03	0.7%	4.76E+03	0.5%
5.00E-01	2.24E+03	0.8%	4.76E+03	0.5%
3.15E-01	1.42E+03	1.0%	3.47E+03	0.6%
1.99E-01	8.76E+02	0.9%	2.49E+03	0.7%
1.26E-01	5.20E+02	1.2%	1.76E+03	0.6%
7.92E-02	2.96E+02	1.2%	1.21E+03	0.7%
5.00E-02	1.62E+02	1.4%	8.22E+02	0.8%
3.15E-02	8.34E+01	0.8%	5.46E+02	1.5%

Table A 3 Oscillatory Shear Experimental Data of the HDB7

Temp.	150 °C				160 °C			
Frequency	G'		G"		G'		G"	
rad/s	Pa	CV	Pa	CV	Pa	CV	Pa	CV
5.00E+02	2.09E+05	1.3%	1.29E+05	1.3%	1.91E+05	0.4%	1.22E+05	0.5%
3.87E+02	1.92E+05	1.5%	1.18E+05	1.1%	1.75E+05	0.3%	1.12E+05	0.6%
3.00E+02	1.75E+05	1.3%	1.09E+05	1.3%	1.59E+05	0.3%	1.03E+05	0.5%
2.32E+02	1.59E+05	1.3%	1.01E+05	1.3%	1.45E+05	0.3%	9.48E+04	0.5%
1.80E+02	1.45E+05	1.4%	9.25E+04	1.2%	1.31E+05	0.3%	8.71E+04	0.5%
1.39E+02	1.32E+05	1.4%	8.50E+04	1.2%	1.19E+05	0.3%	8.02E+04	0.5%
1.08E+02	1.20E+05	1.3%	7.84E+04	1.1%	1.08E+05	0.3%	7.37E+04	0.5%
8.34E+01	1.09E+05	1.4%	7.22E+04	1.2%	9.74E+04	0.3%	6.76E+04	0.5%
6.46E+01	9.84E+04	1.5%	6.65E+04	1.2%	8.78E+04	0.4%	6.22E+04	0.5%
5.00E+01	8.89E+04	1.5%	6.12E+04	1.3%	7.90E+04	0.4%	5.71E+04	0.5%
3.87E+01	8.01E+04	1.5%	5.63E+04	1.3%	7.09E+04	0.3%	5.24E+04	0.4%
3.00E+01	7.21E+04	1.6%	5.18E+04	1.3%	6.34E+04	0.3%	4.80E+04	0.5%
2.32E+01	6.46E+04	1.6%	4.76E+04	1.3%	5.65E+04	0.3%	4.40E+04	0.5%
1.80E+01	5.77E+04	1.7%	4.37E+04	1.3%	5.02E+04	0.3%	4.03E+04	0.4%
1.39E+01	5.15E+04	1.8%	4.01E+04	1.3%	4.45E+04	0.3%	3.68E+04	0.5%
1.08E+01	4.57E+04	1.9%	3.68E+04	1.3%	3.92E+04	0.3%	3.36E+04	0.4%
8.34E+00	4.04E+04	1.9%	3.36E+04	1.3%	3.45E+04	0.3%	3.05E+04	0.5%
6.46E+00	3.56E+04	2.0%	3.06E+04	1.3%	3.01E+04	0.2%	2.76E+04	0.5%
5.00E+00	3.12E+04	2.1%	2.78E+04	1.4%	2.63E+04	0.2%	2.50E+04	0.4%
5.00E+00	3.12E+04	2.1%	2.78E+04	1.4%	2.63E+04	0.3%	2.50E+04	0.4%
3.87E+00	2.72E+04	2.2%	2.52E+04	1.5%	2.27E+04	0.3%	2.26E+04	0.5%
3.00E+00	2.37E+04	2.3%	2.28E+04	1.5%	1.96E+04	0.4%	2.03E+04	0.5%
2.32E+00	2.05E+04	2.4%	2.05E+04	1.6%	1.68E+04	0.3%	1.81E+04	0.5%
1.80E+00	1.77E+04	2.5%	1.84E+04	1.6%	1.44E+04	0.3%	1.62E+04	0.4%
1.39E+00	1.51E+04	2.6%	1.65E+04	1.7%	1.22E+04	0.3%	1.44E+04	0.4%
1.08E+00	1.29E+04	2.8%	1.47E+04	1.7%	1.03E+04	0.3%	1.27E+04	0.5%
8.34E-01	1.09E+04	2.9%	1.31E+04	1.8%	8.63E+03	0.3%	1.12E+04	0.5%
6.46E-01	9.19E+03	3.0%	1.15E+04	1.9%	7.19E+03	0.2%	9.83E+03	0.5%
5.00E-01	7.69E+03	3.2%	1.02E+04	2.0%	5.94E+03	0.3%	8.58E+03	0.5%
5.00E-01	7.67E+03	3.3%	1.02E+04	2.1%	5.92E+03	0.3%	8.59E+03	0.6%
3.15E-01	5.45E+03	3.6%	7.97E+03	2.3%	4.12E+03	0.3%	6.65E+03	0.6%
1.99E-01	3.80E+03	3.9%	6.16E+03	2.4%	2.80E+03	0.3%	5.06E+03	0.6%
1.26E-01	2.58E+03	4.3%	4.69E+03	2.6%	1.85E+03	0.2%	3.78E+03	0.7%
7.92E-02	1.70E+03	4.7%	3.50E+03	2.9%	1.19E+03	0.4%	2.78E+03	0.6%
5.00E-02	1.09E+03	5.4%	2.57E+03	3.0%	7.37E+02	0.2%	2.01E+03	0.6%
3.15E-02	6.78E+02	5.2%	1.85E+03	3.4%	4.40E+02	0.3%	1.42E+03	0.8%
1.99E-02	4.05E+02	5.4%	1.31E+03	3.4%	2.50E+02	2.6%	9.86E+02	1.1%
1.26E-02	2.31E+02	5.5%	9.10E+02	4.0%	1.41E+02	1.2%	6.70E+02	1.8%

Continues Table A3

Temp.	170 °C				180 °C			
Frequency	G'		G"		G'		G"	
rad/s	Pa	CV	Pa	CV	Pa	CV	Pa	CV
5.00E+02	1.76E+05	1.3%	1.16E+05	1.0%	1.65E+05	1.12E+05	1.2%	1.1%
3.87E+02	1.61E+05	1.3%	1.07E+05	1.0%	1.50E+05	1.02E+05	1.2%	1.1%
3.00E+02	1.46E+05	1.3%	9.78E+04	1.0%	1.36E+05	9.39E+04	1.3%	1.1%
2.32E+02	1.32E+05	1.3%	8.97E+04	1.0%	1.23E+05	8.60E+04	1.3%	1.1%
1.80E+02	1.20E+05	1.3%	8.22E+04	0.8%	1.11E+05	7.88E+04	1.3%	1.1%
1.39E+02	1.08E+05	1.4%	7.56E+04	1.0%	9.99E+04	7.21E+04	1.3%	1.1%
1.08E+02	9.77E+04	1.4%	6.93E+04	1.1%	8.98E+04	6.60E+04	1.3%	1.1%
8.34E+01	8.79E+04	1.5%	6.35E+04	1.1%	8.05E+04	6.04E+04	1.3%	1.2%
6.46E+01	7.89E+04	1.6%	5.83E+04	1.2%	7.20E+04	5.52E+04	1.4%	1.2%
5.00E+01	7.07E+04	1.6%	5.33E+04	1.2%	6.42E+04	5.05E+04	1.3%	1.1%
3.87E+01	6.31E+04	1.6%	4.88E+04	1.2%	5.71E+04	4.61E+04	1.4%	1.2%
3.00E+01	5.61E+04	1.7%	4.46E+04	1.2%	5.06E+04	4.21E+04	1.4%	1.2%
2.32E+01	4.98E+04	1.7%	4.08E+04	1.2%	4.46E+04	3.83E+04	1.4%	1.3%
1.80E+01	4.40E+04	1.7%	3.72E+04	1.2%	3.93E+04	3.48E+04	1.5%	1.3%
1.39E+01	3.88E+04	1.7%	3.38E+04	1.3%	3.44E+04	3.15E+04	1.5%	1.3%
1.08E+01	3.40E+04	1.8%	3.07E+04	1.3%	3.00E+04	2.85E+04	1.6%	1.3%
8.34E+00	2.97E+04	1.9%	2.78E+04	1.3%	2.60E+04	2.57E+04	1.6%	1.3%
6.46E+00	2.58E+04	2.0%	2.50E+04	1.4%	2.25E+04	2.31E+04	1.7%	1.3%
5.00E+00	2.23E+04	2.1%	2.25E+04	1.4%	1.93E+04	2.06E+04	1.7%	1.3%
5.00E+00	2.23E+04	1.9%	2.26E+04	1.3%	1.93E+04	2.07E+04	1.6%	1.4%
3.87E+00	1.91E+04	1.8%	2.02E+04	1.3%	1.65E+04	1.84E+04	1.6%	1.4%
3.00E+00	1.64E+04	2.0%	1.81E+04	1.5%	1.40E+04	1.64E+04	1.7%	1.4%
2.32E+00	1.40E+04	2.1%	1.61E+04	1.5%	1.19E+04	1.45E+04	1.8%	1.5%
1.80E+00	1.18E+04	2.3%	1.43E+04	1.5%	9.97E+03	1.28E+04	1.9%	1.4%
1.39E+00	9.93E+03	2.3%	1.26E+04	1.6%	8.32E+03	1.12E+04	1.9%	1.5%
1.08E+00	8.30E+03	2.5%	1.11E+04	1.6%	6.91E+03	9.81E+03	1.9%	1.5%
8.34E-01	6.90E+03	2.6%	9.68E+03	1.6%	5.70E+03	8.53E+03	2.1%	1.5%
6.46E-01	5.69E+03	2.6%	8.44E+03	1.7%	4.66E+03	7.39E+03	2.2%	1.6%
5.00E-01	4.65E+03	2.7%	7.31E+03	1.8%	3.78E+03	6.37E+03	2.3%	1.6%
5.00E-01	4.64E+03	2.8%	7.31E+03	1.7%	3.74E+03	6.36E+03	2.2%	1.6%
3.15E-01	3.16E+03	3.0%	5.58E+03	1.9%	2.50E+03	4.80E+03	2.4%	1.8%
1.99E-01	2.10E+03	3.4%	4.19E+03	1.9%	1.64E+03	3.56E+03	2.7%	1.8%
1.26E-01	1.35E+03	3.6%	3.08E+03	2.1%	1.04E+03	2.60E+03	2.9%	2.0%
7.92E-02	8.43E+02	4.2%	2.23E+03	2.3%	6.39E+02	1.86E+03	3.3%	2.1%
5.00E-02	5.07E+02	4.4%	1.58E+03	2.4%	3.79E+02	1.30E+03	3.4%	2.2%
3.15E-02	2.91E+02	5.1%	1.10E+03	2.8%	2.17E+02	8.98E+02	3.7%	2.2%
1.99E-02	1.63E+02	4.6%	7.52E+02	4.1%	1.21E+02	6.07E+02	4.4%	2.5%
1.26E-02	8.66E+01	4.9%	5.02E+02	4.2%	6.31E+01	4.08E+02	3.2%	3.1%

Continues Table A3

Temp.	190 °C			
Frequency	G'		G"	
rad/s	Pa	CV	Pa	CV
5.00E+02	1.65E+05	1.2%	1.12E+05	1.1%
3.87E+02	1.50E+05	1.2%	1.02E+05	1.1%
3.00E+02	1.36E+05	1.3%	9.39E+04	1.1%
2.32E+02	1.23E+05	1.3%	8.60E+04	1.1%
1.80E+02	1.11E+05	1.3%	7.88E+04	1.1%
1.39E+02	9.99E+04	1.3%	7.21E+04	1.1%
1.08E+02	8.98E+04	1.3%	6.60E+04	1.1%
8.34E+01	8.05E+04	1.3%	6.04E+04	1.2%
6.46E+01	7.20E+04	1.4%	5.52E+04	1.2%
5.00E+01	6.42E+04	1.3%	5.05E+04	1.1%
3.87E+01	5.71E+04	1.4%	4.61E+04	1.2%
3.00E+01	5.06E+04	1.4%	4.21E+04	1.2%
2.32E+01	4.46E+04	1.4%	3.83E+04	1.3%
1.80E+01	3.93E+04	1.5%	3.48E+04	1.3%
1.39E+01	3.44E+04	1.5%	3.15E+04	1.3%
1.08E+01	3.00E+04	1.6%	2.85E+04	1.3%
8.34E+00	2.60E+04	1.6%	2.57E+04	1.3%
6.46E+00	2.25E+04	1.7%	2.31E+04	1.3%
5.00E+00	1.93E+04	1.7%	2.06E+04	1.3%
5.00E+00	1.93E+04	1.6%	2.07E+04	1.4%
3.87E+00	1.65E+04	1.6%	1.84E+04	1.4%
3.00E+00	1.40E+04	1.7%	1.64E+04	1.4%
2.32E+00	1.19E+04	1.8%	1.45E+04	1.5%
1.80E+00	9.97E+03	1.9%	1.28E+04	1.4%
1.39E+00	8.32E+03	1.9%	1.12E+04	1.5%
1.08E+00	6.91E+03	1.9%	9.81E+03	1.5%
8.34E-01	5.70E+03	2.1%	8.53E+03	1.5%
6.46E-01	4.66E+03	2.2%	7.39E+03	1.6%
5.00E-01	3.78E+03	2.3%	6.37E+03	1.6%
5.00E-01	3.74E+03	2.2%	6.36E+03	1.6%
3.15E-01	2.50E+03	2.4%	4.80E+03	1.8%
1.99E-01	1.64E+03	2.7%	3.56E+03	1.8%
1.26E-01	1.04E+03	2.9%	2.60E+03	2.0%
7.92E-02	6.39E+02	3.3%	1.86E+03	2.1%
5.00E-02	3.79E+02	3.4%	1.30E+03	2.2%
3.15E-02	2.17E+02	3.7%	8.98E+02	2.2%
1.99E-02	1.21E+02	4.4%	6.07E+02	2.5%
1.26E-02	6.31E+01	3.2%	4.08E+02	3.1%

Table A 4 Oscillatory Shear Experimental Data of the HPBD

Temp.	150 °C				170 °C			
Frequency	G'		G"		G'		G"	
rad/s	Pa	CV	Pa	CV	Pa	CV	Pa	CV
5.00E+01	8.23E+05	3.4%	2.59E+05	0.1%	7.34E+05	1.3%	2.85E+05	1.2%
3.97E+01	7.89E+05	3.5%	2.74E+05	0.4%	6.93E+05	1.1%	2.97E+05	1.8%
3.16E+01	7.49E+05	3.4%	2.87E+05	0.1%	6.46E+05	1.2%	3.13E+05	0.7%
2.51E+01	7.05E+05	3.6%	3.01E+05	1.0%	5.96E+05	0.9%	3.22E+05	1.4%
1.99E+01	6.56E+05	3.9%	3.15E+05	1.1%	5.40E+05	0.8%	3.29E+05	0.8%
1.58E+01	6.04E+05	4.1%	3.25E+05	2.0%	4.85E+05	0.7%	3.34E+05	0.6%
1.26E+01	5.48E+05	4.0%	3.33E+05	2.3%	4.25E+05	0.3%	3.30E+05	0.3%
9.98E+00	4.89E+05	3.7%	3.35E+05	2.4%	3.65E+05	0.2%	3.18E+05	0.0%
7.93E+00	4.28E+05	4.0%	3.31E+05	2.6%	3.08E+05	0.3%	3.01E+05	0.2%
6.30E+00	3.67E+05	4.2%	3.21E+05	3.2%	2.58E+05	0.2%	2.79E+05	0.4%
5.00E+00	3.11E+05	4.5%	3.03E+05	3.7%	2.14E+05	0.7%	2.53E+05	0.9%
3.97E+00	2.60E+05	4.5%	2.80E+05	3.8%	1.76E+05	0.8%	2.26E+05	1.1%
3.16E+00	2.16E+05	4.2%	2.54E+05	3.9%	1.46E+05	0.2%	1.99E+05	0.7%
2.51E+00	1.79E+05	3.9%	2.26E+05	3.9%	1.21E+05	0.3%	1.73E+05	0.5%
1.99E+00	1.48E+05	3.8%	1.99E+05	4.1%	1.01E+05	0.0%	1.50E+05	0.6%
1.58E+00	1.24E+05	3.5%	1.73E+05	3.9%	8.60E+04	0.1%	1.28E+05	0.7%
1.26E+00	1.04E+05	3.5%	1.50E+05	3.9%	7.29E+04	0.0%	1.10E+05	0.6%
9.98E-01	8.92E+04	3.1%	1.29E+05	3.9%	6.32E+04	0.1%	9.48E+04	0.7%
7.93E-01	7.61E+04	3.2%	1.10E+05	3.9%	5.46E+04	0.2%	8.06E+04	0.5%
6.30E-01	6.57E+04	2.9%	9.46E+04	3.8%	4.76E+04	0.0%	6.89E+04	0.6%
5.00E-01	5.72E+04	2.9%	8.10E+04	3.7%	4.18E+04	0.2%	5.90E+04	0.5%
5.00E-01	5.69E+04	2.9%	8.09E+04	3.9%	4.17E+04	0.0%	5.90E+04	0.8%
3.16E-01	4.51E+04	2.8%	6.03E+04	3.6%	3.35E+04	0.3%	4.40E+04	0.8%
1.99E-01	3.55E+04	2.7%	4.39E+04	3.3%	2.66E+04	0.6%	3.23E+04	0.6%
1.26E-01	2.86E+04	2.8%	3.29E+04	3.3%	2.15E+04	1.1%	2.44E+04	0.7%
7.93E-02	2.34E+04	2.8%	2.50E+04	3.1%	1.76E+04	1.2%	1.87E+04	0.7%
5.00E-02	1.93E+04	3.0%	1.93E+04	3.0%	1.44E+04	1.5%	1.46E+04	0.5%
5.00E-02	1.95E+04	2.8%	1.94E+04	3.0%	1.45E+04	1.2%	1.46E+04	0.5%
3.16E-02	1.63E+04	3.2%	1.53E+04	2.7%	1.21E+04	1.6%	1.17E+04	0.4%
1.99E-02	1.33E+04	3.1%	1.21E+04	2.8%	9.82E+03	1.8%	9.36E+03	0.4%
1.26E-02	1.10E+04	3.2%	9.81E+03	2.8%	8.07E+03	1.9%	7.71E+03	0.1%
7.93E-03	9.10E+03	3.2%	8.10E+03	2.8%	6.71E+03	1.1%	6.46E+03	0.4%
5.00E-03	7.52E+03	3.0%	6.81E+03	2.8%	5.79E+03	0.7%	5.55E+03	0.8%

Continues to Table A4

Temp.	190 C			
Frequency	G'		G"	
rad/s	Pa	CV	Pa	CV
5.00E+01	6.79E+05	2.9%	3.17E+05	2.1%
3.97E+01	6.30E+05	2.7%	3.30E+05	2.4%
3.15E+01	5.76E+05	2.5%	3.40E+05	2.6%
2.51E+01	5.17E+05	2.2%	3.44E+05	2.8%
1.99E+01	4.53E+05	1.8%	3.42E+05	2.7%
1.58E+01	3.91E+05	0.7%	3.32E+05	2.4%
1.26E+01	3.31E+05	0.5%	3.17E+05	2.3%
9.98E+00	2.76E+05	0.1%	2.96E+05	2.5%
7.92E+00	2.30E+05	0.1%	2.71E+05	2.7%
6.29E+00	1.89E+05	0.2%	2.44E+05	2.8%
5.00E+00	1.55E+05	0.1%	2.14E+05	2.4%
3.97E+00	1.28E+05	1.3%	1.86E+05	1.7%
3.15E+00	1.06E+05	1.7%	1.61E+05	1.5%
2.51E+00	8.91E+04	1.5%	1.39E+05	1.5%
1.99E+00	7.50E+04	2.2%	1.19E+05	1.1%
1.58E+00	6.43E+04	2.1%	1.01E+05	0.6%
1.26E+00	5.50E+04	2.4%	8.62E+04	0.5%
9.98E-01	4.82E+04	2.4%	7.41E+04	0.5%
7.92E-01	4.20E+04	2.6%	6.27E+04	0.1%
6.29E-01	3.68E+04	2.8%	5.35E+04	0.3%
5.00E-01	3.25E+04	2.7%	4.58E+04	0.4%
5.00E-01	3.26E+04	3.3%	4.59E+04	0.4%
3.15E-01	2.65E+04	3.1%	3.43E+04	0.4%
1.99E-01	2.11E+04	3.4%	2.53E+04	1.3%
1.26E-01	1.71E+04	3.4%	1.93E+04	1.3%
7.92E-02	1.39E+04	3.9%	1.49E+04	1.6%
5.00E-02	1.13E+04	4.2%	1.17E+04	1.9%
5.00E-02	1.14E+04	4.1%	1.17E+04	1.7%
3.15E-02	9.39E+03	4.7%	9.43E+03	2.2%
1.99E-02	7.55E+03	5.2%	7.58E+03	2.0%
1.26E-02	6.13E+03	6.0%	6.23E+03	2.3%
7.92E-03	4.99E+03	7.3%	5.17E+03	2.4%
5.00E-03	4.08E+03	10.6%	4.33E+03	3.0%

Table A 5 Relaxation Spectra of the HDB5

Temp.	150 C	Temp.	160 C	170 C	180 C	190 C
Time	log(H)	Time	log(H)			
s	Pa	s	Pa			
1.00E-04	5.67E+00	1.00E-04	5.60E+00	5.63E+00	5.64E+00	5.65E+00
1.70E-04	5.56E+00	1.60E-04	5.53E+00	5.55E+00	5.56E+00	5.56E+00
2.89E-04	5.46E+00	2.57E-04	5.46E+00	5.47E+00	5.47E+00	5.47E+00
4.92E-04	5.36E+00	4.12E-04	5.39E+00	5.39E+00	5.39E+00	5.37E+00
8.38E-04	5.28E+00	6.61E-04	5.32E+00	5.32E+00	5.30E+00	5.28E+00
1.43E-03	5.21E+00	1.06E-03	5.25E+00	5.24E+00	5.22E+00	5.19E+00
2.42E-03	5.15E+00	1.70E-03	5.18E+00	5.16E+00	5.13E+00	5.10E+00
4.12E-03	5.08E+00	2.73E-03	5.10E+00	5.07E+00	5.03E+00	5.00E+00
7.02E-03	4.95E+00	4.38E-03	5.00E+00	4.97E+00	4.93E+00	4.89E+00
1.19E-02	4.80E+00	7.02E-03	4.89E+00	4.85E+00	4.81E+00	4.76E+00
2.03E-02	4.64E+00	1.13E-02	4.76E+00	4.72E+00	4.67E+00	4.63E+00
3.46E-02	4.49E+00	1.80E-02	4.62E+00	4.58E+00	4.54E+00	4.49E+00
5.88E-02	4.37E+00	2.89E-02	4.49E+00	4.45E+00	4.41E+00	4.37E+00
1.00E-01	4.25E+00	4.64E-02	4.37E+00	4.33E+00	4.29E+00	4.25E+00
1.70E-01	4.15E+00	7.44E-02	4.26E+00	4.23E+00	4.19E+00	4.15E+00
2.89E-01	4.06E+00	1.19E-01	4.17E+00	4.13E+00	4.10E+00	4.06E+00
4.92E-01	3.96E+00	1.91E-01	4.08E+00	4.05E+00	4.01E+00	3.96E+00
8.38E-01	3.86E+00	3.07E-01	4.00E+00	3.96E+00	3.91E+00	3.86E+00
1.43E+00	3.75E+00	4.92E-01	3.91E+00	3.86E+00	3.81E+00	3.76E+00
2.42E+00	3.61E+00	7.90E-01	3.81E+00	3.76E+00	3.70E+00	3.63E+00
4.12E+00	3.45E+00	1.27E+00	3.70E+00	3.63E+00	3.56E+00	3.48E+00
7.02E+00	3.27E+00	2.03E+00	3.57E+00	3.49E+00	3.40E+00	3.31E+00
1.19E+01	3.06E+00	3.26E+00	3.42E+00	3.33E+00	3.22E+00	3.12E+00
2.03E+01	2.82E+00	5.22E+00	3.26E+00	3.15E+00	3.03E+00	2.90E+00
3.46E+01	2.52E+00	8.38E+00	3.07E+00	2.94E+00	2.81E+00	2.65E+00
5.88E+01	2.19E+00	1.34E+01	2.86E+00	2.70E+00	2.56E+00	2.37E+00
1.00E+02	1.83E+00	2.15E+01	2.61E+00	2.42E+00	2.26E+00	2.04E+00
1.70E+02	1.47E+00	3.46E+01	2.33E+00	2.12E+00	1.91E+00	1.69E+00
2.89E+02	1.10E+00	5.54E+01	2.00E+00	1.79E+00	1.53E+00	1.33E+00
4.92E+02	7.20E-01	8.89E+01	1.66E+00	1.46E+00	1.12E+00	9.55E-01
8.38E+02	3.41E-01	1.43E+02	1.30E+00	1.11E+00	6.97E-01	5.77E-01
1.43E+03	-3.96E-02	2.29E+02	9.33E-01	7.67E-01	2.69E-01	1.98E-01
2.42E+03	-4.20E-01	3.67E+02	5.63E-01	4.19E-01	-1.60E-01	-1.82E-01
4.12E+03	-8.01E-01	5.88E+02	1.91E-01	7.10E-02	-5.91E-01	-5.63E-01
7.02E+03	-1.18E+00	9.43E+02	-1.81E-01	-2.78E-01	-1.02E+00	-9.43E-01
1.19E+04	-1.56E+00	1.51E+03	-5.54E-01	-6.27E-01	-1.45E+00	-1.32E+00
2.03E+04	-1.94E+00	2.42E+03	-9.26E-01	-9.76E-01	-1.88E+00	-1.70E+00
3.46E+04	-2.32E+00	3.89E+03	-1.30E+00	-1.32E+00	-2.31E+00	-2.09E+00
5.88E+04	-2.70E+00	6.24E+03	-1.67E+00	-1.67E+00	-2.75E+00	-2.47E+00
1.00E+05	-3.09E+00	1.00E+04	-2.04E+00	-2.02E+00	-3.18E+00	-2.85E+00

Table A 8 Relaxation Spectra of the HDB7

150 C		190 C	
Time, s	log (H), Pa	Time, s	log (H), Pa
1.00E-03	5.58E+00	1.00E-03	5.02E+00
1.70E-03	5.40E+00	1.60E-03	5.03E+00
2.89E-03	5.24E+00	2.57E-03	5.04E+00
4.92E-03	5.11E+00	4.12E-03	5.07E+00
8.38E-03	5.02E+00	6.61E-03	5.11E+00
1.43E-02	5.01E+00	1.06E-02	5.18E+00
2.42E-02	5.09E+00	1.70E-02	5.30E+00
4.12E-02	5.26E+00	2.73E-02	5.45E+00
7.02E-02	5.47E+00	4.38E-02	5.57E+00
1.19E-01	5.60E+00	7.02E-02	5.55E+00
2.03E-01	5.46E+00	1.13E-01	5.33E+00
3.46E-01	5.11E+00	1.80E-01	5.01E+00
5.88E-01	4.77E+00	2.89E-01	4.72E+00
1.00E+00	4.54E+00	4.64E-01	4.51E+00
1.70E+00	4.40E+00	7.44E-01	4.37E+00
2.89E+00	4.27E+00	1.19E+00	4.24E+00
4.92E+00	4.14E+00	1.91E+00	4.11E+00
8.38E+00	4.01E+00	3.07E+00	4.00E+00
1.43E+01	3.92E+00	4.92E+00	3.92E+00
2.42E+01	3.84E+00	7.90E+00	3.86E+00
4.12E+01	3.74E+00	1.27E+01	3.78E+00
7.02E+01	3.62E+00	2.03E+01	3.67E+00
1.19E+02	3.54E+00	3.26E+01	3.53E+00
2.03E+02	3.54E+00	5.22E+01	3.43E+00
3.46E+02	3.56E+00	8.38E+01	3.41E+00
5.88E+02	3.51E+00	1.34E+02	3.46E+00
1.00E+03	3.36E+00	2.15E+02	3.47E+00
1.70E+03	3.12E+00	3.46E+02	3.30E+00
2.89E+03	2.82E+00	5.54E+02	2.97E+00
4.92E+03	2.50E+00	8.89E+02	2.72E+00
8.38E+03	2.16E+00	1.43E+03	2.69E+00
1.43E+04	1.81E+00	2.29E+03	2.83E+00
2.42E+04	1.46E+00	3.67E+03	2.84E+00
4.12E+04	1.11E+00	5.88E+03	2.32E+00
7.02E+04	7.58E-01	9.43E+03	1.46E+00
1.19E+05	4.06E-01	1.51E+04	4.82E-01
2.03E+05	5.45E-02	2.42E+04	-5.15E-01
3.46E+05	-2.97E-01	3.89E+04	-1.51E+00
5.88E+05	-6.49E-01	6.24E+04	-2.51E+00
1.00E+06	-1.00E+00	1.00E+05	-3.51E+00

Table A 7 Relaxation Spectra of the HDB7

Temp.	150 C	160 C	170 C	180 C	190 C
Time, s	log(H), Pa				
1.00E-04	5.49E+00	5.49E+00	5.49E+00	5.49E+00	5.47E+00
1.70E-04	5.37E+00	5.36E+00	5.35E+00	5.34E+00	5.32E+00
2.89E-04	5.24E+00	5.22E+00	5.21E+00	5.20E+00	5.18E+00
4.92E-04	5.12E+00	5.10E+00	5.08E+00	5.06E+00	5.04E+00
8.38E-04	5.00E+00	4.98E+00	4.95E+00	4.94E+00	4.91E+00
1.43E-03	4.90E+00	4.87E+00	4.85E+00	4.83E+00	4.80E+00
2.42E-03	4.82E+00	4.79E+00	4.76E+00	4.74E+00	4.71E+00
4.12E-03	4.74E+00	4.71E+00	4.69E+00	4.67E+00	4.64E+00
7.02E-03	4.67E+00	4.65E+00	4.62E+00	4.60E+00	4.57E+00
1.19E-02	4.61E+00	4.58E+00	4.55E+00	4.53E+00	4.49E+00
2.03E-02	4.54E+00	4.50E+00	4.47E+00	4.45E+00	4.41E+00
3.46E-02	4.46E+00	4.43E+00	4.39E+00	4.37E+00	4.32E+00
5.88E-02	4.39E+00	4.35E+00	4.31E+00	4.28E+00	4.23E+00
1.00E-01	4.31E+00	4.26E+00	4.22E+00	4.18E+00	4.12E+00
1.70E-01	4.22E+00	4.17E+00	4.12E+00	4.07E+00	4.01E+00
2.89E-01	4.13E+00	4.07E+00	4.01E+00	3.96E+00	3.88E+00
4.92E-01	4.02E+00	3.96E+00	3.89E+00	3.83E+00	3.75E+00
8.38E-01	3.91E+00	3.83E+00	3.76E+00	3.69E+00	3.60E+00
1.43E+00	3.78E+00	3.69E+00	3.61E+00	3.54E+00	3.43E+00
2.42E+00	3.64E+00	3.54E+00	3.45E+00	3.36E+00	3.25E+00
4.12E+00	3.49E+00	3.38E+00	3.27E+00	3.17E+00	3.03E+00
7.02E+00	3.32E+00	3.20E+00	3.08E+00	2.96E+00	2.80E+00
1.19E+01	3.14E+00	3.00E+00	2.85E+00	2.72E+00	2.53E+00
2.03E+01	2.93E+00	2.76E+00	2.59E+00	2.46E+00	2.22E+00
3.46E+01	2.68E+00	2.48E+00	2.28E+00	2.15E+00	1.86E+00
5.88E+01	2.40E+00	2.16E+00	1.94E+00	1.80E+00	1.46E+00
1.00E+02	2.08E+00	1.82E+00	1.56E+00	1.42E+00	1.05E+00
1.70E+02	1.74E+00	1.46E+00	1.18E+00	1.02E+00	6.18E-01
2.89E+02	1.38E+00	1.10E+00	7.85E-01	6.17E-01	1.85E-01
4.92E+02	1.02E+00	7.32E-01	3.90E-01	2.10E-01	-2.50E-01
8.38E+02	6.59E-01	3.64E-01	-6.52E-03	-1.99E-01	-6.86E-01
1.43E+03	2.96E-01	-4.59E-03	-4.03E-01	-6.08E-01	-1.12E+00
2.42E+03	-6.72E-02	-3.73E-01	-8.01E-01	-1.02E+00	-1.56E+00
4.12E+03	-4.31E-01	-7.42E-01	-1.20E+00	-1.43E+00	-1.99E+00
7.02E+03	-7.95E-01	-1.11E+00	-1.59E+00	-1.84E+00	-2.43E+00
1.19E+04	-1.16E+00	-1.48E+00	-1.99E+00	-2.24E+00	-2.87E+00
2.03E+04	-1.52E+00	-1.85E+00	-2.39E+00	-2.65E+00	-3.30E+00
3.46E+04	-1.89E+00	-2.22E+00	-2.79E+00	-3.06E+00	-3.74E+00
5.88E+04	-2.25E+00	-2.59E+00	-3.18E+00	-3.47E+00	-4.17E+00
1.00E+05	-2.61E+00	-2.96E+00	-3.58E+00	-3.88E+00	-4.61E+00

Table A 6 Relaxation Spectra of the HDB6

Temp.	150 C	170 C	190 C
Time	log(H)		
s	Pa		
1.00E-04	5.61E+00	5.64E+00	5.63E+00
1.70E-04	5.51E+00	5.51E+00	5.50E+00
2.89E-04	5.41E+00	5.39E+00	5.36E+00
4.92E-04	5.31E+00	5.26E+00	5.23E+00
8.38E-04	5.21E+00	5.14E+00	5.10E+00
1.43E-03	5.11E+00	5.03E+00	4.97E+00
2.42E-03	5.01E+00	4.92E+00	4.85E+00
4.12E-03	4.90E+00	4.81E+00	4.74E+00
7.02E-03	4.79E+00	4.69E+00	4.62E+00
1.19E-02	4.66E+00	4.58E+00	4.50E+00
2.03E-02	4.54E+00	4.46E+00	4.39E+00
3.46E-02	4.44E+00	4.35E+00	4.29E+00
5.88E-02	4.34E+00	4.26E+00	4.19E+00
1.00E-01	4.25E+00	4.16E+00	4.08E+00
1.70E-01	4.17E+00	4.07E+00	3.97E+00
2.89E-01	4.07E+00	3.96E+00	3.85E+00
4.92E-01	3.97E+00	3.84E+00	3.71E+00
8.38E-01	3.85E+00	3.70E+00	3.55E+00
1.43E+00	3.72E+00	3.54E+00	3.36E+00
2.42E+00	3.57E+00	3.36E+00	3.15E+00
4.12E+00	3.40E+00	3.17E+00	2.93E+00
7.02E+00	3.22E+00	2.95E+00	2.70E+00
1.19E+01	3.00E+00	2.70E+00	2.41E+00
2.03E+01	2.76E+00	2.41E+00	2.03E+00
3.46E+01	2.48E+00	2.07E+00	1.58E+00
5.88E+01	2.16E+00	1.69E+00	1.07E+00
1.00E+02	1.82E+00	1.28E+00	5.45E-01
1.70E+02	1.46E+00	8.57E-01	9.94E-03
2.89E+02	1.09E+00	4.25E-01	-5.27E-01
4.92E+02	7.12E-01	-9.04E-03	-1.06E+00
8.38E+02	3.36E-01	-4.44E-01	-1.60E+00
1.43E+03	-4.01E-02	-8.80E-01	-2.14E+00
2.42E+03	-4.17E-01	-1.32E+00	-2.68E+00
4.12E+03	-7.94E-01	-1.75E+00	-3.22E+00
7.02E+03	-1.17E+00	-2.19E+00	-3.75E+00
1.19E+04	-1.55E+00	-2.62E+00	-4.29E+00
2.03E+04	-1.92E+00	-3.06E+00	-4.83E+00
3.46E+04	-2.30E+00	-3.49E+00	-5.37E+00
5.88E+04	-2.68E+00	-3.93E+00	-5.90E+00
1.00E+05	-3.05E+00	-4.36E+00	-6.44E+00